Identification of Genes Involved in Hereditary Hearing Impairment and Alopecias

A thesis submitted in partial fulfillment of the requirements for the degree of Doctor of Philosophy

in

Biochemistry / Molecular Biology

by

GHAZANFAR ALI

Department of Biochemistry
Faculty of Biological Sciences
Quaid-i-Azam University
Islamabad
2009

CERTIFICATE

This thesis by **Mr. Ghazanfar Ali** is accepted in its present form by the Department of Biochemistry, Quaid-i-Azam University, Islamabad as satisfying the thesis requirements for the degree of Doctor of Philosophy (PhD) in Biochemistry / Molecular Biology.

External Examiner:_____

(Dr. Hamid Rashid)

External Examiner:_____

(Dr. Allah Nawaz)

Supervisor & Chairman:_____

(Prof. Dr. Wasim Ahmad)

Dated: February 04, 2009

DECLARATION

I hereby declare that the work presented in the following thesis is my own effort, except where otherwise acknowledged, and that thesis is my own composition. No part of this thesis has been previously presented for any other degree.

Ghazanfar Ali

Dedicated to

My Loving Parents

&

My Loving Son

(M. Qasim Hassan)

In the name of Allah, the most Beneficent,
the most Merciful

CONTENTS

ACKNOWLEDGEMENTS

All praise is to Allah who granted me the urge and ability to seek knowledge of His creation.

I offer my profound gratitude to my research supervisor Dr. Wasim Ahmad, Professor, Chairman, Department of Biochemistry, Quaid-i-Azam University Islamabad, whose guidance, support and encouragement facilitated the completion of my research work. His energy, optimism, intelligence and continuous encouragement at every step during the course of this whole project enabled me to achieve my goals. I must say that without his support and kind efforts, this task would have been impossible.

I present my deepest regards to Dr. Muhammad Ansar, Assistant Professor, Department of Biochemistry, Faculty of Biological sciences, Quaid-i-Azam University, Islamabad for his guidance and cooperation.

I am extremely thankful for the invaluable help I received from Dr. Muhammad Naeem, Dr. Peter John, Mr. Muhammad Salman Chisti, Mr. Jawad Hassan Raja, Dr. Abdul Wali Tareen, Dr. Asma Gul, Dr. Attya Bhatti, Dr. Shaeen Sikander, Mr. Zahid Azeem, Mr. Muhammad Tariq, Mr. Syed Kamran Naqvi, Mr. Naveed Wasif, Mr. Salman Basit, Mr. Yasrab Arafat and Miss Gulnaz from Quaid-i-Azam University Islamabad, Others deserving of my thanks from Quaid-i-Azam University Islamabad.

I am indebted to Dr. Huma Qureshi, Executive Director, and Dr. Mubashar A Khan, Pakistan Medical Research Council, Islamabad for their kindness, continuous support and encouragement throughout my period of research. I deeply appreciate the steady support I received from Agha Sadaruddin, Centre Incharge, and Dr. Jehangir A Khan from the Pakistan Medical Research Council, Islamabad.

I am extremely grateful to Dr. Arshad Mamtaz from the Department of Histopathalogy, National Institute of Health, Islamabad for his invaluable contributions.

I am grateful to my colleagues Abid Khan, Dr. Najma Javaid and junior staff members, Muhammad Jamil, Liaqat Hayat, Nasib Zaman, Zia-ul-Haq, Asghar Ali, Abdul Haq and Qari Sheraz for their cooperation.

I'm extremely obliged to all the patients and their families on whom this research was conducted for their participation and cooperation.

Finally, I wish to thank the Higher Education Commission (HEC), Islamabad Pakistan, for funding this project through different research grant to my supervisor.

A particular note of gratitude is owed to my Uncles Malik Muhammad Afzal and Muhammad Khan, for their help, devotion, inspiration and prayers.

I am blessed and strengthened by the unconditional support and love from my father, mother, brothers, sisters, my wife Nazia Malik and my loving son Muhammad Qasim Hassan. I am thankful to all of them for their help, devotion, inspiration, prayers.

Ghazanfar Ali

LIST OF TABLES

LIST OF FIGURES

LIST OF ACRONYMS

AA	Alopecia Areata
ACPTA	Air Conduction Pure Tone Average
ARNSHI	Autosomal Recessive Non-syndromic Hearing Impairment
AH	Autosomal Recessive Hypotrichosis
APL	Atrichia with Papular Lesions
APMR	Alopecia with Mental Retardation
AR	Androgen Receptor
bp	Base Pair
CDH3	Cadherin 3
CDSN	Corneodesmosin
CHLC	Cooperative Human linkage Center
cM	Centimorgans
dB	Decibels
DNA	Deoxyribonucleic Acid
dNTP	Deoxynucleoside Triphosphate
DSC	Desmocollin
DFN	Non-syndromic Deafness
DFNA	Autosomal Dominant Non-syndromic Deafness
DFNB	Autosomal recessive non-syndromic deafness
DSG	Desmoglein
DSP	Desmoplakin
EDAR	Ectodysplasin 1 Anhidrotic Receptor
EDTA	Ethylenediamine Tetra Acetic Acid
ESTs	Expressed Sequence Tags
EVPL	Envoplakin
GJB2	Gap Junction Beta-2
GJB6	Gap Junction Beta-6
hHb1, hHb3	Trichocyte Keratin Genes
HDF	Hi Di Formamide
hHb	Keratin Hair Basic
HJMD	Hypotrichosis Congenital with Juvenile Macular Dystrophy

HI	Hearing Impairment
HR	Hairless
Hz	Hertz (Unit of sound frequency)
HSS	Hypotrichosis Simplex of the Scalp
HTS	Hypotrichosis Simplex
IBD	Identity-by-Descend
IQ	Intelligence Quotient
KCNRG	Potassium Channel Regulator Isoform 2
Kb	Kilo base
KDa	Kilo Dalton
LAH	Localized Autosomal Recessive Hypotrichosis
LEKTI	Lympho-epithelial Kazal-type related Inhibitor
LIPH	Lipase-H
LPA	2-acyl Lysophosphatidic Acid
LOD	Logarithm of Odds
LOR	Loricrin
LPA	2-Acyl Lysophosphatidic Acid
Mb	Megabase
Mg	Milligram
MHC	Major Histocompatibility
MIM	Mendelian Inheritance in Man
ml	Milli Litre
mM	Milli Molar
MPB	Male Pattern Baldness
MUUH	Marie Unna Hereditary Hypotrichosis
NCBI	National Center for Biotechnology Information
ng	Nanogram
NIH	National Institute of Health
NS	Netherton Syndrome
OD	Optical density
PCR	Polymerase Chain Reaction
PCDH15	Protocadherin 15
PIMS	Pakistan Institute of Medical Sciences

PKP1	Plakophillin 1
PLA1	Phosphatidic Acid-Selective Phospholipase A1
PVRL1	Poliovirus Receptor 1
rpm	Revolution Per Minute
RT-PCR	Reverse transcriptase-polymerase chain reaction
SDS	Sodium Dodecyl Sulfate
SNPs	Single Nucleotide Polymorphism
SLC	Solute Carrier Family
TI	Trichorrhexis Invaginata
TMC1	Transmembrane Channel-like Gene 1
TMIE	Transmembrane Inner Ear Expressed Gene
TMPRSS3	Transmembrane Protease Serine-3 Gene
TNF	Tumor Necrosis Factor
TNFSF10	Tumor Necrosis Factor Ligand Superfamily Member 10
TR	Thyroid Hormone Receptor
UV	Ultra Violet
µl	Micro Liter
uM	Micro Molar
WHN	Winged Helix Nude
WHRN	Whirlin
ZNF	Zinc Finger

ABSTRACT

A study of rare monogenetic disorders in humans is often invaluable for discovery of the previously unknown genes and physiological pathways. In Pakistan, due to strict social customs, inbreeding has led to unique large families with un-described phenotypes. These families represent the opportunity to clinically describe new entities, and large family size allows the variability and natural history to be documented. The families also provide an ideal solution to the linkage problem, as individual families contain enough power to allow the disease genes to be localized, the first step in defining the defective genes. For the present study, Pakistani families with autosomal recessive disorders, Hearing Impairment or Alopecias, have been studied as described below.

In the present investigation, five highly consanguineous families (A-E) with hereditary hearing impairment and four families (F-I) with hereditary alopecias have been studied from Punjabi, Sindhi and Balochi speaking population of Pakistan. In all these families, a classical linkage analysis approach was used to identify the underlying genes.

In family A, screening of the human genome led to the identification of a novel autosomal recessive non-syndromic hearing impairment locus, DFNB62, on chromosome 12p13.2-p11.23. Significant evidence of linkage to this chromosomal region was found with two-point LOD score of 4.0 and multipoint LOD score of 5.3. Haplotype analysis located the DFNB62 locus in 22.4 cM (15.0 Mb) region flanked by markers D12S358 and D12S1042. DFNB62 represents the second autosomal recessive non-syndromic hearing impairment (ARNSHI) locus that mapped on chromosome 12p13.2.

In family B, linkage data obtained from genome scan and saturation of several chromosomal regions with additional markers failed to define a region harboring a causative gene for deafness.

In three families (C, D, E), linkage was established to known hearing impairment loci. Family C showed linkage to DFNB9 locus on chromosome 2p23.3 containing *OTOF* gene. In families D and E, linkage was established to DFNB8/10 on chromosome 21q22.3. The entire coding region, as well as intron-exon boundaries of *TMPRSS3*

gene was sequenced in affected and unaffected individuals of both the families, but the efforts failed to detect the functional sequence variants.

In family F with hereditary hypotrichosis, linkage was established to AH/LAH2 locus on chromosome 3q27. The entire coding region, as well as intron-exon boundaries of *LIPH* gene were sequenced in all the three affected and one normal individuals of the family. Sequence analysis of a candidate gene Lipase-H (*LIPH*) revealed a novel five base pair deletion mutation (c.346–350delATATA) in exon 2 of the gene leading to frameshift and downstream premature termination codon. The deletion mutation identified in the family is the second mutation identified in *LIPH* gene.

In family G with alopecia and mental retardation syndrome, hairs were completely absent by birth from all areas of body of the affected individuals. Candidate gene mapping showed linkage of this family to microsatellite markers linked to APMR1 and APMR2 loci on chromosome 3q26.2-q28. A maximum two-point LOD score of 1.74 (θ=0.0) was obtained with nine markers. Multipoint linkage analysis resulted in a maximum LOD score of 3.17 with markers D3S2433, D3S2427 and D3S3676 which supports the linkage. Haplotype analysis located the APMR locus between markers D3S3622 and D3S3596, spanning 32.53 cM (20.14 Mb) region on chromosome 3q26.2–q28. Sequence analysis of five candidate genes, *LIPH, ETS* variant gene 5, *TNFSF10, AP2M1* and *CamK2* from DNA samples of two affected and one unaffected individuals of the family failed to reveal pathogenic sequence variants.

In family H with hypotrichosis, initial genome wide scan revealed five chromosomal regions including D1S1151 at 1p36.22, D3S1544 at 3q12.2, D8S1832 at 8q24.13, D10S1700 at 10q26.3 and D12S291 at 12q12, which were found to be homozygous in all the three affected members of the family. Saturation of these five regions with additional markers, however, failed to generate a significant LOD score with any of the markers, thus excluding these regions from harboring a causative gene for hypotrichosis in family H.

The family I was tested for linkage by using polymorphic microsatellite markers linked to hairless (*HR*) gene on chromosome 8p21.2. Genotyping of five members including two affected and three unaffected individuals with polymorphic microsatellite markers D8S322, D8S282, D8S560, D8S298, established linkage to the *HR* locus. Subsequently, the entire coding region as well as intron-exon boundaries of

the *HR* gene was sequenced in two affected individuals, but failed to identify functional sequence variant suggesting that the mutation is probably present in the regulatory sequence of the gene.

The work presented in the thesis has been published in the following articles.

1. **Ali G**, Santos RL, John P, Wambangco MA, Lee K, Ahmad W, Leal S. The mapping of DFNB62, a new locus for autosomal recessive non-syndromic hearing impairment, to chromosome 12p13.2-p11.23. **Clinical Genetics 69(5):429-33, 2006.**
2. **Ali G**, Chishti MS, Raza SI, John P, Ahmad W. A mutation in the lipase H (LIPH) gene underlie autosomal recessive hypotrichosis. **Human Genetics 121(3-4):319-325, 2007.**

INTRODUCTION

Human population is characterized by some parameters including consanguineous marriages, frequencies of genetic disorders, birth rate, morbidity and mortality. Among these population parameters, consanguineous marriages are customary in various human societies that lead to an increased prevalence of severe genetic disorders. Hence, consanguinity and genetic disorders, being related to serious health problems, are always considered most important in genetic studies (Bittles, 2002).

Genetic disorders are found almost in every human population though their nature, prevalence and distribution vary in different regions of the world (El-Hazmi, 1999). Consequently, the genetic disorders impose a heavy medical and financial burden on the affected individuals and their families, as well as on the society at large due to their chronic nature (Abdel-Meguid *et al.*, 2000).

The consanguineous marriage pattern has significant implication for increased rate of recessive genetic disorders (Bittles, 2005; Al-Gazali, 2005). High rate of consanguinity in any population along with other factors such as religion, ethnicity, language, geography etc, usually lead to create genetically isolated groups in which typically confined, well-documented, extended and multigenerational pedigrees with several cases of rare diseases are expected (Peltonen *et al.*, 2000; Bittles, 2001). The extended pedigrees were readily used by geneticists for their linkage studies and for mapping many monogenic autosomal recessive disorders. In this regard, various isolated Pakistani population such as many small communities have played prominent role in identifying the novel mutations in these autosomal recessive disorders.

The huge population of Indian sub-continent including Pakistan, India and Bangladesh also provides an opportunity for studies of genetic disorders (Gadgil *et al.*, 1998). But the population of Pakistan is the goldmine for these studies due to its unique geography and history. In addition, it is a mixture of diverse ethnicities with unique familial and social characteristics (Mehdi *et al.*, 1999).

For the present study consanguineous Pakistanies families with genetic disorders like hearing impairment and alopecia have been ascertained and investigated.

Hearing Impairment

Hearing impairment (HI) is the loss of ability to hear normally, whether permanent loss or fluctuating. Hearing impairment is clinically and genetically heterogeneous and can be caused by environmental as well as genetic factors.

Type of Hearing Impairment

Primarily there are four forms of hearing impairment:

Conductive

It is related to disease of outer or middle ear. Audiometrically normal bone conduction thresholds are <20 dB HL and an air-bone gap >15 dB HL averaged over 0.5, 1 and 2 kHz.

Sensorineural

It is related to disease of the inner ear or cochlear nerve with an air/bone gap < 15 dB HL averaged over 0.5, 1 and 2 kHz.

Mixed

It is related to combined involvement of the outer/middle ear and the inner ear/cochlear nerve. Audiometrically there are >20 dB HL in the bone conduction threshold together with >15 dB HL air-bone gap averaged over 0.5, 1 and 2 kHz.

Central Auditory Dysfunction

It occurs when auditory centers of the brain are affected by injury, disease, tumor and hereditary or unknown causes.

Onset and Severity of Hearing Impairment

Prelingual hearing loss

Prelingual hearing loss is present before speech develops. All congenital hearing loss is prelingual, but not all prelingual hearing loss is congenital.

Postlingual hearing loss

It occurs after the development of normal speech.

Hearing is measured in **decibels** (dB). The threshold or 0 dB mark for each frequency refers to the level at which normal young adults perceive a tone burst 50% of the time.

Hearing is considered normal if an individual's thresholds are within 15 dB of normal thresholds.

Air conduction pure tone average (ACPTA) thresholds in the conversational frequencies (0.5, 1, 2 and 4 kHz) were calculated for each deaf ear and were used to define the severity of deafness: mild (20 db<ACPTA≤39 db), moderate (40 db<ACPTA≤69 db), severe (70 db<ACPTA≤89 db) and profound (≥90 db) (Albert *et al.*, 2006).

Genetics of Hearing Impairment

The genetically determined hearing impairment can be divided into two categories; syndromic and non-syndromic forms. The syndromic forms include several hundred deafness syndromes, with the underlying genetic defect being found in about 30 of them (Petit, 1996; Resendes *et al.*, 2001; Petersen and Willems, 2006). In non-syndromic genetic deafness of pre-lingual onset, autosomal recessive inheritance predominates (80%), but autosomal dominant (20%), X-linked (1%), and mitochondrial (<1%) forms have also been described. In post-lingual, non-syndromic deafness, autosomal recessive inheritance is very rare. The autosomal recessive forms are usually more severe than the other forms and are almost exclusively due to cochlear defects (Petersen and Willems, 2006).

Syndromic Hearing Impairment

Syndromic hearing impairment may account for up to 30% of prelingual deafness, which in most cases is of conductive and mixed type but its relative contribution to all deafness is much smaller, reflecting the occurrence and diagnosis of post lingual hearing loss. Over 400 genetic syndromes that include hearing loss have been described (Petersen and Willems, 2006). Syndromic hearing loss is categorized according to the mode of inheritance. Syndromic hearing loss can have many modes of transmission, including maternal inheritance due to a mitochondrial mutation.

Non-Syndromic Hearing Impairment

Non-syndromic deafness is a paradigm of genetic heterogeneity. It is estimated that more than 70% of hereditary hearing loss is non-syndromic (Van Camp *et al.*, 1997; Petersen and Willems, 2006). The different gene loci for non-syndromic deafness are designated DFN (for DeaFNess). Loci for genes inherited in an autosomal dominant

forms are referred to as DFNA, and for genes inherited in an autosomal recessive forms as DFNB, and those for genes inherited in an X-linked forms as DFN.

Approximately 126 different gene loci associated with non-syndromic hearing impairment have been identified to date (Hereditary Hearing Loss. http://www.dnalab-www.uia.ac.be/dnalab/hhh, September 2007). Presently 54 gene/loci associated with autosomal dominant mode of inheritance, 72 with autosomal recessive mode of inheritance, 7 are X-chromosome linked and 4 mitochondrial have been identified. In total 21 genes have been characterized for autosomal dominant (DFNA), 27 for autosomal recessive (DFNB), and 2 for X-linked (DFN) disorders (Van Camp and Smith, 2008; Hereditary Hearing Loss Homepage; http://www.dnalab-www.uia.ac.be /dnalab/hhh).

Autosomal Dominant Non-Syndromic Hearing Impairment

Autosomal dominant non-syndromic hearing loss is a heterogeneous disorder. Most forms of autosomal dominant non-syndromic deafness are difficult to distinguish phenotypically. The majority of autosomal dominant genes are associated with hearing impairment that is postlingual in onset, often beginning before the age of 20 years. Some forms, however, notably DFNA4, DNFA9 and DFNA10 are associated with hearing impairment starting somewhat later during the third and fourth decades. Mutations at the DFNA6/14/38 locus as well as those associated with the DFNA9 locus tend to have distinguishable clinical phenotypes, and DFNA12, DFNA13 and DFNA21 are characterised by mid frequency hearing impairment.

Autosomal Recessive Non-Syndromic Hearing Impairment

Autosomal recessive non-syndromic hearing impairment is clinically, the most important group because it accounts for about 80% of non-syndromic deafness. Most of the recessively inherited forms of hearing impairment cause a phenotypically identical severe to profound, prelingual hearing loss (Van Camp and Smith Hereditary Hearing Loss Homepage, 2003), but mutations at a few loci DFNB2 (*MYO7A*) (Liu *et al.,* 1997), DFNB8/10 (*TMPRSS3*) (Veske *et al.,* 1996) and DFNB16 (*STRC*) (Verpy *et al.,* 2001) cause a delayed, childhood onset hearing impairment.

Genes for Autosomal Recessive Non-Syndromic Hearing Impairment

Hereditary hearing impairment is genetically a highly heterogeneous disease with many different genes responsible for auditory dysfunction. Of the 30,000-35,000 human genes, 1%, i.e., 300-500 genes are estimated to be necessary for hearing (Friedman and Griffith, 2003). Most of the genes for recessive deafness have been identified by positional genetics in inbred multiplex families in ethnic isolates. Only a few of the genes including *OTOA*, *PCDH15*, *GJB3*, *GJA1*, and *SLC26A5* have been found to be associated with recessive deafness by a functional candidate gene approach.

A total of 27 different DFNB genes have been identified, and 21 genes are categorized by their function into four groups as described briefly below.

Cytoskeletal Genes

MYO3A

Dose and Burnside, (2000) mapped the *MYO3A* gene to chromosome 10p11.1 (DFNB30). Sequencing of the *MYO3A* gene from genomic DNA revealed three different mutations of this gene cosegregating with hearing loss. *MYO3A* gene is specifically expressed in photoreceptors and cochlea and is important for the phototransduction and hearing processes.

MYO6

The *MYO6* gene was mapped at 6q13 and defined the DFNB37 locus (Ahmed *et al.*, 2003). Vreugde *et al.* (2006) described that *MYO6* modulates RNA polymerase II-dependent transcription of active genes and suggested that an actin-myosin-based mechanism may be involved in transcription. Myosin VI participates in 2 steps of endocytic trafficking; it is recruited to both clathrin-coated pits and to ensuing uncoated endocytic vesicles (Naccache *et al.*, 2006). To date more than five mutations in affected individuals of various ethnic origins have been identified (Mohiddin *et al.*, 2004).

MYO7A

The *MYO7A* gene was mapped to 11q13.5 in a highly consanguineous family from Tunisia (Guilford *et al.*, 1994). *MYO7A* may be important for the original organization of stereocilia on the cell's apical surface, as the stereocilia are disorganized in the

MYO7A null mutant. More than 50 distinct *MYO7A* mutations in affected individuals have been identified, which are responsible for DFNB2 and dominant deafness (DFNA11) (Tamagawa *et al.*, 1996; Liu *et al.*, 1997; Bolz *et al.*, 2004; Ouyang *et al.*, 2005).

MYO15A

The human *MYO15A* gene was identified and mapped to the DFNB3 region on chromosome 17p11.2 (Liang *et al.*, 1998; Wang *et al.*, 1998). *MYO15A* have a role in maintenance of stereocilia, as recent studies suggest actin replacement in stereocilia occurs every 48 h. *MYO15A* is essential for normal actin organization within the inner hair cells (IHCs) of the cochlea, and may function similarly in stereocilia (Probst *et al.*, 1998; Friedman *et al.*, 2000, 2002; Anderson *et al.*, 2000). To date more than nine different pathogenic mutations have been identified in *MYO15A* gene (Nal *et al.*, 2007).

Structural Genes

STRC

The *STRC* gene was mapped to DFNB16 chromosomal region on 15q21-q22 (Verpy *et al.*, 2001). *STRC* gene may function to anchor the tectorial membrane to organ of corti cell structures (Jovine *et al.*, 2002). Verpy *et al.* (2001) identified three pathogenic mutations in affected individuals including an insertion mutation of a cytosine in exon 13, a 4-bp deletion in exon 5 and a large deletion of the *STRC* gene.

TECTA

The *TECTA* gene was identified to a locus for recessive deafness DFNB21 in a region on chromosome 11q23–q25 (Mustapha *et al.*, 1999). The function of this gene is to optimize the sensitivity of the basilar membrane to frequency-tuned mechanical oscillations and to provide mechanical feedback to the outer hair cells in order to adjust the gain of the cochlear amplifier (Legan *et al.*, 2000). Sequence analysis of the *TECTA* gene identified a G-to-A transition mutation in the donor splice site (GT) of intron 9, homozygosity for 649insC and 6037delG mutation in the *TECTA* gene, respectively (Mustapha *et al.*, 1999; Naz *et al.*, 2003).

OTOA

Zwaenepoel *et al.* (2002) mapped the *OTOA* gene on chromosome 16p12.2 (DFNB22). The mouse Otoa gene is expressed only in the inner ear. Otoancorin was suggested to mediate attachment of the tectorial membrane in the cochlea, and the otoconial membranes and cupulae in the vestibule. Zwaenepoel *et al.* (2002) identified a T-to-C transition at the exon 12/intron 12 junction of the *OTOA* gene.

COL11A2

Chen *et al.* (2005) localized the *COL11A2* gene to 6p21.3 (DFNB53). The *COL11A2* gene helps in the production of type XI collagen. Type XI collagen helps to maintain the spacing and diameter of type II collagen fibrils. Type II collagen is an important component of the eye and mature cartilage tissue. The size and arrangement of type II collagen fibrils are essential for the normal structure of these tissues. Several pathogenic mutations in *COL11A2* have been reported, including 11 nonsense or frameshift/stop mutations, three in-frame deletions and four missense mutations (Temtamy *et al.*, 2006).

Ion Transport genes

GJB2 & GJB6

Brown *et al.* (1996) found *GJB2* and *GJB6* genes linkage to the DFNB1 locus on chromosome 13q11–q12. This family of genes produces protein subunits for gap junctions (channels) that connect adjacent cells. These channels are important for the movement of nutrients, charged ions, intercellular communication and homeostasis in the inner ear. Elias *et al.* (2007) concluded that gap junction adhesions are necessary for glial-guided neuronal migration. To date more than thirty seven different mutations have been identified in the *GJB2* gene (Seeman *et al.*, 2004; Dahl *et al.*, 2006). However only two mutations have been detected in the *GJB6* gene (del Castillo *et al.*, 2002).

GJB3

The *GJB3* gene (connexin 31) was cloned and mapped to chromosome 1p35–p33 (Xia *et al.*, 1998). This *GJB3* gene family encoded protein, which is a component of gap junctions, and are composed of arrays of intercellular channels that provide a route for the passage of low molecular weight materials from cell to cell (Abrams *et al.*, 2006).

Mutation screening in Chinese families with compound heterozygosity for the same two *GJB3* mutations, heterozygous R32W mutation and 3 bp *GJB3* deletion was detected in a Spanish family (Liu *et al.*, 2000; Lopez-Bigas *et al.*, 2001; Mhatre *et al.*, 2003; Uyguner *et al.*, 2003).

TMC1

The transmembrane channel-like gene 1 (*TMC1)* gene was mapped to locus DFNB7/ DFNB11 on chromosome 9q13-q21 in highly consanguineous families segregating non-syndromic deafness. It was suggested that the gene function of *TMC1* might be an ion channel or transporter, which mediates K+ homeostasis in the inner ear (Keresztes *et al.*, 2003). Seven different *TMC1* mutations in affected individuals of various ethnic origins including nonsense, frameshift, missense, deletion, and splice site were identified in 11 recessive families (Kurima *et al.*, 2002; Santos *et al.*, 2005).

CLDN14

Wilcox *et al.* (2001) showed that the *CLDN14* gene maps to locus DFNB29 on chromosome 21q22.1. The protein encoded by this *CLDN14* gene is a component of tight junction strands. Tight junctions represent one mode of cell-to-cell adhesion and serving as a physical barrier to prevent solutes and water from passing freely through the paracellular space.

SLC26A5

Liu *et al.* (2003) mapped *SLC26A5* gene to chromosome 7q22.1. Nine human *SLC26A* genes have already been identified, and mutations in the *SLC26A2*, *SLC26A3*, and *SLC26A4* genes are responsible for three distinct recessive disorders: diastrophic dysplasia, congenital chloride diarrhea, and Pendred syndrome/DFNB4, respectively (Everett and Green, 1999; Lohi *et al.*, 2002). Zheng *et al.* (2000) concluded that prestin is the motor protein of cochlear outer hair cells. Weber *et al.* (2002) suggested thyroid hormone as a first transcriptional regulator of the motor protein prestin and as a direct or indirect modulator of subcellular prestin distribution.

Genes Having Unknown Functions

TMIE

The transmembrane inner ear expressed gene (*TMIE)* was mapped to locus DFNB6 on chromosome 3p14-p21. *TMIE* gene has a conserved critical role in the auditory

system. This gene is required for correct development of stereocilia bundles, including normal postnatal maturation of sensory hair cells in the cochlea (Mitchem *et al.*, 2002). The mutations in *TMIE* gene indicate that loss of function of *TMIE* causes hearing loss in humans (Naz *et al.*, 2002; Mitchem *et al.*, 2002; Santos *et al.*, 2006).

TMPRSS3

Transmembrane protease, serine 3 gene *(TMPRSS3)* was mapped to locus DFNB8/ DFNB10 on chromosome 21q22. Wattenhofer *et al.* (2005) concluded that precleavage of *TMPRSS3* is mandatory for normal function because this gene significantly activates epithelial sodium channel EnaC, which is involved in the regulation of sodium concentration in the endolymph.

OTOF

The *OTOF* gene was mapped to DFNB9 locus on 2p23-p22 (Yasunaga and Petit, 2000). Roux *et al.* (2006) showed that otoferlin localized to ribbon-associated synaptic vesicles and may play a role in releasing chemical signals (neurotransmitters) from nerve cells that are involved in hearing. Otoferlin bound Ca (2+) and displayed Ca (2+)-dependent interactions with the other molecules like SNARE proteins syntaxin-1 (STX1A) and SNAP25. To date 11 distinct mutations have been identified in the *OTOF* gene (Yasunaga *et al.*, 1999, 2000; Adato *et al.*, 2000; Houseman *et al.*, 2001; Migliosi *et al.*, 2002; Mirghomizadeh *et al.*, 2002).

CDH23

The *CDH23* gene was localized to DFNB12 locus on chromosome 10q21-22. *CDH23* was shown to be part of the tip links involved in cross-linking stereocilia (Di Palma *et al.*, 2001; Siemens *et al.*, 2002). Kazmierczak *et al.* (2007) demonstrated that *CDH23* and *PCDH15* interact to form tip links, extracellular filaments that connect the stereocilia and are thought to gate the mechanoelectrical transduction channel. To date, 36 different pathogenic mutations in affected individuals of various ethnic origins have been reported for the *CDH23* gene including two nonsense and two frameshift mutations in families with *USH1D* (Bork *et al.*, 2001).

USH1C

Verpy *et al.* (2000) mapped the *USH1C* gene to the locus DFNB18, which maps to the region of chromosome 11p14-15.1. Adato *et al.* (2005) proposed that, via its

binding to myosin VIIa and/or harmonin, it controls the hair bundle cohesion and plays a role in the development and maintenance of hair like projections called stereocilia. To date, 10 different pathogenic mutations in affected individuals of various ethnic origins have been reported for the *USH1C* gene.

PCDH15

The *PCDH15* gene was mapped to locus DFNB23 on chromosome 10p11.2-q21. *PCDH15* may play a role in early stages of inner ear development and maintenance of specialized photoreceptor cells that detect light and color. The *PCDH15* gene encoding protocadherin 15 had previously been shown to be reponsible for Usher syndrome type 1F (Ahmed *et al.*, 2001; Alagramam *et al.*, 2001).

WHRN

The *WHRN* gene was mapped to locus DFNB31 on chromosome 9q32–q34 (Mustapha *et al.*, 2002). Whirlin is known to be essential for the elongation process of the stereocilia of sensory hair cells in the inner ear, though its complete spatial and temporal expression patterns remained elusive. Whirlin has a pleiotropic function in both retina and inner ear (van Wijk *et al.*, 2006). The murine region syntenic to the DFNB31 interval on chromosome 4 contains the locus for the recessive deafness mutant whirler (wi), which in the homozygous adult causes the shaker waltzer syndrome: deafness and circling with tossing of the head (Mustapha *et al.*, 2002; Mburu *et al.*, 2003).

ESPN

The *ESPN* gene was mapped to DFNB36 locus on chromosome 1p36.3 (Naz *et al.*, 2004). Espin localizes to stereocilia of hair cells and is involved in establishing and stabilizing the actin filament structure (Zheng *et al.*, 2000). Stereocilia, bend in response to sound waves for converting them to nerve impulses and for conveying information about the movement.

Alopecia

Hereditary alopecia is a heterogeneous group of inherited hair loss disorders with different clinical features, modes of inheritance, and genetic bases. It is characterized by diffuse or localized thinning or absence of hairs beginning at birth or early childhood. The loss of hair affects the scalp, eyebrows, eyelashes, body hairs, axillary and pubic hairs.

Total or partial absence of hair may occur either in isolation or with associated ectodermal abnormalities as a part of syndrome of a very diverse nature. On the bases of such associations, several different syndromes featuring congenital alopecia can be distinguished. The major defects reported to be associated with total or partial absence of hair, either single or in various combinations include mental retardation, dwarfism, epilepsy, nail dystrophy, total or partial anodontia, hyperkeratosis, impaired sweating, cataracts, retinitis pigmentation etc (Pinheiru *et al.,* 1985; Feinstein *et al.,* 1987; John *et al.,* 2006). In familial cases, inheritance is usually autosomal recessive, but families with autosomal dominant or X-linked recessive inheritance have also been reported. Patients with recessive form tend to have a more sever phenotype, often with complete absence of hair development, affecting scalp and body hair.

Different Patterns of Hair Loss

Monilethrix

Monilethrix (MIM 158000) is a congenital autosomal dominant hair disorder, which mapped to locus 12q13 that can cause scarring alopecia in affected individuals (Carreras, 1996). Monilethrix may occur either alone or in association with physical retardation, keratosis pilaris, cataracts, syndactyly and nail or teeth abnormalities. The hallmark of hair abnormality in monilethrix is a beading of the hair shaft caused by periodic narrowing with nodes separated by about 0.7 mm. The cause of the beading is unknown. The expression of monilethrix is variable (Winter *et al.,* 1998). Monilethrix has been linked to the type I and type II keratin gene clusters on chromosome 17q and 12q13, respectively.

Most cases of monilethrix described so far are associated with mutations in the type II (basic) trichocyte keratin genes *hHb1*, *hHb3* and *hHb6* (Horev *et al.,* 2000; 2003; Winter *et al.,* 2000; Muramatsu *et al.,* 2003; Sprecher *et al.,* 2003). Hair keratins have

acidic and basic forms. At least one acidic human hair keratin maps to the type I keratin gene cluster at 17q12-q21 and at least one basic hair keratin maps to the corresponding type II cluster at 12q13 (Rogers *et al.*, 1995)

To date, 10 different pathogenic mutations in affected individuals of various ethnic origins have been reported for the human monilethrix gene. These include, missense, nonsense, deletions, insertion, and splice sites mutations (Rothnagel *et al.*, 1992; Syder *et al.*, 1994; Sybert *et al.*, 1999; Hatsell *et al.*, 2001; Sprecher *et al.*, 2001; Whittock *et al.*, 2001, 2002; Terron-Kwiatkowski *et al.*, 2002; Lee *et al.*, 2002; Ishida-Yamamoto *et al.*, 2003; Van Steensel *et al.*, 2005).

Congenital Atrichia

Congenital atrichia (MIM 209500) is a rare form of irreversible autosomal recessive disorder. Clinical features of affected individuals with this form of alopecia include: atrichia at birth or shedding of normal scalp hair several months after birth with failure to regrow; appearance of skin papules within the first year of life; sparse eyebrows and eyelashes; lack of secondary axillary, pubic, or body hair; and normal nails, teeth, and sweating (Zlotogorski *et al.*, 2002). To date, families with congenital atrichia have been reported from 17 backgrounds, including Pakistani, Japanese, Polish, German, Israeli, Palestinian, Mexican, Italian, Korean and Mediterranean populations.

Congenital atrichia has been linked to 8p21, where several mutations of the hairless gene (*HR*, MIM 602302) have been reported as the underlying cause of congenital atrichia. To date, more than 38 different pathogenic mutations in affected individuals of various ethnic origins have been reported for the human *HR* gene (Ahmad *et al.*, 1998a; Cichon *et al.*, 1998; John *et al.*, 2005; Wali *et al.*, 2006b; Betz *et al.*, 2007; Kim *et al.*, 2007; Kraemer *et al.*, 2008; Roelandt *et al.*, 2008).

Marie Unna Hereditary Hypotrichosis (MUHH)

Marie Unna hereditary hypotrichosis (MUHH; OMIM 146550) is a rare autosomal dominant disorder. Light microscopic examination from hair of the scalp could show thick, irregular, and twisted hair (He *et al.*, 2004). They detected linkage on 8p22–p21 by several groups (van Steensel *et al.*, 1999; Cichon *et al.*, 2000; Lefevre *et al.*, 2000; Sreekumar *et al.*, 2000; He *et al.*, 2004). Because the MUHH locus mapped to the same region of chromosome 8 as the human *HR* gene which had been shown to carry

recessive mutations responsible for congenital atrichia with papules (Ahmad *et al.*, 1998, 1999; Cichon *et al.*, 1998; Zlotogorski *et al.*, 2002; Wali *et al.*, 2006b), therefore mutation analysis of the *HR* gene was performed, but no mutations were found in MUHH pedigrees.

Yang *et al.* (2005) found a second novel locus for MUHH on chromosome 1p21.1–1q21.3 in a Chinese family. This indicated that MUHH is a genetically heterogeneous disorder.

Netherton Syndrome

Netherton syndrome (NS, MIM 256500) is a severe autosomal recessive skin disorder characterized by congenital ichthyosis, a specific hair shaft abnormality (Trichorrhexis Invaginata (TI) or ''bamboo hair''), and atopic manifestations (Netherton, 1958; Plantin *et al.*, 1991). The gene for NS was mapped to 5q31-q32, and was subsequently identified as *SPINK5* (Chavanas *et al.*, 2000a). The gene spans a region of 61 kb and is composed of 33 exons. It encodes LEKTI (Lympho-epithelial Kazal-type related Inhibitor), a predicted serine protease inhibitor highly expressed in thymus and mucous epithelia (Magert *et al.*, 1999; Chavanas *et al.*, 2000b).

To date, 45 different pathogenic mutations in affected individuals of various ethnic origins have been reported for the *SPINK5* gene (Chavanas *et al.*, 2000a; Sprecher *et al.*, 2001, 2004; Mizuno *et al.*, 2006; Zhao *et al.*, 2007).

Hereditary Hypotrichosis Simplex

Hereditary hypotrichosis simplex can be divided into two main forms; generalized (universal or total) in which the defects involve all the body hair and localized (hereditary hypotrichosis of the scalp) in which hair loss is limited to the scalp with the rest of pilary system being normal. Hypotrichosis simplex of the scalp (HSS; MIM 146520) is an autosomal dominant form of nonsyndromic alopecia that affects men and women equally. Affected individuals with the scalp have normal hair in early childhood but experience progressive loss of the scalp hair beginning in the middle of first decade almost complete baldness by the third decade. The body hair, beard, eyebrows, eyelashes, axillary hair, teeth and nail are normal.

Betz *et al.* (2000) mapped a locus for hypotrichosis simplex of the scalp to human chromosome 6p21.3 in two Danish families and one Spanish family. Levy-Nissenbaum *et al.* (2003) identified nonsense mutations in corneodesmosin gene

(CDSN; MIM 602593) in three families suffering from hypotrichosis simplex of the scalp. CDSN, a glycoprotein of 529 amino acids expressed in the epidermis and inner root sheath of hair follicles, is a keratinocyte adhesion molecule.

Autosomal Recessive Hypotrichosis

To date, three clinically similar forms of autosomal recessive hypotrichosis have been reported. Localized autosomal recessive hypotrichosis (LAH; MIM 607903) has been mapped to the region of the desmosomal cadherin gene cluster on chromosome 18q12.1 (Kljuic *et al.*, 2003a; Rafiq *et al.*, 2003), which contains the genes for desmogleins (DSG1, DSG2, DSG3, and DSG4) and desmocollins (DSC1, DSC2, and DSC3). A large, intragenic deletion of exons 5-8 (EX5_8del) in desmoglein 4 gene (*DSG4*; MIM 607892) was found to be the underlying defect in two unrelated LAH families of Pakistani origin (Kljuic *et al.*, 2003b). DSG4, a novel member of the desmosomal cadherin family that is expressed in the inner epithelial layers of the hair follicle, where its function appears to be crucial during differentiation of the hair follicle layers. The same deletion mutation was subsequently detected in six additional Pakistani kindreds (Moss *et al.*, 2004; Rafiq *et al.*, 2004; John *et al.*, 2006b), suggesting that it represents an ancestral mutation that has been widely dispersed. Messenger *et al.* (2005) reported a missense mutation (A129S) in *DSG4* gene in an Iraqi family. More recently, Wajid *et al.* (2007) identified a single nucleotide deletion 87delG with in exon 3 of the *DSG4* gene.

A second autosomal recessive hypotrichosis locus (AH / LAH2; MIM 604379) was mapped on chromosome 3q27 (Aslam *et al.*, 2004). The AH locus overlaps with an alopecia mental retardation syndrome (APMR1) locus (John *et al.*, 2006a). Interestingly, another alopecia with mental retardation syndrome (APMR2) locus (Wali *et al.*, 2006a) was mapped proximal to AH and APMR1 loci.

Recently, Kazantseva *et al.* (2006) have reported the identification of a deletion mutation in Lipase H (*LIPH*) gene (MIM 607365) on chromosome 3q27 (Kazantseva *et al.*, 2006). The gene was cloned earlier by Sonoda *et al.* (2002). LIPH is a phosphatidic acid-selective phospholipase A1 (PLA1) that produces 2-acyl lysophosphatidic acid (LPA), which is a lipid mediator with diverse biologic properties. The deletion mutation involves 985 bp containing exon 4 and the flanking intronic sequences of *LIPH* gene. The deletion of exon 4 does not alter the reading

frame of the gene however this eliminates the evolutionary conserved domain in the protein structure (Kazantseva *et al.*, 2006). Recently, Ali *et al.* (2007, present study) have reported a five base pair deletion mutation (c.346–350delATATA) in exon 2 of the gene leading to frameshift and downstream premature termination codon.

Recently, Wali *et al.* (2007a) ascertained two consanguineous Pakistani families demonstrating autosomal recessive form of hereditary hypotrichosis. The affected individuals in these two families exhibited typical features of the hereditary hypotrichosis. Genome wide scan using polymorphic microsatellite markers led to the identification of a third locus (LAH3; MIM 611452) for this form of hypotrichosis in a 17.35 cM region on chromosome 13q14.11-q21.32.

Alopecia with Mental Retardation Syndrome

Alopecia with mental retardation syndrome (APMR, MIM 203650) is a rare autosomal recessive form of alopecia which show hair loss on the scalp, absence of eyebrows, eyelashes, axillary and pubic hair, and mild to severe mental retardation (Perniola *et al.*, 1980; Baraitser *et al.*, 1983; Benke and Hajianpour 1985; John *et al.*, 2006a; Wali *et al.*, 2006a; 2007b). John *et al.* (2006a) have mapped the *APMR1* locus to human chromosome 3q26.33–q27.3 in a family with severe mental retardation (IQ from 25–30). The second locus for alopecia and mental retardation (*APMR2*) was mapped to chromosome 3q26.2–q26.31 (Wali *et al.*, 2006a) in a family with total alopecia and mild to moderate mental retardation (IQ from 53–61). Recently, Wali *et al.* (2007b) reported the mapping of a third locus for alopecia and mental retardation syndrome (*APMR3*) in a large family at chromosome 18q11.2–q12.2.

Alopecia areata (AA)

Alopecia areata (AA; MIM 104000) is a nonscarring, autoimmune, inflammatory, hair loss on the scalp and/or body (Olsen, 2003). Recognized subgroups of this disease include those patients with the complete absence of terminal scalp hair (alopecia totalis or AT) and those patients with total loss of terminal scalp and body hair (alopecia universalis or AU) (Sehgal and Jain, 2003; Olsen *et al.*, 2004). In the initial stages, the number of hair follicles appears to remain the same; however, in the more advanced stages this number decrease and miniaturization of the anagen hair follicles is observed (McDonagh and Messenger, 1996).

Martinez-Mir *et al.* (2007) performed a genome wide search for linkage in 20 families with AA consisting of 102 affected and 118 unaffected individuals from the United States and Israel. Linkage analysis resulted in the localization of at least four susceptibility loci on chromosome 6, 10, 16, and 18. Interestingly, the major loci on chromosome 16 and 18 reported in this study coincide with loci for psoriasis. The results suggest that these regions may harbor genes involved in a number of different skin and hair disorders.

In the present study, nine families with hereditary hearing loss or alopecias have been described. Molecular genetic studies and DNA sequencing have been performed to locate the disease loci and pathogenic mutations.

MATERIALS AND METHODS

Families Studied

Five families (A-E) with autosomal recessive non-syndromic hereditary hearing impairment and four families (F-I) with alopecia, residing in different regions of Pakistan, have been located and studied for the present investigation. The families have been ascertained by identifying probands during the field visits. The families were visited at their places of residence to collect all possible information. The well informed elders and relatives of the families were interviewed to obtain maximum information about the family history and individuals having hereditary hearing impairment and alopecias. All the information on the degree of hereditary hearing loss, number of affected individuals, number of generations involved, miscarriages in the family, the associated defects if any and onset of the hearing and hair loss were carefully recorded. All the information obtained was crosschecked by independently interviewing different persons associated with the family. Audiometry was performed on selected individuals to detect the level of hearing impairment. Dermatologists at Pakistan Institute of Medical Sciences (PIMS) Islamabad and Government Hospital Quetta, Balochistan examined the affected individuals from all the alopecia families. Histopathologists at National Institute of Health (NIH) Islamabad examined scalp biopsy of affected individuals with hypotrichosis. The phenotypes of affected persons, indicated, in the pedigrees, were recorded for clinical diagnosis of the disorders. Blood samples from affected and normal individuals of each family were collected for DNA extraction.

Pedigree Analysis

Pedigree is the most important step while studying human genetic disorder. This helps geneticists to infer the mode of inheritance of the trait. For genetic inference an extensive pedigree was constructed for each family using the standard methods described by Bennett *et al.* (1995). Males were symbolized by squares and females by circles. The normal individuals were designated with unfilled symbols while the affected individuals by filled symbols. Each generation has been numbered consecutively and was denoted by Roman numeral. The individuals within a generation were designated by Arabic numerals. A number enclosed within a symbol

indicates the number of sibs. The exact genealogical relationships of all the affected individuals were obtained through extensive personal interviews of elders of the families. The information was checked and rechecked by interviewing different persons. The segregation or transmission of the hereditary hearing loss and hair loss within the families were deduced by observing the pattern of inheritance of hereditary disorders studied and were expressed in the form of pedigree.

Blood Sampling

Before the onset of the study, approval was obtained from Quaid-i-Azam University Institutional Review Board. After obtaining informed consent from all individuals venous blood samples were drawn from both affected and normal members of the families by the aid of 10 ml sterilized syringes (0.7 x 40 mm, 22G x 1 ½) and blood vacutainer sets. Attempts were made to collect the blood samples of all the affected and normal family members, but some of them were not available for the study. The blood was immediately transferred into the blood vacutainer sets containing ethylenediaminetetraacetic acid (EDTA). The blood samples, collected in the field were kept at 4°C, before being processed for extraction of genomic DNA.

Genomic DNA Extraction

Two methods were used for genomic DNA extraction and purification from blood samples:

- Phenol-Chloroform Method for DNA Extraction
- Inorganic Method for DNA Extraction

Phenol-Chloroform Method for DNA Extraction

Genomic DNA extraction from venous blood sample was performed using standard phenol-chloroform procedure (Sambrook *et al.*, 1989). Equal volume of the blood and solution A [0.32 M Sucrose, 10 mM Tris (pH 7.5), 5 mM $MgCl_2$, 1% v/v Triton X-100] was mixed in a 1.5 ml microcentrifuge tube and was kept at room temperature for 10-15 minutes. The tubes were centrifuged at 13,000 rpm for 1 minute in a Microfuge® 18 Centrifuge (Eppendorf Centrifuge 5415 R, Germany). Supernatant was discarded and pellet was re-suspended in 400 µl of solution A, and was centrifuged again. Supernatant was again discarded and the nuclear pellet was re-suspended in 400 µl of solution B [10 mM Tris (pH 7.5), 400 mM NaCl, 2 mM

EDTA (pH 8.0)] and 12 µl of 20% SDS solution and 25 µl of Proteinase K (2 mg/ml stock) and incubated at 37^0C overnight.

On the following day, after complete digestion of the nuclear pellet, 0.5 ml of freshly prepared mixture of equal volumes of solution C (phenol) and solution D (chloroform and iso-amyle alcohol 24:1) were added in the tubes; mixed and centrifuged for 10 minutes at 13,000 rpm. The aqueous phase (upper phase) was transferred in a new tube containing 500 µl of solution D, centrifuged again at 13,000 rpm for 10 minutes. The aqueous phase was placed in a new tube, and after adding 55 µl of 3 M sodium acetate (pH 6) and equal volume of iso-propanol, the tubes were inverted several times to precipitate DNA. After washing DNA with 70% ethanol; dried it in the vaccum DNA concentrator (Eppendorf Concentrator 5301, Germany) and dissolved in Tris-EDTA (TE) buffer. DNA concentration was determined by spectrophotometer (Biometra GeneRay UV-Photometer) at OD_{260} nm.

Inorganic Method for DNA Extraction

Two and a half milliliter of blood was taken in a 15 ml conical tube with 7.5 ml lysis buffer [155 mM Ammonium Chloride, 10 mM Potassium Hydrogen Carbonate, 0.1 mM EDTA, pH 7.4]. After mixing the contents by inversion, the tubes were placed on ice for 15 minutes. Centrifugation was carried out at 2,000 rpm (Eppendorf Centrifuge 5810 R, Germany) for 15 minutes at 4°C. The supernatant was discarded and the pellet was resuspended in 5 ml of lysis buffer. The nuclear pellet was digested overnight in 3 ml of nuclear lysis solution [10 mM Tris-HCl (pH 8.0), 400 mM NaCl, 2 mM EDTA, pH 8.2] containing 85 µl of 20% SDS and 8 µl proteinase K (50 mg/ml). The protein contaminants were then salted out by centrifugation at 4,000 rpm for 30 minutes after adding 0.83 ml of sodium chloride (6 M). Equal volume of iso-propanol was added to the supernatant to precipitate the DNA. The precipitated DNA was fished out and transferred in a microcentrifuge tube containing 70% ethanol for washing. After evaporation of residual ethanol by using vaccum DNA concentrator (Eppendorf Concentrator 5301, Germany), DNA was dissolved in appropriate amount of Tris-EDTA (TE) buffer and stored at 4°C.

Polymerase Chain Reaction (PCR)

PCR was performed in total volume of 25 µl reaction mixture containing 2.5 µl of 10 X PCR buffer (KCl 50 mM, Tris-HCl 100 mM, pH 8.3, 1.5 mM $MgCl_2$) with 0.5 mM

dNTP, 0.3 μl microsatellite marker, 1 unit Taq DNA polymerase (MBI-Fementase, UK) and 40 ng genomic DNA. The reaction mixture was centrifuged for few seconds for thorough mixing. Reactions were performed by means of thermocyclers obtained from Biometra, Germany. The conditions were set as, an initial denaturation at 95°C for 5 min, followed by 40 cycles of denaturation at 95°C for 1 min, annealing at 55-57°C for 1 min, and elongation at 72°C for 1 minute. The final additional elongation step at 72°C for 10 minutes.

Horizontal Gel Electrophoresis

The amplified PCR product were analyzed on 2% agarose gel, which was prepared by melting 2 grams of agarose in 100 ml 1X TBE buffer (0.89 mM Tris-Borate, 0.025 M EDTA pH 8.3) in a microwave oven for one minute. Ethidium bromide (0.5 μg/ml final concentration) was added to stain the gel to visualize the DNA after electrophoresis.

PCR products were mixed with loading dye (0.25% bromophenol blue, 40% sucrose), samples were loaded into the wells. Electrophoresis was performed at 100 volts for half an hour in 1X TBE running buffer. Amplified products were visualized by placing the gel on UV Transilluminator (Biometra TI 2, Germany)

Vertical Gel Electrophoresis

The amplified PCR products were resolved on 8% non-denaturing polyacrylamide gel (13.5 ml of 30% acrylamide solution, 5 ml of 10X TBE, 350 μl of 10% ammonium persulphate and 17.5 μl of TEMED). 30 % acrylamide solution was prepared by dissolving 29 g of acrylamide and 1 g of NN'-Methylenebisacrylamide in respective amount of de-ionized water. Electrophoresis was performed at 100 V. The gel was stained with ethidium bromide solution (10 mg/ml) and visualized on UV transilluminator (Biometra TI 2, Germany), for photography with the help of a Digital Camera DC120 (Kodak, USA).

Genotyping

Analysis of the microsatellie markers was performed by PCR, and the amplified products were resolved on 8% standard non-denaturing gel as described above. Microsatellite markers were visualized by placing the ethidium bromide stained gel on UV transilluminator and genotypes were assigned by visual inspection.

Microsatellite markers mapped by Cooperative Human linkage Center (CHLC) were obtained from Invitrogen (USA). Approximately 94% heterozygous tri and tetra nucleotide repeats sequence polymorphic markers were used in current study. Average heterozygosity for each marker was 78%, implying that these markers were highly informative for allelotyping pedigree members. The cytogenetic location of these markers as well as the length of amplified products was obtained from genome data base homepage (http://genome.ucsc.edu/). Table 2.1 summarizes microsatellite markers used for exclusion mapping of known loci.

Linkage Studies

Linkage to Known Loci

To elucidate the gene defect in the nine families (A-I), presented here, an initial search for linkage was carried out by using polymorphic markers mapped within some of the autosomal recessive non-syndromic deafness loci listed on the hereditary hearing loss homepage (http://dnalab-www.uia.ac.be/be/dnalab/hhh). Table 2.1-2.2 summarizes microsatellite markers located in the region of known deafness and alopecia loci, which were used as first pass analysis for genetic linkage in the families. Selected markers had an average heterozygosity of >70%. Genotyping of these markers was performed as described above.

Mutations in *GJB2* (Connexin 26) gene, at DFNB1 locus on chromosome 13q12, account for up to 50% of non-syndromic recessive deafness in some populations. Genomic DNA of an affected individual of each hearing impaired family was screened for mutation in the *GJB2* of hereditary hearing loss.

Genome-wide Search

Genome-wide search was carried out by a method known as homozygosity mapping (Lander and Botstein, 1987). Homozygosity mapping uses families that are genetically homozygous for recessive diseased genes by virtue of consanguinity. Genome-wide screen was conducted with microsatellite markers spaced approximately at 10 cM intervals. Information about the markers map order was obtained from Rutgers maps (Kong *et al.*, 2005) and deCode genetic maps (Kong *et al.*, 2002). Genotyping and PCR conditions used were as described above.

Lod Score Calculations

Lod scores were calculated using the FASTLINK computer package (Schaffer, 1996) and MLINK was used for two-point lod scores (Cottingham *et al.*, 1993). Multipoint linkage analysis was performed using ALLEGRO (Gudbjartsson *et al.*, 2005). A fully penetrant recessive model with no phenocopies and a disease allele frequency of 0.001 was assumed. Equal allele frequencies were used in the analysis. However, since it is well known that using allele frequencies, which are too low can lead to false positive results, a sensitivity analysis was performed. The marker allele that was segregating with the disease was varied between 0.2 and 0.8 and both two-points and multipoints linkage analysis was carried out. Microsatellite markers positions and map distances were derived from the Marshfield (Broman *et al.*, 1998) (http://www.research.marshfieldclinic.org/) and Decode (Kong *et al.*, 2002) genetic maps. Haplotypes were constructed using SIMWALK2 (Week *et al.*, 1995; Sobel and Lange, 1996). Meiotic recombination frequencies were considered to be equal for males and females and allele frequencies for microsatellite markers were calculated by genotyping 100 unrelated unaffected individuals from the same population.

Mutation Screening

Mutation Analysis of Hearing Impairment and Alopecia Genes

To screen for mutations in genes involved in hereditary hearing impairment *(MGP, TMPRSS3* and *GJB2)* and alopecias *(HR, TNFSF 10, ETV5, LIPH, AP2M1* and *CAM-K2N2),* all exons and splice junctions were PCR amplified from genomic DNA. Primer3 software (Rozen and Skaletsky, 2000) was used to design primers from the intronic sequences of these genes. The primer sequences, their amplified products and the annealing temperatures are described in Tables 2.3-2.10. Amplification was carried out on 100 ng of genomic DNA in a 30 cycle PCR, in which initial 5 min denaturation of template DNA at 95°C was followed by 30 cycles of 95°C for 1 min, 55-60°C for 1 min and 72°C for 1 min in a volume of 50 µl containing 10 mM Tris-HCl, pH 8.3, 50 mM KCl, 0.2 mM of each dNTP, 1.5 mM $MgCl_2$, 0.5 µM of each primer and 1.0 unit of Taq DNA polymerase (MBI Fermentas, UK). PCR products were analyzed on 2% agarose gel and purified in centri-sep spin columns (Marligen Biosciences, USA) to remove the unincorporated primers and nucleotides. The purified PCR products were subjected to cycle sequencing using Big Dye Terminator

V 3.0 ready reaction mix and sequencing buffer (PE Applied Biosystems, Foster city, CA, USA). The sequencing products were purified to remove unincorporated nucleotides and primers with CentriflexTM Gel Filteration Cartridges (Biosystems, Gaithersburg, MD, USA). The purified products were resuspended in 20 µl of HDF (Hi Di Formamide) and were placed in 0.5 ml septa tubes to be directly sequenced in an ABI Prism 310 Genetic Analyzer (Applera, Foster City, CA, USA). Chromatograms from normal and affected individuals were compared with the corresponding control gene sequences from NCBI (National Center for Biotechnology Information) database to identify the aberrant nucleotide base-pair change (http://www.ncbi.nlm.nih.gov/).

Sequence variants were identified via Bioedit sequence alignment editor, version 6.0.7. When a potentially functional sequence variant was found, the exon in which the variant was found was sequenced in all other family members for whom DNA was available. When the identified sequence variant was shown to segregate with the disease status within a family, a minimum 100 unrelated ethnically matched control individuals were also screened for the same exon.

Table 2.1: List of microsatellite markers used to test linkage to known hearing impairment genes

Locus/ Gene/ Cytogenetic Band	Markers	Location (cM)	Locus/ Gene/ Cytogenetic Band	Markers	Location (cM)
DFNB 1	D13S175	0.00	**DFNB 2**	D11S4081	85.51
(GJB2, GJB6)	D13S1316	0.55	***(MYO7A)***	D11S527	86.91
13q11–q12	D13S633	3.10	**11q13.5**	D11S906	88.12
	D13S1236	5.41			
DFNB 3	D17S2196	50.99	**DFNB 4**	D7S2453	115.66
(MYO15)	D17S1794	51.64	***(SLC26A4)***	D7S496	117.99
17p11.2	D17S805	52.6	**7q31**	D7S2459	118.18
	D17S969	53.30			
DFNB 6	D3S3647	72.07	**DFNB 7/11**	D9S1822	68.91
(TMIE)	D3S1767	74.49	***(TMC1)***	D9S1876	69.4
3p14-p21	D3S3640	75.26	**9q13-q21**	D9S927	70.2
DFNB 8/10	D21S1260	55.54	**DFNB 9**	D2S2223	50.79
(TMPRSS3)	D21S212	58.54	***(OTOF)***	D2S2350	50.79
21q22	D21S1411	61.33	**2p23-p22**	D2S174	50.94
DFNB 12	D10S1759	91.3	**DFNB 16**	D15S994	41.37
(CDH23)	D10S1694	92.44	***(STRC)***	D15S537	42.58
10q21-22	D10S1432	93.7	**15q21-q22**	D15S659	43.74
DFNB 18	D11S902	30.69	**DFNB 21**	D11S925	130.7
(USH1C)	D11S4130	32.1	***(TECTA)***	D11S1345	133.83
11p14-15.1	D11S2368	33.91	**11q23–q25**	D11S4464	136.99
DFNB 22	D16S3046	43.87	**DFNB 23**	D10S1762	72.54
(OTOA)	D16S2974	45.70	***(PCDH15)***	D10S1642	73.01
16p12.2	D16S403	46.66	**10p11.2-q21**	D10S1227	74.45
DFNB24	D11S1294	113.13	**DFNB28**	D22S1045	49.77
(RDX)	D11S927	114.27	***(TRIOBP)***	D22S272	51.85
11q23	D11S1391	115.14	**22q13.1**	D22S423	53.62
DFNB 29	D21S211	41.28	**DFNB 30**	D10S1749	48.31
(CLDN14)	D21S167	44.92	***(MYO3A)***	D10S2481	50.83
21q22.1	D21S267	44.92	**10p11.1**	D10S1771	52.98

DFNB 31	D9S1824	122.39	**DFNB35**	D14S61	72.79
(WHRN)	D9S1855	123.56	***(ESRRB)***	D14S53	73.27
9q32–q34	D9S1776	123.79	**14q24.3**	D14S42	74.0
DFNB 36	D1S47	15.25	**DFNB 37**	D6S1659	91.90
(ESPN)	D1S2731	16.17	***(MYO6)***	D6S1031	93.11
1p36.3	D1S1646	17.15	**6q13**	D6S1625	93.11
DFNB49	D5S629	80.77	**DFNB 53**	D6S1666	54.10
(MARVELD2)	D5S589	81.17	***(COL11A2)***	D6S1939	54.92
5q13.1	D5S1999	82.09	**6p21.3**	D6S1701	55.48
DFNB59	D2S2173	197.32	**DFNB 66/67**	D6S1645	57.00
(PJVK)	D2S385	197.50	***(LHFPL5)***	D6S291	57.66
2q31.1-q31.3	D2S2978	199.17	**6p22.3-p21.2**	D6S1051	58.42

Table 2.2: List of microsatellite markers used to test linkage to known genes involved in skin disorders

S. No.	Candidate Genes	Chromosomal Location	Markers	Distance (cM)*
1	Plakophillin1 (*PKP1*)	1q32.1-q44	D1S1660 D1S2716 D1S2738 D1S306 D1S1171 D1S2686 D1S2655	213.11 215.44 215.63 216.6 217.41 218.94 218.81
2	Loricrin (*LOR*)	1q21.3	D1S534 D1S442 D1S498 D1S305	155.97 157.78 160.46 163.48
3	ED3 gene ectodysplasin1anhidrotic receptor (*EDAR*)	2q11-13	D2S1343 D2S2954 D2S1893 D2S1891 D2S2236 D2S321 D2S141	123.96 127.74 128.62 128.62 169.92 172.66 175.22
4	Alopecia with Mental Retardation 1, Autosomal Recessive Hypotrichosis (*APMR1, AH*)	3q26.33-q27.2	D3S3699 D3S2314 D3S3578 D3S3583 D3S3592 D3S1530 D3S1262 D3S1314	200.19 201.92 205.94 205.94 206.82 208.12 210.41 221.44
5	Corneodesmosin (*CDSN*)	6p21.33	D6S1615 D6S273 D6S1666 D6S439	53.70 53.70 54.10 57.00
6	Desmoplakin (*DSP*)	6p24	D6S1640 D6S1547 D6S1674 D6S296 D6S410	20.26 20.85 22.28 22.97 23.33
7	Hairless (*HR*)	8p21.3	D8S258 D8S560 D8S298 D8S1786 D8S1739 D8S1048	37.51 39.68 40.11 41.41 45.23 48.52
8	ED4 gene poliovirus receptor-like 1 (*PVRL1*)	11q23.3	D11S1998 D11S4104 D11S924 D11S4129 D11S4171	126.24 127.01 128.16 128.16 128.16

9	Keratin Type II (*KRT1*)	12q13	D12S87 D12S1301 D12S297 D12S368 D12S398 D12S90	54.21 59.20 67.04 67.04 68.15 73.71
10	ED2 gene gap junction protein b-6 (*GJB6*)	13q12.11	D13S1316 D13S175 D13S633 D13S250 D13S787	0.00 0.55 3.10 3.10 8.75
11	Transglutaminase 1 (*TGM 1*)	14q11.2	D14S50 D14S283 D14S990 D14S972 D14S264	9.33 10.29 10.93 15.00 15.95
12	Nail Dysplasia Isolated Congenital Gene (*NDIC*)	17q13	D17S1866 D17S926 D17S849 D17S1840 D17S1529	0.00 0.63 0.63 1.35 2.81
13	Type-I Hair Keratin & Plakoglobin Genes. (*KRTHA 1*)	17q21.2	D17S1788 D17S1814 D17S1787 D17S934 D17S791 D17S797	64.18 66.44 67.65 69.99 70.65 72.85
14	Envoplakin (*EVPL*)	17q25.1	D17S1807 D17S1301 D17S801 D17S1847 D17S784	111.10 111.65 114.23 122.28 127.80
15	Desmogleins and Desmocollins (*DSG & DSC* Cluster)	18q21	D18S1107 D18S478 D18S847 D18S36 D18S457 D18S536	45.89 50.50 53.29 54.83 55.14 56.29
16	Transglutaminase II/III (*TGM 2& 3*)	20q11.2	D20S195 D20S865 D20S834 D20S478 D20S107 D20S108 D20S119	54.15 55.42 56.41 58.90 60.00 61.97 67.18

*Average-sex distance in cM according to Rutgers combined linkage-physical human genome map (Kong *et al.*, 2004).

Table 2.3: Sequences of primers used in screening *MGP* gene

Exon No.	PRIMER (5′→ 3′)		Product Size (bp)	Annealing Temp (°C)
	Forward	**Reverse**		
1	GGAGCCTCTCTCCCTACTGC	GAAGTAAGCCAAAGTCAGAGGC	183	61
2	CAGCAAGGCCAGAGCTAGAG	TCGCCTGTAGCTTAAATCCC	463	55
3	GAGTTGCATAAGTTAAGGCACTTTC	GCTGTTTCCCACTCCAATTC	263	60
4	GGGGCATGGAGAGAAAGTC	TACAAAATCAGGTGCCAGCC	201	55

bp= base pair

°C= Centigrade

Table 2.4: Sequences of primers used in screening *TMPRSS3* gene

Exon No.	PRIMER (5'→ 3')		Product Size (bp)	Annealing Temp (°C)
	Forward	**Reverse**		
1	TAGAAAGGTCTCTGGTCTCC	GTGGTACACCTACCATAAGC	319	55
2	ACCGTATGACCAAGATGCAC	GACAGTCAGTCACATTGGTC	295	55
3	GTTTCATGGCACTCCAAGTC	TCCAGTAATTAAGGCTGGGC	286	55
4	GGGACAGTTGTTAGTGTTGC	ATCCCAGCTGAAGACATGAC	307	55
5	AGAAGTGGGTCAGATTTGGC	ATCCTCTCTGTGTTTTGCCC	287	55
6	GCACATCGGTTGAATGCTTC	ACAAATCCAGCAGGTGACTC	252	55
7	GAACGGCCTGTTGTGTACAC	AGGACTTAGCATGTGCTTGC	333	56
8	ATGGTGGTGACACCATGTCC	GACATGACCCAGGAGTGAAC	288	57
9	TAACCTCTCCCACCATCTTC	AGCAGCCATCATAAGAATGC	364	57
10	TAACCAAGGGCTTGACCTTC	TGGGAACATCACAATGGGAC	319	55
11	TTTCCGCTGTTGCGACACAC	TTGTCCTGTCACAGGGAAAC	368	55
12	AGAAAGCAATCTCGCATGGC	TATAGCAAGACCAGGGTTGC	297	55
13	TCTTCATCGTGGAGAACAGC	AAGCAGCTTGAAGGTTGTGC	325	55

bp= base pair

°C= Centigrade

Table 2.5: Sequences of primers used in screening *HR* gene

Exon No.	PRIMER (5′→ 3′)		Product Size (bp)	Annealing Temp (°C)
	Forward	Reverse		
2-1$^{\alpha}$	GCCTTACTGGTTTGAGCTGC	TGAGATGGCCACCACTATGC	548	58
2-2$^{\alpha}$	TCCTGAGCACCCCAGACTCC	CTTGGGGTTGACTGTGGGGC	614	61
3-1$^{\beta}$	GAGGGCTTCAGTATTCTCCC	AGTGGGTGGGTAGGATGAAC	494	56
3-2$^{\beta}$	GAATCCTTGCCCGCTCTTCC	CTGAGGAACTCCCAGAGAGC	757	58
4	CATCCTCAGACTCCCTGCTC	TGGCTGTGTCTTCCTCCTGC	474	59
5	CTGCCACTCTCAGCAAGTGC	CCTTAGGTCTAGGAGCTGGC	393	58
6	CTCTCCATGGAAGCTGCTCC	GCCAACGAATGACCACAGGC	360	59
7	GCTGTGTCTCTATGTGACCC	GGTGGTGAGTGTAGACCAAC	393	56
8	AGCTTCCCGTCTGATTGTCC	GGGAATTAGCCTGATCCCAC	370	57
9	GGTAGAAGTCCATGAGCAAC	AAGGTGTTTGGAGGCATGTC	421	55
10	TGCAGGAAAAGCAGTAGAGC	ATGTTGGTGATGCGGTCATC	462	56
11	AGCGAATACACATGGCCTTC	TAAGGGCAGTAGAACAGCTC	529	55
12	TCCCCGAGCTGTTCTACTGC	ACAGGAGGAGACAGAACGGC	430	60
13	AGCGTAAGTGTCCCCAACAC	ACATGAGAGTACCAGGGACC	358	57
14	CCTGGTACTCTCATGTTTGC	TGGAATCAGAGAAGCGCTTC	358	55
15	ACTCCTGACCTCAGGTGATC	TCCAGGCCTGAAAGGAAGTC	357	56
16	TCAGCATCCTGGTGCATGCC	TTGGGTCTGTGCAGCTCACC	400	61
17	CTGCCCTTCAAGACTTGACC	CTCAGTGACTTCAAGGCCTC	465	56
18	GAATCTGCTCTCTGAGAGCC	AGGGTGGGATCTGCTATGTC	347	56
19	CTGGGATTACAGGTGTGAGC	AGATCTTTTGGCAGGAGGGC	677	57

bp= base pair

^{o}C= Centigrade

$^{\alpha}$ exon 2 was amplified by 2 sets of overlapping primers.

$^{\beta}$ exon 3 was amplified by 2 sets of overlapping primers.

Table 2.6: Sequences of primers used in screening *TNFSF10* gene

Exon No.	PRIMER (5'→ 3')		Product Size (bp)	Annealing Temp (°C)
	Forward	Reverse		
1	CAGGTTCAATAGATGTGGG	GAAGCAGGAAAGTCTTCAG	391	55
2	AAGGACAAAGGAGAGCATGC	GGAATTCTTCTGGCCTTCTC	357	58
3	AGACATCAGCAAGATGAGC	TGAGTGGATGAGAACACAG	229	58
4	TGACAACACCTATGAAGAGC	TCGTGGCAATAATTGAGCTG	372	55
5	AATATAGGCTGGCCACAGCTG	GTGGCTGCTCTACTCAGATTG	668	55

bp= base pair

°C= Centigrade

Table 2.7: Sequences of primers used in screening *ETV5* gene

Exon No.	PRIMER (5′→ 3′)		Product Size (bp)	Annealing Temp (°C)
	Forward	Reverse		
1	CTGGCCAATGGGAACAAGGC	TCAGCCCGTGAACTCTAGCC	351	59
2	CATCCTGTACCTCTGATACC	CCAACAGAAAGTGAAGGCTC	408	55
3	ACGCTGAAAGCACCATGGAC	CCTTCAGCTAACCAAGCCTC	436	57
4	ACAGATCTGGCTCACGATTC	TGCCATCACCAGAAAGGTAC	370	55
5	CTCAGTCAACTTCAAGAGGC	GGATTATAGGTGTGAGCCAC	471	55
6	GGGAGGTTGTGTGTTTAAGC	GTCTGCTGGGTAAGTAACTC	390	55
7	ATTTCCTGGCAACAATGGGC	CATCAACCATCTGGAGTACC	597	55
8	GCCACATTTAGCCTTGTACC	GGCACATGTCTGAACATGTC	592	55
9	CTTCCTGACTCAAGAGCTTC	ATGTCAGCTCTACTAGCTCC	612	55
10	TTGCTTATTGGTGTGGCACC	TCTTAGCCTGGAAACTGAGC	374	55
11	CAGCAGTAGGACTTAGGATC	GTTTGGGACAAGGACACATC	363	55
12	AGGTTTGGAGGTGTCAGAAC	GAAGCAAGAGCAGACTTGAC	419	55
13	AGTCAGGTTACAGAACTGGC	ATTTCCTCGTAGCGACGATC	296	55
14	ATAGGTTCCCAGGAGTTCTC	GTCTTTAAGGGTGCCAATCC	536	55

bp= base pair

°C= Centigrade

Table 2.8: Sequences of primers used in screening *LIPH* gene

Exon No.	PRIMER (5′→ 3′)		Product Size (bp)	Annealing Temp (°C)
	Forward	Reverse		
1	AAAGATCCTGAAAGGGTTGG	CTATGGACTTAAGTTCACCG	333	52
2	ATAGAACAGCACTCTTGCTTG	GCTCACTGTAGCTATCTCTTG	529	54
3	CTCCAAAGTCAACAGCCAGG	CCACACTCAGAGAGGTTAGG	323	56
4	TCATCCAGAAGGATCAAAGG	TAGAGGAACCTGATCTGCTC	277	53
5	TTCCTGCTTATACCTGGCAGG	TCGTCTCAAACTCCTGACCTC	310	57
6	AATACACTGAAAGAGCGCAG	GTGGCTCATGCCTGTAATCC	433	57
7	CTCTCAGAAGTGGTGGATAC	TCCAGCTCCAAAGTTGATGC	327	55
8	CTTTGCAGAGAAACCAGAGAG	GCAACTAAGCAATAGTTCCCC	389	54
9	TACCAGTGACTTGCAGGCTTC	CCCATCATGTCCCTCATTGTG	377	57
10	TGGGATTACAGGCATGAGTC	ATGTGACATCCATAGGACGC	394	55

bp= base pair

°C= Centigrade

Table 2.9: Sequences of primers used in screening *AP2M1* gene

Exon No.	PRIMER (5′→ 3′)		Product Size (bp)	Annealing Temp (°C)
	Forward	Reverse		
1	ATTGCAAGCAAGGAGGCCGC	AGTGCAGGGCAGGACAAAGC	285	59
2	AAGAAGCTCCAGTGACCTGC	ACCATGCCATTCCACAGGTC	426	57
3	TTGGAGTGTGTGTGTCAGAC	AGTTCAGAGTGTACCAGAGC	494	55
4	TGCCGGTCAGATGTGTAGGC	GAGGGCTCATGAGTCAGCTC	261	59
5-1$^{\alpha}$	TAGGATCCAAGCCTCATAGC	AATGTCAAGAGCGAACAGCC	817	55
5-2$^{\alpha}$	GCTCCCCATTTATCTGTTCC	AATGTCAAGAGCGAACAGCC	---	55
6-1$^{\beta}$	TCATAGTCTCTGGTGCCAGC	GCAGGCGTGTACATACTCAC	823	57
6-2$^{\beta}$	CACTGCTGGCTCAGAAGATC	GCAGGCGTGTACATACTCAC	---	57
7	GTTAGCAGGGTCCTGACCAC	CCTCACCTCTAAGGTGCAGC	343	59
8-1ω	CCTCTTAGAAGGTCCCACGC	GGATAAGGGCTTGGATGGCC	910	59
8-2ω	GAGTTCTGAGGCTCCTGCTC	GGATAAGGGCTTGGATGGCC	---	59

bp= base pair

°C= Centigrade

$^{\alpha}$ exon 5 was amplified by 2 sets of overlapping primers

$^{\beta}$ exon 6 was amplified by 2 sets of overlapping primers

ω exon 8 was amplified by 2 sets of overlapping primers

Table 2.10: Sequences of primers used in screening *CAM-K2N2* gene

Exon No.	PRIMER (5′→ 3′)		Product Size (bp)	Annealing Temp (°C)
	Forward	**Reverse**		
1	TCGGGCGCTCATCGTCATTC	TTCCAGAGGTGGCGAGCATC	625	59
2	ACGCGGGGCTCATTCTCATC	AGAAAGAGGCTGAGGCTGGG	652	59
3	GGCTGCGTACTTGCATGAGC	ACTTGGCAACCGTCCCTCAC	641	59

bp= base pair

°C= Centigrade

HEARING IMPAIRMENT

Hearing impairment is the most common sensory disorder and it is clinically and genetically heterogeneous. It is estimated that 1–2 per 2,000 newborns are affected with profound hearing impairment (HI) (Parving, 1983; Morton, 2002). For congenital hearing impairment, roughly half of the cases are expected to be genetic. Of the genetic cases of HI, 30% are known to be syndromic, with the remaining cases displaying non-syndromic hearing impairment (NSHI). For non-syndromic hearing impairment, 75–80% of the cases are due to autosomal recessive (AR) inheritance, 15–20% display autosomal dominant inheritance, 2–3% of cases show X-linked inheritance, and less than 1% of cases are due to mitochondrial inheritance (Keat and Berlin, 1999; Bitner-Glindzicz *et al.*, 2000; Morton, 2002). This extreme heterogeneity reflects involvement of different molecular mechanisms within the auditory system that malfunction to cause hearing impairment.

The extreme genetic heterogeneity for hearing impairment (HI) testifies to the inherent complexity of the mammalian inner ear. As more hearing impaired genes are identified, the elucidation of the function of the proteins that these genes encode contributes greatly to the understanding of cochlear mechanisms and their role in disease causation. Currently, 27 genes have been identified for autosomal recessive non-syndromic hearing impairment (ARNSHI) (Van Camp and Smith, 2008) (URL:http://webhol.ua.ac.be/hhh/); however, for more than 60% of the mapped NSHI loci a gene has yet to be identified. The identification of linkage of multiple NSHI families to a single locus validates the linkage finding and can make gene identification more attainable due to a smaller physical interval for the NSHI locus.

The first successful linkage study of an autosomal recessive form of non-syndromic deafness was reported in 1994, and the first recessive deafness genes (*GJB2* and *MYO7A*) were identified in 1997. Several of the genes are involved in both recessive and dominant non-syndromic deafness (*GJB2, GJB3, GJB6, MYO6, MYO7A, TMC1, TECTA, COL11A2*) or in both non-syndromic and syndromic deafness (*GJB2, GJB3, GJB6, MYO7A, SLC26A4, CDH23, USH1C, PCDH15, COL11A2, MYO6*). Nearly all genes both for recessive and dominant non-syndromic forms cause sensorineural hearing loss. Only a few of the genes including *OTOA, PCDH15, GJB3, GJA1, and SLC26A5* have been found to be associated with recessive deafness by a functional

candidate gene approach.

Advances in genomics have facilitated rapid progress in identifying genes for hearing impairment, and consequently increased insight into the normal development and function of cells in the auditory system.

Description of the Families Studied

Family A

Family A resides in Jalal Pur district of the Punjab province, Pakistan. Traditionally, owing to strict social customs, the family members rarely marry outside their community. Pedigree of this consanguineous family is shown in figure 3.1. Five individuals including one male and four females are affected by prelingual non-syndromic hearing impairment. The affected persons are present in generations V and VI of the pedigree. In generation V two female (V-6 and V-7), in generation VI two females (VI-2 and VI-4) and one male (VI-6) are affected. Analysis of the pedigree is strongly suggestive of an autosomal recessive mode of inheritance. All affected individuals have a history of prelingual profound hearing impairment (HI) involving all frequencies and use sign language for communication. The transmission of hearing impairment within the family is consistent with autosomal recessive inheritance. Regardless of age, affected family members display the same level of profound HI (Figure 3.2), implying that the hearing loss is not progressive.

Medical and physical examinations of the affected individuals were performed by trained otolaryngologists affiliated with government hospitals. The hearing-impaired individuals underwent careful examination for balance problems, mental retardation, defects in ear morphology, dysmorphic facial features, eye disorders including night blindness and tunnel vision and were not found to have any syndromic features or vestibular disorders.

After informed consent was obtained, blood samples were collected from five affected (V-6, V-7, VI-2, VI-4 and VI-6) and nine normal individuals (IV-7, IV-8, V-1, V-2, V-3, V-4, V-5, VI-1 and VI-3) and processed for genomic DNA extraction.

Family B

The family B is settled in Larkana district of Sindh province, Pakistan. The family members are engaged in subsistence farming and local market business. They

traditionally marry within the family due to strict social customs. The pedigree comprising of four generations (Figure 3.3) and five affected individuals, including one male (IV-6) and four females (IV-2, IV-3, IV-4, and IV-5). All the affected individuals have a history of prelingual hearing impairment and regardless of the age all of them display the same level of hearing loss. The physical examination of the affected individuals for defects in ear morphology, mental retardation and other clinical features indicated that no abnormality was associated with hearing impairment, thus excluding syndromic form of hearing loss. Analysis of the pedigree suggests an autosomal recessive mode of inheritance.

After informed consent was obtained, blood samples collected from 10 family members, including five affected (IV-2, IV-3, IV-4, IV-5, and IV-6) and five normal (III-1, III-2, III-3, IV-1 and IV-7) individuals, were processed for DNA extraction.

Family C

Family C lives in a village near Chishtian of the Punjab province, Pakistan. The family members are engaged in subsistence farming and local market business. Traditionally, they prefer to marry within the family and consequently consanguineous marriages are common. Pedigree of this consanguineous family is shown in Figure 3.4. Eleven individuals including five males and six females are affected by prelingual non-syndromic hearing impairment. The affected persons are present in generations V and VI of the pedigree (Figure 3.4). In generation V four females (V-1, V-5, V-6 and V-13) and four males (V-2, V-3, V-12 and V-14), in generation VI two females (VI-1 and VI-2) and one male (VI-3) are affected. Analysis of the pedigree is strongly suggestive of an autosomal recessive mode of inheritance. All the affected individuals use sign language for communication.

Physical examinations were performed to exclude the stigmata of syndromic hearing impairment. External ear abnormalities were not observed in any of the affected individuals. The age of the affected individual vary from 5 to 50 years.

After informed consent was obtained, blood samples collected from nineteen family members, including eleven affected (V-1, V-2, V-3, V-5, V-6, V-12, V-13, V-14, VI-1, VI-2 and VI-3) and eight normal (IV-1, IV-4, IV-11, V-4, V-10, V-11, VI-4 and VI-5) individuals, were processed for DNA extraction.

Family D

Family D lives in a remote village Jahaniyan of the Punjab province, Pakistan. The family members are engaged in subsistence farming and unskilled labor. They follow the local tradition of marrying within the family, resulting in a high rate of consanguineous marriages. Five generation pedigree (Figure 3.5) comprised of three affected male individuals (IV-1, V-1 and V-2). One Affected individual (IV-1) was not present at the time of study. Analysis of the pedigree strongly suggests an autosomal recessive mode of inheritance, and consanguineous loops accounted for all the affected persons being homozygous for a mutant allele.

After informed consent was obtained, blood samples collected from four family members, including two affected (V-1 and V-2) and two normals (III-3 and IV-2), were processed for DNA extraction.

Family E

The family E resides in Rahim Yar Khan district of the Punjab province, Pakistan. These people are engaged in farming and trade; they rarely marry out side the family and consequently consanguineous unions are very common. The affected persons are present in generation IV of the pedigree (Figure 3.6). In this generation four females (IV-3, IV-4, IV-6, and IV-7) and three males (IV-1, IV-2, and IV-5) are affected. Analysis of the pedigree is strongly suggestive of an autosomal recessive mode of inheritance. All the affected individuals use sign language for communication.

After informed consent was obtained, blood samples collected from ten family members including seven affected (IV-1, IV-2, IV-3, IV-4, IV-5, IV-6, and IV-7) and three normals (III-1, III-2, and III-3), were processed for DNA extraction.

Molecular Genetic Studies

Linkage Studies

The order of the markers, used in the present study, was based on National Center for Biotechnology Information (NCBI) Build 36 sequence-based physical map (International Human Genome Sequence Consortium, 2001). The Rutgers combined linkage-physical map of the human genome (Kong *et al.*, 2004) was used for genetic map distances in linkage analysis for the markers. PEDCHECK (O'Connell and Weeks, 1998) was used to identify Mendelian inconsistencies while the MERLIN

(Abecasis *et al.*, 2002) program was used to detect potential genotyping errors that did not produce a Mendelian inconsistency. Haplotypes were constructed using SIMWALK2 (Weeks *et al.*, 1995; Sobel and Lange, 1996). Two-point linkage analysis was carried out using MLINK program of the FASTLINK computer package (Cottingham *et al.*, 1993). Multipoint linkage analysis was performed using ALLEGRO version 2 (Gudbjartsson *et al.*, 2002). An autosomal recessive mode of inheritance with complete penetrance and a disease allele frequency of 0.001 were used.

On the basis of genetic linkage studies in hereditary hearing impairment, it is clear that at least some candidate gene intervals should be tested for either linkage or exclusion mapping before embarking on genome wide search. In the present study, families A-E with hereditary hearing impairment were tested first for linkage to several known loci by genotyping microsatellite markers mapped within the candidate linkage intervals (Table 2.1).

As prevalence of *GJB2* gene mutations in non-syndromic and syndromic hearing impairment has been well documented in different world population, therefore, DFNB1 locus was tested for linkage to *GJB2* gene in preference. Purified DNA samples from affected and normal individuals of all the five families, presented here, were tested first for linkage to DFNB1 locus by using four microsatellite markers (D13S1275, D13S787, D13S292, D13S1294). However, results obtained (not shown) excluded all the families from linkage to DFNB1 locus. Sequence analysis of the coding exon of *GJB2* further supported the exclusion of *GJB2* as a causative gene for deafness in families A-E.

In order to test linkage to several other known loci in the families (A-E), three or more microsatellite markers tightly linked to these loci were genotyped. Table 2.1 summarizes microsatellite markers in the region of known deafness loci, which were used as first pass analysis for genetic linkage in these families. Linkage to the known loci was conclusively excluded in two families (A and B) indicated the involvement of novel loci responsible for hearing loss in these families. Therefore, these families were subjected to genome-wide search to map the disease causing loci.

In the consanguineous Pakistani family A, an initial genome-wide scan was performed by using 396 highly polymorphic fluorescently labeled markers and DNA

from five of the affected individuals (V-6, V-7, VI-2, VI-4, and VI-6). Evidence suggestive of genetic linkage was obtained initially with two markers AAC040 at 32.19 cM and D12S320 at 32.19 cM (Figure 3.7) on chromosome 12p13.31. For fine mapping of the region, 22 additional markers (D12S336, D12S1697, D12S89, D12S358, D12S1581, D12S364, D12S62, D12S1715, D12S1669, D12S1682, D12S1688, D12S1057, D12S1034, D12S1042, D12S1584, D12S291, D12S1301, D12S85, D12S1701, D12S1661, D12S347, D12S297) were selected from Rutgers combined linkage-physical map of the human genome (Kong *et al.,* 2004). Sixteen of these 22 fine mapping markers (D12S336, D12S1697, D12S89, D12S358, D12S364, D12S62, D12S1669, D12S1682, D12S1057, D12S1584, D12S291, D12S1301, D12S85, D12S347, D12S1042, D12S297) (Figures 3.8-3.21) were informative for linkage and six markers (D12S1581, D12S1715, D12S1688, D12S1034, D12S1701, D12S1661) were non-informative, although the markers had an average heterozygosity of more than 0.70. After genotyping these markers, the data was analyzed using two-point and multipoint linkage analysis. The maximum two-point LOD score of 4.0 (θ=0.0) was obtained at marker AAC040 (Table 3.1). A maximum multipoint LOD score of 5.3 was achieved at D12S320. The three-unit support interval extended from marker D12S89 to marker D12S1042, spanning a 24.3 cM region according to the Rutgers combined linkage-physical map of the human genome (Kong *et al.,* 2004). This interval includes 15.7 Mb on the sequence-based physical map (International Human Genome Sequence Consortium, 2001). Using SIMWALK2, haplotypes were constructed to determine the critical recombination events (Figure 3.22). The disease haplotype (region of homozygosity) is flanked by markers D12S358 and D12S1042 and is smaller than the three-unit support interval. It is 22.4 cM long and contains 15.0 Mb. The critical recombination defining the co-segregating interval occurred in the affected individuals. The telomeric boundary of this interval was defined by a recombination between markers D12S358 and AAC040 observed in individual V-6. The affected individuals in both branches of the family were homozygous at genome scan marker D12S1042 but for different alleles in each family branch. Therefore the centromeric boundary of the region of homozygosity was assigned between markers D12S1057 and D12S1042. This novel non-syndromic hearing impairment locus has been assigned number DFNB62 on chromosome 12p13.2-p11.23.

At present the DFNB62 linkage interval contains 75 known genes, 15 of which encode hypothetical proteins. The family A was screened for *MGP* and *EMP1* genes, which were sequenced directly in an ABI Prism 310 automated DNA sequencer and no functional variants were discovered in unaffected and affected individuals.

In family B (Figure 3.3), an initial genome-wide screen with microsatellite markers was conducted on the DNA of five affected individuals (IV-2, IV-3, IV-4, IV-5 and IV-6). In the course of screening 390 markers, the affected individuals showed homozygosity with a marker D13S1306 on chromosome 13q22.3. This region was saturated with 10 additional markers (D13S1231, D13S279, D13S800, D13S269, D13S792, D13S317, D13S1235, D13S628, D13S1283, D13S265) located in the vicinity of D13S1306 and selected from Rutgers combined linkage-physical map of the human genome (Kong *et al.,* 2004). However, two-point and multipoint analysis failed to generate significant LOD score with any of these markers. Therefore, no further work was performed on this family in this present study.

Family C (Figure 3.4), showed linkage with seven markers D2S1400, D2S2952, D2S149, D2S1360, D2S220, D2S158 and D2S1356 (Figures 3.23-3.29) linked to DFNB9 locus on chromosome 2p23.3. Two point linkage analysis generated a maximum LOD score of 6.4 at marker D2S1360 (Table 3.2). Otoferlin (*OTOF*), the causative gene for DFNB9 locus, consists of 48 exons spanning approximately ~90 Kb of genomic DNA (Mirghomizadeh *et al.,* 2002). Due to large size of the gene and limited sequenceing facility available, this gene has not been sequenced in the present study.

In family D (Figure 3.5), both the affected individuals (V-1 and V-2) were homozygous at markers D21S212 at 58.54 cM (Figure 3.31), D21S1411 at 61.33 cM (Figure 3.32) and D21S1446 at 69.08 cM (Figure 3.33), linked to DFNB8/10 locus harboring *TMPRSS3* gene on chromosome 21q22.3. All the 13 exons and splice junction sites of *TMPRSS3* gene were PCR amplified using the primer sets shown in Table 2.4. PCR products were sequenced directly in an ABI Prism 310 automated DNA sequencer, however no disease causing mutation was detected in family D.

In family E (Figure 3.6), all the affected members (IV-1, IV-2, IV-3, IV-4, IV-5, IV-6, and IV-7) were homozygous at markers D21S212 (Figure 3.34), D21S1411 (Figure 3.35) and D21S1446 (Figure 3.36) while normal individuals were heterozygous, thus

linking family E to DFNB8/10 locus harboring *TMPRSS3* gene on chromosome 21q22.3. All the 13 exons and splice junction sites of *TMPRSS3* gene were PCR amplified using the primer sets shown in Table 2.4. PCR products were sequenced directly in an ABI Prism 310 automated sequencer, however, this failed to detect any functional sequence variant.

DISCUSSION

In the present study, five consanguineous Pakistani families (A-E), demonstrating autosomal recessive form of non-syndromic hearing impairment, have been ascertained from remote regions of Pakistan. The affected individuals in these families had prelingual severe to profound haring loss with no associated features of syndromic and acquired forms of deafness. The affected individuals from various age groups showed the same level of severe hearing impairment implying that deafness was not progressive in any of the families studied. To identify the gene defect in these families, linkage studies were performed by a method known as "Homozygosity Mapping". The homozygosity mapping revolves around the underlying principle that fraction of genome of consanguineous matings would be expected to be homozygous in the offspring because of an expected identity by descent (Sheffield *et al.*, 1995). It can be predicted that approximately $1/16^{th}$ of the genome of offspring of first cousin matings would be predicted to be homozygous. The region of homozygosity should be random between different offsprings of such matings, except at common disease locus shared by the affected offspring (Sheffield *et al.*, 1995). The minimum detectable length of a homozygous segment depends on marker density of screening set and their heterozygosity. For markers with 70% heterozygosity, a homozygous segment as short as 9 cM may be detected when the markers are 1 cM apart. This may suggest that with the density of a genome scan of 20 cM, only very large homozygous segments can be detected (Broman and Weber, 1999).

Miano *et al.* (2000) have indicated potential problems encountered during linkage studies performed by homozygosity mapping, which include: (i) unexpected allelic heterogeneity, causing region containing the disease locus to be missed; (ii) identification of homozygosity identical by descent (IDB) region unrelated to the disease locus; and (iii) the potential for inflation of LOD scores, as a result of underestimation of the extent of inbreeding.

In the present study prior to embarking on a genome-wide scan, co-segregation and homozygosity analysis were performed with microsatellite markers corresponding to candidate genes involved in related autosomal recessive non-syndromic deafness phenotypes. Two to three markers per locus were used to genotype both affected and normal individuals in each family. In two families, A and B, linkage to known loci was conclusively excluded, thus indicating the involvement of novel loci responsible

for deafness in these families. In family C linkage was established to DFNB9 locus on chromosome 2p23.3. In two families D and E, linkage was detected on chromosome 21q22.3 at DFNB8/10 locus.

In family A, screening of the human genome led to the identification of a new autosomal recessive non-syndromic hearing loss locus, DFNB62, on chromosome 12p13.2-p11.23. Significant evidence of linkage to this chromosomal region was found with two-point LOD score of 4.0 and multipoint LOD score of 5.3. Haplotypes analysis located the DFNB62 locus in 22.4 cM (15.0 Mb) region flanked by markers D12S358 and D12S1042. DFNB62 represents the second ARNSHI locus to map to chromosome 12p13.2.

Previously, three deafness loci including DFNA25 (Greene *et al.*, 2001), DFNA41 (Blanton *et al.*, 2002) and DFNA48 (D'Adamo *et al.*, 2003) were mapped on the same chromosome 12. It has been observed that different mutations in the same gene can cause both autosomal dominant and recessive non-syndromic hearing impairment (e.g. *GJB2, MYO7A, TECTA and TMC1*) (Van Camp and Smith, 2005). Mutations of *MYO7A* can cause both non-syndromic hearing impairment (DFNB2 and DFNA11) and syndromic deafness (USH1B) (Weil *et al.*, 1995, 1997; Liu *et al.*, 1997).

At present the DFNB62 linkage interval contains 75 known genes, 15 of which encode hypothetical proteins (UCSC Genome Browser, http://genome.ucsc.edu/). Among the known genes is a gene for Keutel syndrome, which is caused by mutations in matrix Gla protein (*MGP*) (Hur *et al.*, 2005). Patients with Keutel syndrome are found mostly in consanguineous families and have the following as cardinal features: midface hypoplasia, flat nasal bridge, cartilage calcification, and brachytelephalangism or 'drumstick' fingers (Hur *et al.*, 2005). Additional clinical signs include heart defects (e.g., pulmonary artery stenosis), developmental delay, and respiratory abnormalities. About 70% of cases report HI with or without otitis media. This Family A was screened for the *MGP* gene through direct sequencing and no functional variants were discovered. *EMP1* and other candidate genes have not been associated with inner ear disorders, but it is highly expressed in the developing murine nervous system including the peripheral (cranial) nerves (Wulf and Suter, 1999). The *EMP1* gene was negative for functional variants in one unaffected and two affected individuals from family A.

In family B, the linkage data obtained from genome scan and further saturation with additional markers failed to define a region harboring a causative gene for deafness. However, it has been planned that for future studies clinical status of all the normal and affected individuals of the family B will be checked again and genome scan will be performed with microsatellite markers spaced at 5 cM intervals.

The family C showed linkage to DFNB9 locus on chromosome 2p23.3. Otoferlin (*OTOF*), the causative gene for this locus, consists of 48 exons spanning approximately ~90 kb of genomic DNA (Mirghomizadeh *et al.*, 2002). The otoferlin gene is expressed in the inner hair cells, the utriculus, and the sacculus. It is probably involved in the transport of membrane vesicles to the plasma membrane. Several mutations in the *OTOF* gene have been reported in various families (Yasunaga *et al.*, 1999, 2000; Adato *et al.*, 2000; Migliosi *et al.*, 2002). Due to large size of the gene, this has not been sequenced in the present study.

In two families D and E, linkage was detected at locus DFNB8/10 located on chromosome 21q22.3. These two families were screened for the *TMPRSS3* gene, located at DFNB9/10 locus, through direct sequencing and no functional variants were discovered. However, the presence of the mutations in the regulatory sequences of the gene cannot be ruled out.

This *TMPRSS3* gene contains 13 exons spanning 24 kb (Scott *et al.*, 2001). *TMPRSS3* encodes a serine protease with two LDLRA and SRCR domains and is the cause of deafness in DFNB8/10 families (Ben-Yosef *et al.*, 2001; Masmoudi *et al.*, 2001; Scott *et al.*, 2001; Wattenhofer *et al.*, 2002). All the domains have been shown to be important for the ability of *TMPRSS3* to activate ENaC and for its catalytic activity (Guipponi *et al.*, 2002; Lee *et al.*, 2003). ENaC is a sodium channel known to be regulated by serine protease activity (Vallet *et al.*, 1997). It is expressed in the inner ear, where it has been proposed to be involved in maintaining a low Na^+ concentration in the endolymph (Couloigner *et al.*, 2001). Previously, *TMPRSS3* mutations have been reported very low in the studied deaf populations, i.e. 2.5% (4/159) in Pakistani, 0.4% (2/448) in European Mediterranean, and even 0% (0/64) in North American populations (Wattenhofer *et al.*, 2005).

The study presented here, includes mapping of a novel locus, DFNB62, for non-syndromic autosomal recessive deafness on human chromosomes 12p13.2-p11.23,

thus demonstrating the extensive genetic heterogeneity of this condition. Since in the affected individuals of family A, abnormalities other than deafness were not observed, one might predict that defect in genes responsible for deafness in this family affect protein that have fundamental role in hearing.

The recent identification of several genes for hearing impairment provides an important step towards understanding the molecular mechanism of hearing. The genes identified encode proteins that have a role in hair cell transduction, ionic homeostasis in cochlear duct and integrity of the tectorial membrane. Many of the genes, known to be responsible for human hereditary deafness, have been identified in the past few years making this a very exciting and fast moving field. The function of some of these genes is still a mystery, but valuable clues to the function of others have come from establishing the type of protein that they encode and their expression patterns. Understanding the function of these genes has not only provided us with insight into the molecular basis of deafness, but also of normal auditory function. Consequently, we now have a better understanding of the genetic control of inner ear development, melanocytes development, hair cell maintenance and survival, and potassium movement during auditory transduction. In coming years, further deafness genes are sure to be identified, and mouse models for the human disease will be constructed as a starting point in the understanding the pathological processes involved in deafness. The rate of discovery of deafness genes by positional cloning in human will be accelerated by the freely available human genome sequence and by a catalogue of ESTs (expressed sequence tags) within genetic intervals known to contain locus for human hereditary hearing loss.

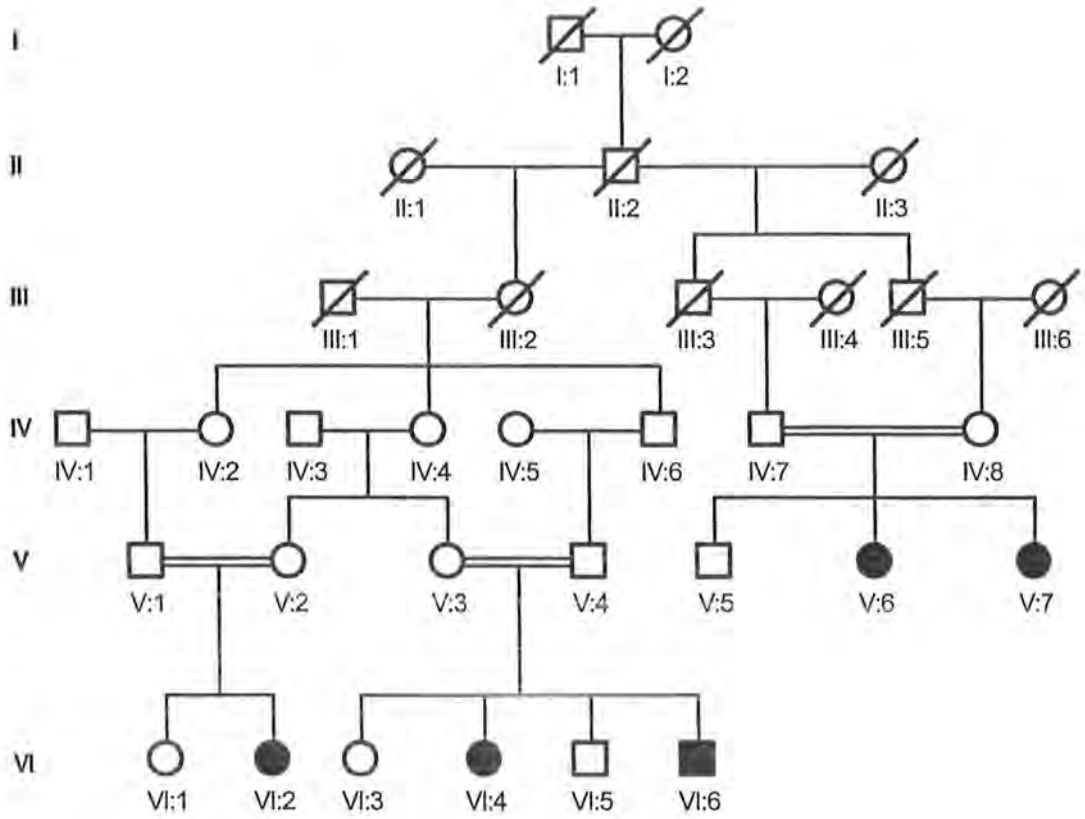

Figure 3.1: Pedigree of family A with autosomal recessive non-syndromic hereditary hearing impairment. Circles represent females, squares represent males. Filled circles and squares represent affected individuals. Double lines indicate consanguineous marriages. Cross lines on the symbols represent deceased individuals.

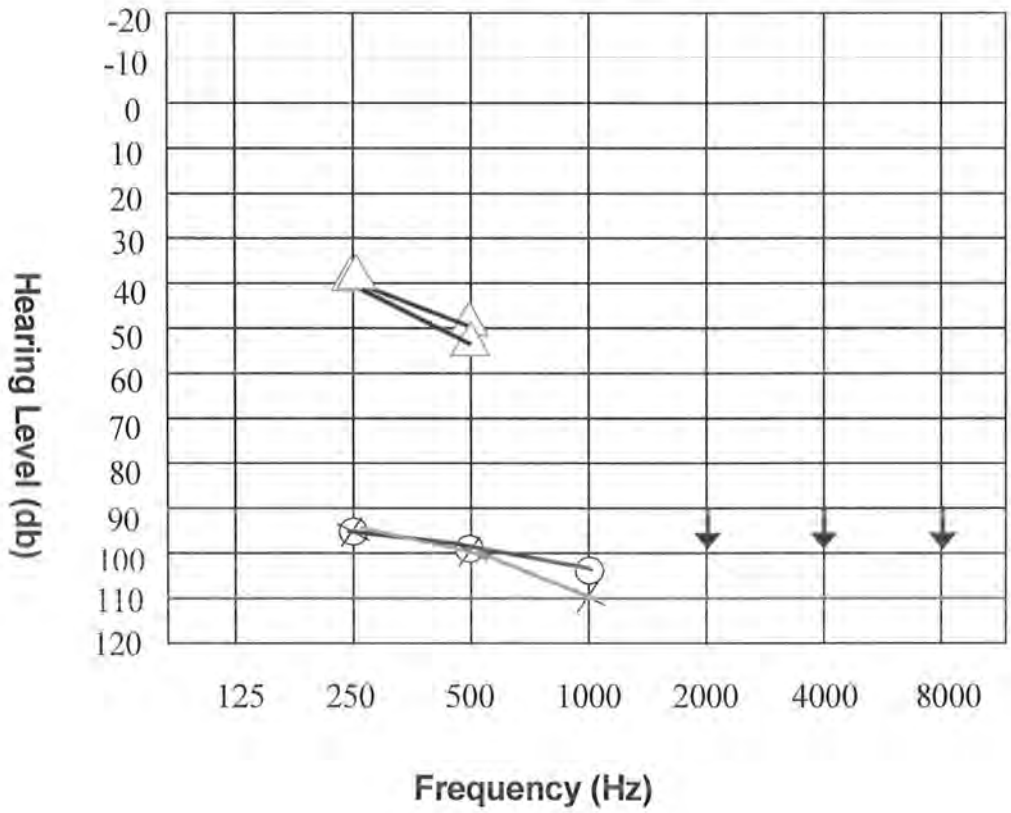

Figure 3.2: Audiogram of an affected individual (VI-6) of family A demonstrating profound hearing impairment that involves all frequencies in both ears. Circles and crosses represent air conduction for right and left ear, respectively. Arrows indicate residual hearing at 2–8 kHz.

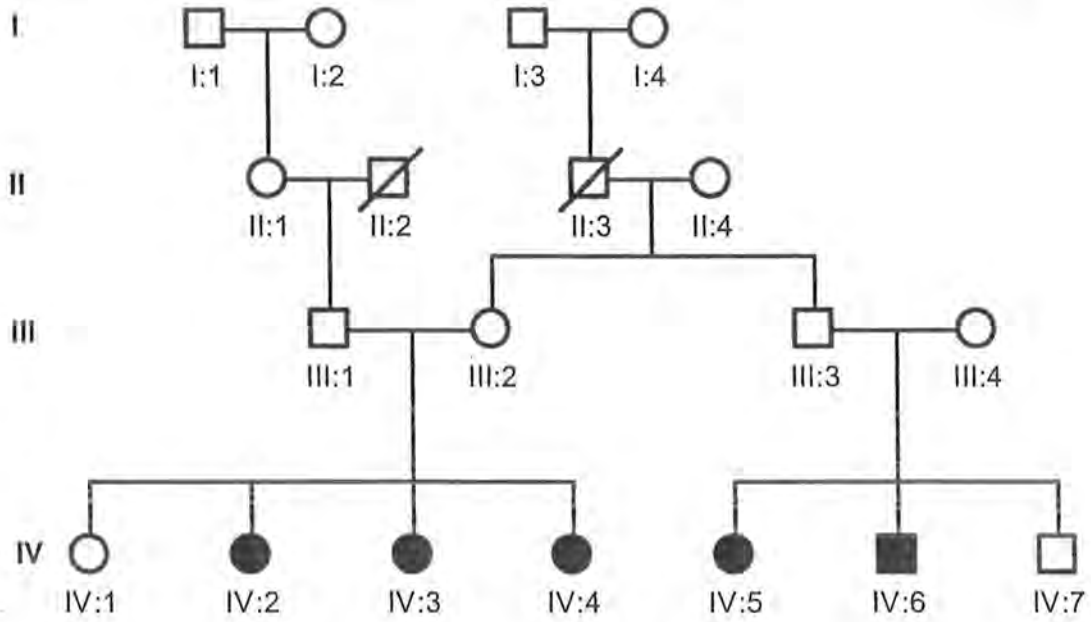

Figure 3.3: Pedigree of family B with autosomal recessive non-syndromic hereditary hearing impairment. Circles represent females, squares represent males. Filled circles and squares represent affected individuals. Double lines indicate consanguineous marriages. Cross lines on the symbols represent deceased individuals.

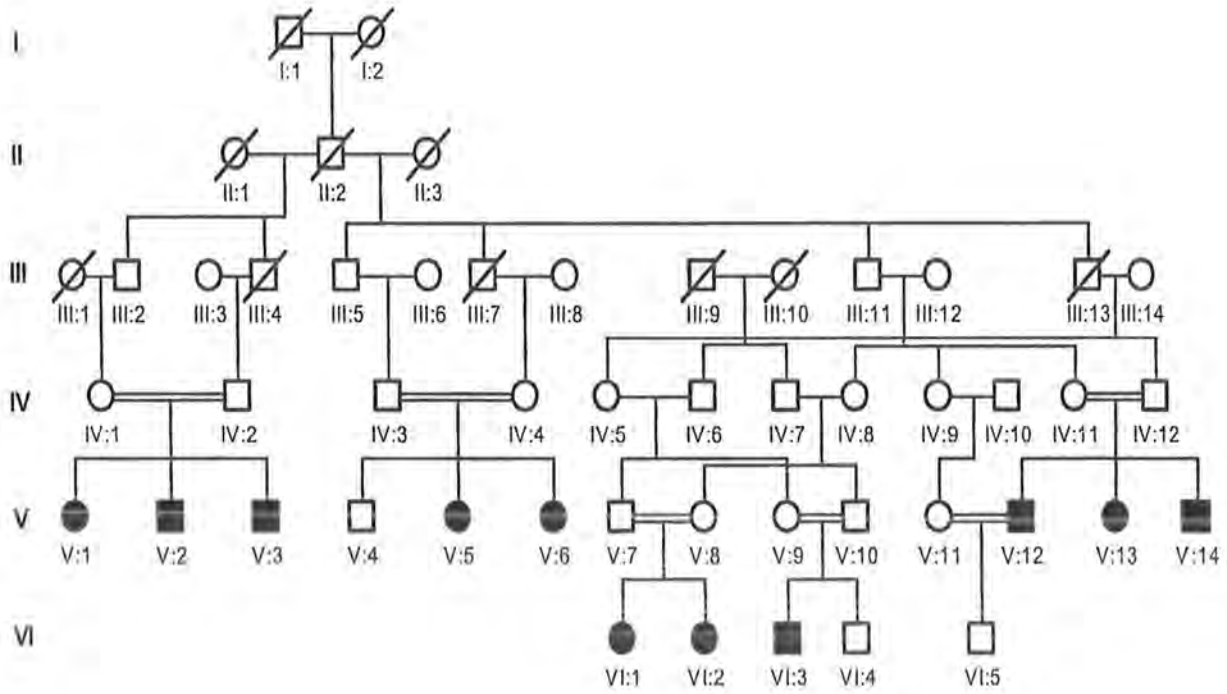

Figure 3.4: Pedigree of family C with autosomal recessive non-syndromic hereditary hearing impairment. Circles represent females, squares represent males. Filled circles and squares represent affected individuals. Double lines indicate consanguineous marriages. Cross lines on the symbols represent deceased individuals.

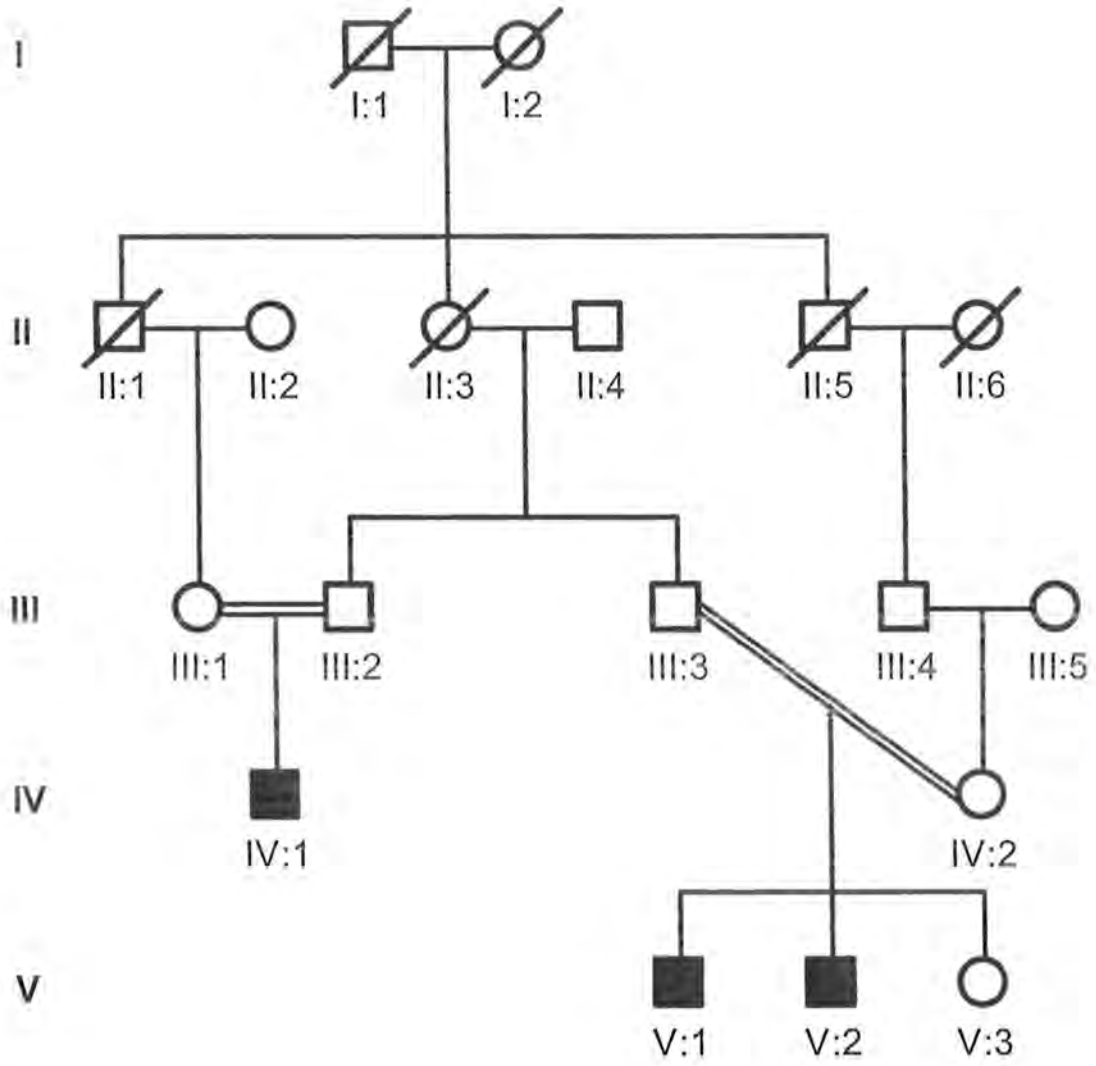

Figure 3.5: Pedigree of family D with autosomal recessive non-syndromic hereditary hearing impairment. Circles represent females, squares represent males. Filled circles and squares represent affected individuals. Double lines indicate consanguineous marriages. Cross lines on the symbols represent deceased individuals.

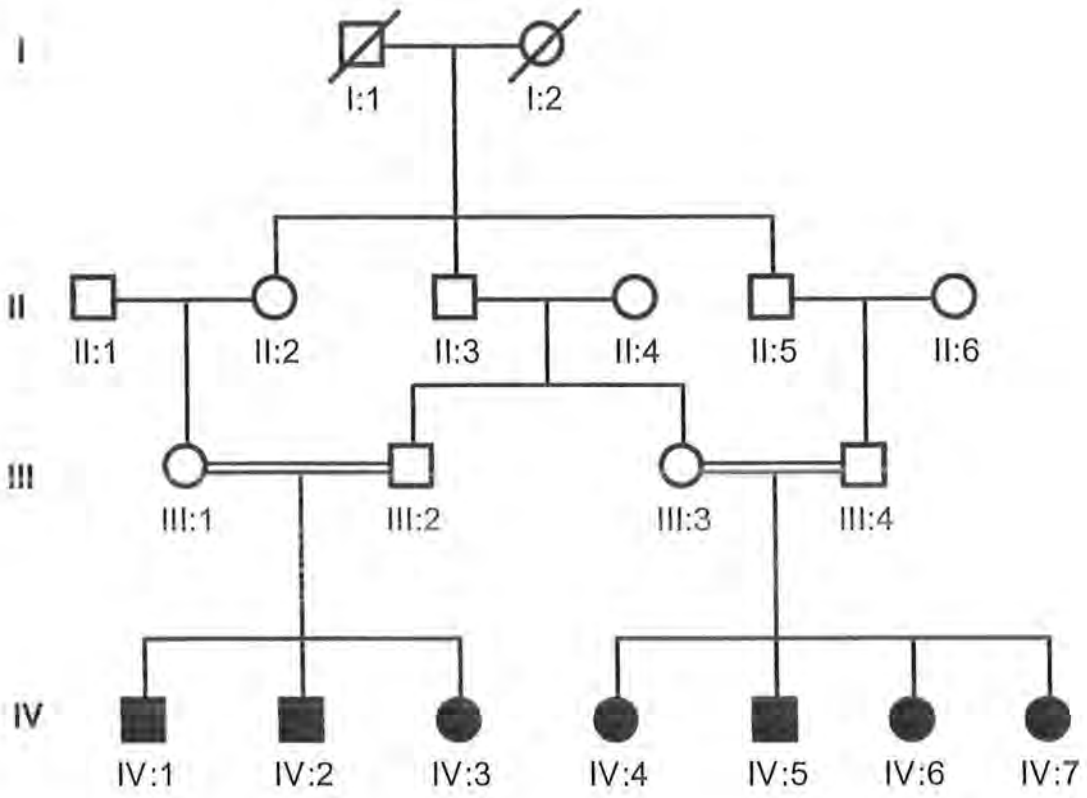

Figure 3.6: Pedigree of family E with autosomal recessive non-syndromic hereditary hearing impairment. Circles represent females, squares represent males. Filled circles and squares represent affected individuals. Double lines indicate consanguineous marriages. Cross lines on the symbols represent deceased individuals.

1 2 3 4 5 6 7 8 9 10 11 12 13 14

Family A

Lane 1- VI-4	Lane 5- VI-3	Lane 9- V-2	Lane 13- V-6
Lane 2- VI-6	Lane 6- VI-2	Lane 10- V-5	Lane 14- IV-7
Lane 3- V-4	Lane 7- VI-1	Lane 11- IV-8	
Lane 4- V-3	Lane 8- V-1	Lane 12- V-7	

Figure 3.7: Electropherogram of ethidium bromide stained 8% non-denaturing polyacrylamide gel for marker D12S320 at 32.19 cM on chromosome 12p13.1 showing homozygosity among the affected individuals (V-6, V-7, VI-2, VI-4 and VI-6) of family A. The Roman numerals indicate the generation number of the individuals within a pedigree while Arabic numerals indicate their positions within a generation.

1 2 3 4 5 6 7 8 9 10 11 12 13 14

Family A

Lane 1- VI-4	Lane 5- VI-3	Lane 9- V-2	Lane 13- V-6
Lane 2- VI-6	Lane 6- VI-2	Lane 10- V-5	Lane 14- IV-7
Lane 3- V-4	Lane 7- VI-1	Lane 11- IV-8	
Lane 4- V-3	Lane 8- V-1	Lane 12- V-7	

Figure 3.8: Electropherogram of ethidium bromide stained 8% non-denaturing polyacrylamide gel for marker D12S336 at 24.51 cM on chromosome 12p13.31. The Roman numerals indicate the generation number of the individuals within a pedigree while Arabic numerals indicate their positions within a generation.

Family A

Lane 1- VI-4	Lane 5- VI-3	Lane 9- V-2	Lane 13- V-6
Lane 2- VI-6	Lane 6- VI-2	Lane 10- V-5	Lane 14- IV-7
Lane 3- V-4	Lane 7- VI-1	Lane 11- IV-8	
Lane 4- V-3	Lane 8- V-1	Lane 12- V-7	

Figure 3.9: Electropherogram of ethidium bromide stained 8% non-denaturing polyacrylamide gel for marker D12S1697 at 26.72 cM on chromosome 12p13.2. The Roman numerals indicate the generation number of the individuals within a pedigree while Arabic numerals indicate their positions within a generation.

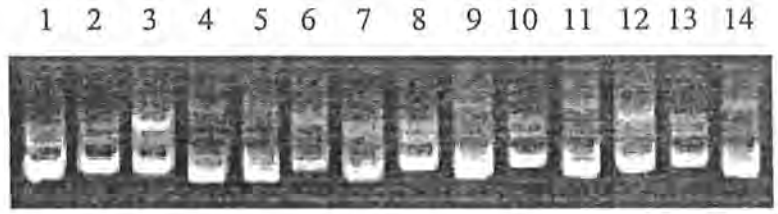

Family A

Lane 1- VI-4	Lane 5- VI-3	Lane 9- V-2	Lane 13- V-6
Lane 2- VI-6	Lane 6- VI-2	Lane 10- V-5	Lane 14- IV-7
Lane 3- V-4	Lane 7- VI-1	Lane 11- IV-8	
Lane 4- V-3	Lane 8- V-1	Lane 12- V-7	

Figure 3.10: Electropherogram of ethidium bromide stained 8% non-denaturing polyacrylamide gel for marker D12S89 at 27.00 cM on chromosome 12p13.2 showing homozygosity among the affected individuals (V-6, V-7, VI-2, VI-4 and VI-6) of family A. The Roman numerals indicate the generation number of the individuals within a pedigree while Arabic numerals indicate their positions within a generation.

1 2 3 4 5 6 7 8 9 10 11 12 13 14

Family A

Lane 1- VI-4	Lane 5- VI-3	Lane 9- V-2	Lane 13- V-6
Lane 2- VI-6	Lane 6- VI-2	Lane 10- V-5	Lane 14- IV-7
Lane 3- V-4	Lane 7- VI-1	Lane 11- IV-8	
Lane 4- V-3	Lane 8- V-1	Lane 12- V-7	

Figure 3.11: Electropherogram of ethidium bromide stained 8% non-denaturing polyacrylamide gel for marker D12S358 at 28.89 cM on chromosome 12p13.2-p13.1 showing homozygosity among the affected individuals (V-6, V-7, VI-2, VI-4 and VI-6) of family A. The Roman numerals indicate the generation number of the individuals within a pedigree while Arabic numerals indicate their positions within a generation.

1 2 3 4 5 6 7 8 9 10 11 12 13 14

Family A

Lane 1- VI-4	Lane 5- VI-3	Lane 9- V-2	Lane 13- V-6
Lane 2- VI-6	Lane 6- VI-2	Lane 10- V-5	Lane 14- IV-7
Lane 3- V-4	Lane 7- VI-1	Lane 11- IV-8	
Lane 4- V-3	Lane 8- V-1	Lane 12- V-7	

Figure 3.12: Electropherogram of ethidium bromide stained 8% non-denaturing polyacrylamide gel for marker D12S364 at 32.19 cM on chromosome 12p13.1 showing homozygosity among the affected individuals (V-6, V-7, VI-2, VI-4 and VI-6) of family A. The Roman numerals indicate the generation number of the individuals within a pedigree while Arabic numerals indicate their positions within a generation.

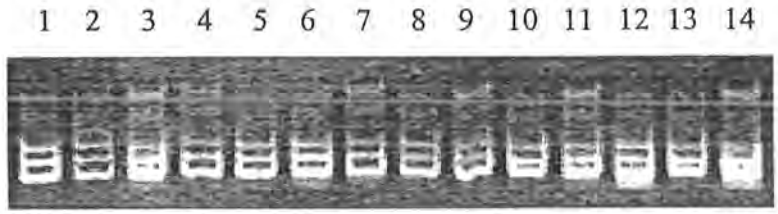

Family A

Lane 1- VI-4	Lane 5- VI-3	Lane 9- V-2	Lane 13- V-6
Lane 2- VI-6	Lane 6- VI-2	Lane 10- V-5	Lane 14- IV-7
Lane 3- V-4	Lane 7- VI-1	Lane 11- IV-8	
Lane 4- V-3	Lane 8- V-1	Lane 12- V-7	

Figure 3.13: Electropherogram of ethidium bromide stained 8% non-denaturing polyacrylamide gel for marker D12S62 at 34.32 cM on chromosome 12p12.3 showing homozygosity among the affected individuals (V-6, V-7, VI-2, VI-4 and VI-6) of family A. The Roman numerals indicate the generation number of the individuals within a pedigree while Arabic numerals indicate their positions within a generation.

Family A

Lane 1- VI-4	Lane 5- VI-3	Lane 9- V-2	Lane 13- V-6
Lane 2- VI-6	Lane 6- VI-2	Lane 10- V-5	Lane 14- IV-7
Lane 3- V-4	Lane 7- VI-1	Lane 11- IV-8	
Lane 4- V-3	Lane 8- V-1	Lane 12- V-7	

Figure 3.14: Electropherogram of ethidium bromide stained 8% non-denaturing polyacrylamide gel for marker D12S1669 at 37.83 cM on chromosome 12p12.3 showing homozygosity among the affected individuals (V-6, V-7, VI-2, VI-4 and VI-6) of family A. The Roman numerals indicate the generation number of the individuals within a pedigree while Arabic numerals indicate their positions within a generation.

1 2 3 4 5 6 7 8 9 10 11 12 13 14

Family A

Lane 1- VI-4	Lane 5- VI-3	Lane 9- V-2	Lane 13- V-6
Lane 2- VI-6	Lane 6- VI-2	Lane 10- V-5	Lane 14- IV-7
Lane 3- V-4	Lane 7- VI-1	Lane 11- IV-8	
Lane 4- V-3	Lane 8- V-1	Lane 12- V-7	

Figure 3.15: Electropherogram of ethidium bromide stained 8% non-denaturing polyacrylamide gel for marker D12S1682 at 40.34 cM on chromosome 12p12.3 showing homozygosity among the affected individuals (V-6, V-7, VI-2, VI-4 and VI-6) of family A. The Roman numerals indicate the generation number of the individuals within a pedigree while Arabic numerals indicate their positions within a generation.

1 2 3 4 5 6 7 8 9 10 11 12 13 14

Family A

Lane 1- VI-4	Lane 5- VI-3	Lane 9- V-2	Lane 13- V-6
Lane 2- VI-6	Lane 6- VI-2	Lane 10- V-5	Lane 14- IV-7
Lane 3- V-4	Lane 7- VI-1	Lane 11- IV-8	
Lane 4- V-3	Lane 8- V-1	Lane 12- V-7	

Figure 3.16: Electropherogram of ethidium bromide stained 8% non-denaturing polyacrylamide gel for marker D12S1057 at 46.46 cM on chromosome 12p12.1 showing homozygosity among the affected individuals (V-6, V-7, VI-2, VI-4 and VI-6) of family A. The Roman numerals indicate the generation number of the individuals within a pedigree while Arabic numerals indicate their positions within a generation.

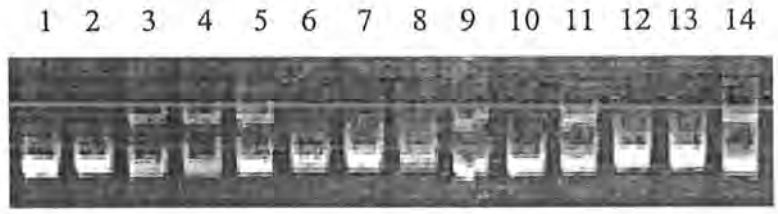

Family A

Lane 1- VI-4	Lane 5- VI-3	Lane 9- V-2	Lane 13- V-6
Lane 2- VI-6	Lane 6- VI-2	Lane 10- V-5	Lane 14- IV-7
Lane 3- V-4	Lane 7- VI-1	Lane 11- IV-8	
Lane 4- V-3	Lane 8- V-1	Lane 12- V-7	

Figure 3.17: Electropherogram of ethidium bromide stained 8% non-denaturing polyacrylamide gel for marker D12S1584 at 55.41 cM on chromosome 12p11.21 showing homozygosity among the affected individuals (V-6, V-7, VI-2, VI-4 and VI-6) of family A. The Roman numerals indicate the generation number of the individuals within a pedigree while Arabic numerals indicate their positions within a generation.

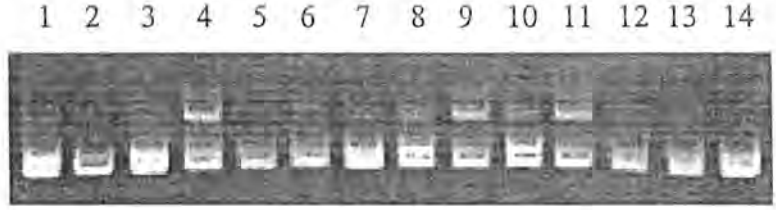

Family A

Lane 1- VI-4	Lane 5- VI-3	Lane 9- V-2	Lane 13- V-6
Lane 2- VI-6	Lane 6- VI-2	Lane 10- V-5	Lane 14- IV-7
Lane 3- V-4	Lane 7- VI-1	Lane 11- IV-8	
Lane 4- V-3	Lane 8- V-1	Lane 12- V-7	

Figure 3.18: Electropherogram of ethidium bromide stained 8% non-denaturing polyacrylamide gel for marker D12S291 at 59.08 cM on chromosome 12q12 showing homozygosity among the affected individuals (V-6, V-7, VI-2, VI-4 and VI-6) of family A. The Roman numerals indicate the generation number of the individuals within a pedigree while Arabic numerals indicate their positions within a generation.

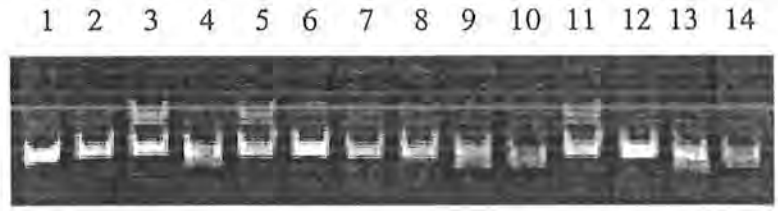

Family A

Lane 1- VI-4	Lane 5- VI-3	Lane 9- V-2	Lane 13- V-6
Lane 2- VI-6	Lane 6- VI-2	Lane 10- V-5	Lane 14- IV-7
Lane 3- V-4	Lane 7- VI-1	Lane 11- IV-8	
Lane 4- V-3	Lane 8- V-1	Lane 12- V-7	

Figure 3.19: Electropherogram of ethidium bromide stained 8% non-denaturing polyacrylamide gel for marker D12S1301 at 59.08 cM on chromosome 12q12 showing homozygosity among the affected individuals (V-6, V-7, VI-2, VI-4 and VI-6) of family A. The Roman numerals indicate the generation number of the individuals within a pedigree while Arabic numerals indicate their positions within a generation.

Family A

Lane 1- VI-4	Lane 5- VI-3	Lane 9- V-2	Lane 13- V-6
Lane 2- VI-6	Lane 6- VI-2	Lane 10- V-5	Lane 14- IV-7
Lane 3- V-4	Lane 7- VI-1	Lane 11- IV-8	
Lane 4- V-3	Lane 8- V-1	Lane 12- V-7	

Figure 3.20: Electropherogram of ethidium bromide stained 8% non-denaturing polyacrylamide gel for marker D12S85 at 60.52 cM on chromosome 12q13.11 showing homozygosity among the affected individuals (V-6, V-7, VI-2, VI-4 and VI-6) of family A. The Roman numerals indicate the generation number of the individuals within a pedigree while Arabic numerals indicate their positions within a generation.

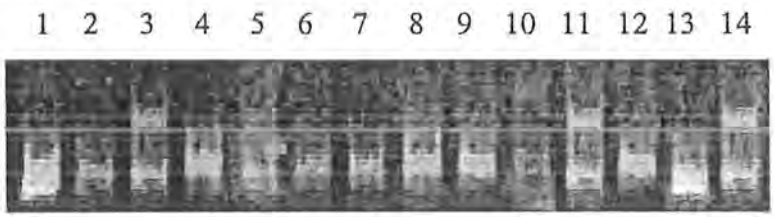

Family A

Lane 1- VI-4	Lane 5- VI-3	Lane 9- V-2	Lane 13- V-6
Lane 2- VI-6	Lane 6- VI-2	Lane 10- V-5	Lane 14- IV-7
Lane 3- V-4	Lane 7- VI-1	Lane 11- IV-8	
Lane 4- V-3	Lane 8- V-1	Lane 12- V-7	

Figure 3.21: Electropherogram of ethidium bromide stained 8% non-denaturing polyacrylamide gel for marker D12S347 at 65.70 cM on chromosome 12q13.13 showing homozygosity among the affected individuals (V-6, V-7, VI-2, VI-4 and VI-6) of family A. The Roman numerals indicate the generation number of the individuals within a pedigree while Arabic numerals indicate their positions within a generation.

Table 3.1: Two-point LOD score results between the DFNB62 locus and chromosome 12p13.2-p11.23 markers. Also displayed are the genetic and sequence-based physical map distances. Markers displayed in bold flank the region for DFNB62

Marker[a]	Genetic Map Position[b]	Physical map Position[c]	Lod score at recombination fraction θ =				
			0.0	0.02	0.05	0.20	0.30
D12S336	24.51	9,385,296	-4.60	-1.61	-0.92	-0.14	-0.04
D12S1697	26.72	11,685,470	-3.31	-0.31	0.26	0.51	0.29
D12S89	27.00	11,793,257	-1.12	0.26	0.52	0.49	0.29
D12S358	28.89	**12,530,590**	**1.74**	**1.64**	**1.50**	**0.82**	**0.44**
AAC040	32.19	13,065,278	4.02	3.85	3.58	2.21	1.30
D12S320	32.19	13,513,310	1.15	1.08	0.98	0.52	0.29
D12S364	32.19	13,724,570	1.64	1.55	1.42	0.80	0.45
D12S62	34.32	15,219,370	2.30	2.18	2.00	1.13	0.63
D12S1669	37.83	19,429,661	1.62	1.53	1.39	0.77	0.42
D12S1682	40.34	20,570,897	2.30	2.17	1.98	1.06	0.53
D12S1057	46.46	24,568,387	2.30	2.18	2.00	1.13	0.63
D12S1042	**51.27**	**27,538,599**	**- ∞**	**0.69**	**1.17**	**1.18**	**0.78**
D12S1584	55.41	31,610,488	2.30	2.18	2.00	1.13	0.63
D12S291	59.08	41,688,390	1.55	1.47	1.35	0.80	0.47
D12S1301	59.08	42,348,809	- ∞	1.94	1.79	1.06	0.62
D12S85	60.52	45,622,954	2.98	2.83	2.61	1.52	0.85
D12S347	65.70	50,298,255	1.57	1.49	1.37	0.79	0.46
D12S297	66.82	50,899,108	- ∞	-1.15	-0.25	0.49	0.38

[a]Markers in bold type flank the haplotype. Genome scan markers are shown in italics.

[b]Cumulative sex-averaged Kosambi genetic map distances (cM) from the Rutgers combined linkage-physical map of the human genome (Kong *et al.*, 2004).

[c]Sequence-based physical map distances in bases according to Build 34 of the human reference sequence (International Human Genome Sequence Consortium, 2001).

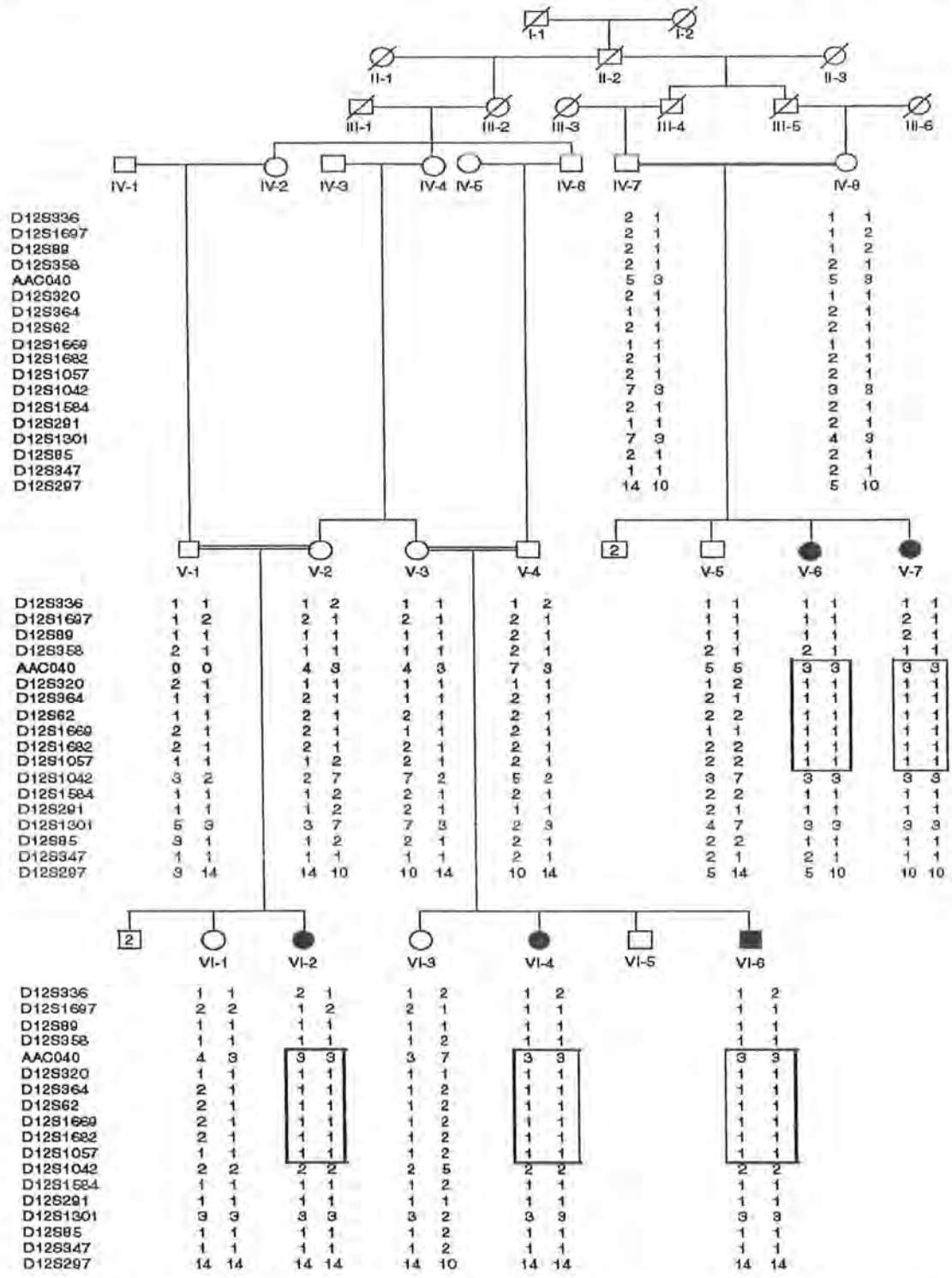

Figure 3.22: Pedigree of family A with autosomal recessive non-syndromic hearing impairment due to DFNB62. Haplotypes for the most closely linked short tandem repeats (STRPs) are shown below each symbol. Boxes on the haplotypes of the corresponding individuals indicate key recombination event. The alleles are denoted by 1-3 according to their sizes. Size of the alleles was determined by using 5 bp ladder (O'RangeRuler™, Fermentas, Life Sciences, UK).

1 2 3 4 5 6 7 8 9 10 11 12 13 14 15 16 17 18 19

Family C

Lane 1- V-6	Lane 6- VI-3	Lane 11- V-2	Lane 16- IV-11
Lane 2- V-5	Lane 7- VI-4	Lane 12- IV-1	Lane 17- V-3
Lane 3- IV-4	Lane 8- V-1	Lane 13- VI-2	Lane 18-VI-5
Lane 4- V-4	Lane 9- V-13	Lane 14- VI-1	Lane 19-V-11
Lane 5- V-12	Lane 10-V-14	Lane 15- V-10	

Figure 3.23: Electropherogram of ethidium bromide stained 8% non-denaturing polyacrylamide gel for marker D2S1400 at 28.38 cM on chromosome 2p25.1 showing homozygosity among the affected individuals (V-1, V-2, V-3, V-5, V-6, V-12, V-13, V-14, VI-1, VI-2 and VI-3) of family C. The Roman numerals indicate the generation number of the individuals within a pedigree while Arabic numerals indicate their positions within a generation.

1 2 3 4 5 6 7 8 9 10 11 12 13 14 15 16 17 18 19

Family C

Lane 1- V-6	Lane 6- VI-3	Lane 11- V-2	Lane 16- IV-11
Lane 2- V-5	Lane 7- VI-4	Lane 12- IV-1	Lane 17- V-3
Lane 3- IV-4	Lane 8- V-1	Lane 13- VI-2	Lane 18-VI-5
Lane 4- V-4	Lane 9- V-13	Lane 14- VI-1	Lane 19-V-11
Lane 5- V-12	Lane 10-V-14	Lane 15- V-10	

Figure 3.24: Electropherogram of ethidium bromide stained 8% non-denaturing polyacrylamide gel for marker D2S2952 at 18.44 cM on chromosome 2p25.1. The Roman numerals indicate the generation number of the individuals within a pedigree while Arabic numerals indicate their positions within a generation.

1 2 3 4 5 6 7 8 9 10 11 12 13 14 15 16 17 18 19

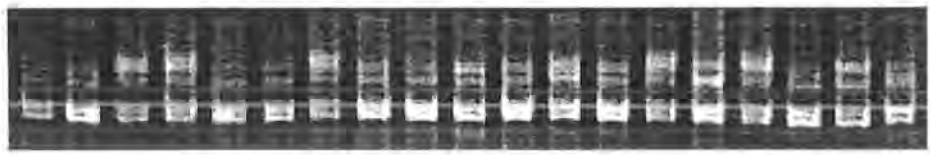

Family C

Lane 1- V-6	Lane 6- VI-3	Lane 11- V-2	Lane 16- IV-11
Lane 2- V-5	Lane 7- VI-4	Lane 12- IV-1	Lane 17- V-3
Lane 3- IV-4	Lane 8- V-1	Lane 13- VI-2	Lane 18-VI-5
Lane 4- V-4	Lane 9- V-13	Lane 14- VI-1	Lane 19-V-11
Lane 5- V-12	Lane 10-V-14	Lane 15- V-10	

Figure 3.25: Electropherogram of ethidium bromide stained 8% non-denaturing polyacrylamide gel for marker D2S149 at 33.12 cM on chromosome 2p24.3 showing homozygosity among the affected individuals (V-1, V-2, V-3, V-5, V-6, V-12, V-13, V-14, VI-1, VI-2 and VI-3) of family C. The Roman numerals indicate the generation number of the individuals within a pedigree while Arabic numerals indicate their positions within a generation.

1 2 3 4 5 6 7 8 9 10 11 12 13 14 15 16 17 18 19

Family C

Lane 1- V-6	Lane 6- VI-3	Lane 11- V-2	Lane 16- IV-11
Lane 2- V-5	Lane 7- VI-4	Lane 12- IV-1	Lane 17- V-3
Lane 3- IV-4	Lane 8- V-1	Lane 13- VI-2	Lane 18-VI-5
Lane 4- V-4	Lane 9- V-13	Lane 14- VI-1	Lane 19-V-11
Lane 5- V-12	Lane 10-V-14	Lane 15- V-10	

Figure 3.26: Electropherogram of ethidium bromide stained 8% non-denaturing polyacrylamide gel for marker D2S1360 at 39.05 cM on chromosome 2p24.2 showing homozygosity among the affected individuals (V-1, V-2, V-3, V-5, V-6, V-12, V-13, V-14, VI-1, VI-2 and VI-3) of family C. The Roman numerals indicate the generation number of the individuals within a pedigree while Arabic numerals indicate their positions within a generation.

1 2 3 4 5 6 7 8 9 10 11 12 13 14 15 16 17 18 19

Family C

Lane 1- V-6	Lane 6- VI-3	Lane 11- V-2	Lane 16- IV-11
Lane 2- V-5	Lane 7- VI-4	Lane 12- IV-1	Lane 17- V-3
Lane 3- IV-4	Lane 8- V-1	Lane 13- VI-2	Lane 18-VI-5
Lane 4- V-4	Lane 9- V-13	Lane 14- VI-1	Lane 19-V-11
Lane 5- V-12	Lane 10-V-14	Lane 15- V-10	

Figure 3.27: Electropherogram of ethidium bromide stained 8% non-denaturing polyacrylamide gel for marker D2S220 at 44.46 cM on chromosome 2p24.1 showing homozygosity among the affected individuals (V-1, V-2, V-3, V-5, V-6, V-12, V-13, V-14, VI-1, VI-2 and VI-3) of family C. The Roman numerals indicate the generation number of the individuals within a pedigree while Arabic numerals indicate their positions within a generation.

1 2 3 4 5 6 7 8 9 10 11 12 13 14 15 16 17 18 19

Family C

Lane 1- V-6	Lane 6- VI-3	Lane 11- V-2	Lane 16- IV-11
Lane 2- V-5	Lane 7- VI-4	Lane 12- IV-1	Lane 17- V-3
Lane 3- IV-4	Lane 8- V-1	Lane 13- VI-2	Lane 18-VI-5
Lane 4- V-4	Lane 9- V-13	Lane 14- VI-1	Lane 19-V-11
Lane 5- V-12	Lane 10-V-14	Lane 15- V-10	

Figure 3.28: Electropherogram of ethidium bromide stained 8% non-denaturing polyacrylamide gel for marker D2S158 at 49.22 cM on chromosome 2p23.3. The Roman numerals indicate the generation number of the individuals within a pedigree while Arabic numerals indicate their positions within a generation.

1 2 3 4 5 6 7 8 9 10 11 12 13 14 15 16 17 18 19

Family C

Lane 1- V-6	Lane 6- VI-3	Lane 11- V-2	Lane 16- IV-11
Lane 2- V-5	Lane 7- VI-4	Lane 12- IV-1	Lane 17- V-3
Lane 3- IV-4	Lane 8- V-1	Lane 13- VI-2	Lane 18-VI-5
Lane 4- V-4	Lane 9- V-13	Lane 14- VI-1	Lane 19-V-11
Lane 5- V-12	Lane 10-V-14	Lane 15- V-10	

Figure 3.29: Electropherogram of ethidium bromide stained 8% non-denaturing polyacrylamide gel for marker D2S1356 at 68.85 cM on chromosome 2p21 showing homozygosity among the affected individuals (V-1, V-2, V-3, V-5, V-6, V-12, V-13, V-14, VI-1, VI-2 and VI-3) of family C. The Roman numerals indicate the generation number of the individuals within a pedigree while Arabic numerals indicate their positions within a generation.

Table 3.2: Two-point LOD score results between the DFNB9 locus and chromosome 2p23.3 markers. Also displayed are the genetic and sequence-based physical map distances.

Marker	Genetic Map Position[a]	Physical map Position[b]	Lod score at recombination fraction θ =				
			0.00	0.05	0.20	0.30	0.40
D2S2952	18.44	8,028,636	-Infinity	0.8206	1.4955	1.0540	0.4952
D2S1400	28.38	11,557,537	4.1754	3.6621	2.2019	1.3172	0.5473
D2S149	33.12	14,343,670	-Infinity	2.2527	1.7590	1.0702	0.4233
D2S1360	39.05	17,413,585	6.4493	5.7237	3.5565	2.1664	0.9079
D2S220	44.46	21,007,648	4.1808	3.6431	2.1170	1.2126	0.4683
D2S158	49.22	26,363,815	5.5513	4.9041	2.9878	1.7932	0.7535
D2S1356	68.85	43,285,172	5.7603	5.1071	3.1291	1.8703	0.7682

[a]Cumulative sex-averaged Kosambi genetic map distances (cM) from the Rutgers combined linkage-physical map of the human genome (Kong *et al.*, 2004).

[b]Sequence-based physical map distances in bases according to Build 36 of the human reference sequence (International Human Genome Sequence Consortium, 2007).

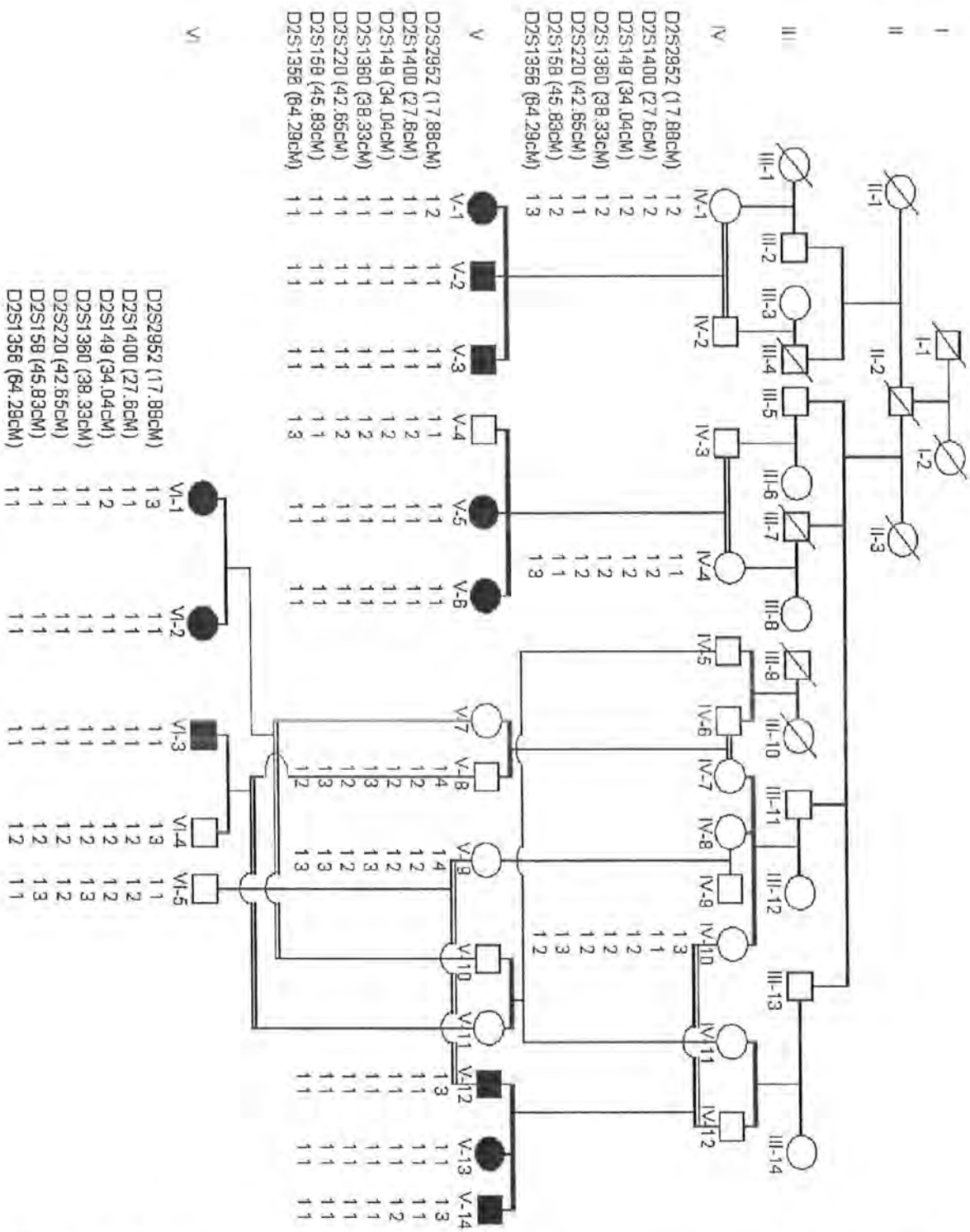

Figure 3.30: Pedigree of family C with autosomal recessive non-syndromic hearing impairment due to DFNB9. Haplotypes for the most closely linked short tandem repeats (STRPs) are shown below each symbol. The genetic map distances in centimorgans (cM) according to the decode genetic map are shown in Parenthesis next to the marker name. The alleles are denoted by 1-3 according to their sizes. Size of the alleles was determined by using

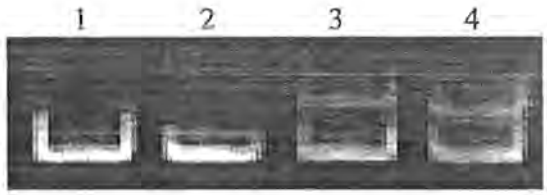

Family D

Lane 1- V-1 Lane 3- III-3
Lane 2- V-2 Lane 4- IV-2

Figure 3.31: Electropherogram of ethidium bromide stained 8% non-denaturing polyacrylamide gel for marker D21S212 at 58.54 cM on chromosome 21 showing homozygosity among the affected individuals (V-1 and V-2) of family D. The Roman numerals indicate the generation number of the individuals within a pedigree while Arabic numerals indicate their positions within a generation.

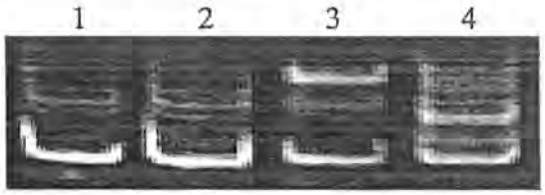

Family D

Lane 1- V-1 Lane 3- III-3
Lane 2- V-2 Lane 4- IV-2

Figure 3.32: Electropherogram of ethidium bromide stained 8% non-denaturing polyacrylamide gel for marker D21S1411 at 61.33 cM on chromosome 21q22.3 showing homozygosity among the affected individuals (V-1 and V-2) of family D. The Roman numerals indicate the generation number of the individuals within a pedigree while Arabic numerals indicate their positions within a generation.

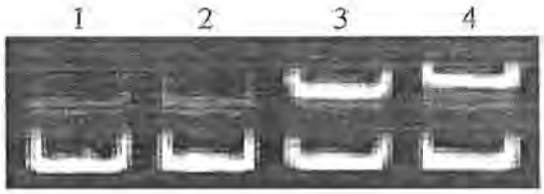

Family D

Lane 1- V-1 Lane 3- III-3

Lane 2- V-2 Lane 4- IV-2

Figure 3.33: Electropherogram of ethidium bromide stained 8% non-denaturing polyacrylamide gel for marker D21S1446 at 69.08 cM on chromosome 21q22.3 showing homozygosity among the affected individuals (V-1 and V-2) of family D. The Roman numerals indicate the generation number of the individuals within a pedigree while Arabic numerals indicate their positions within a generation.

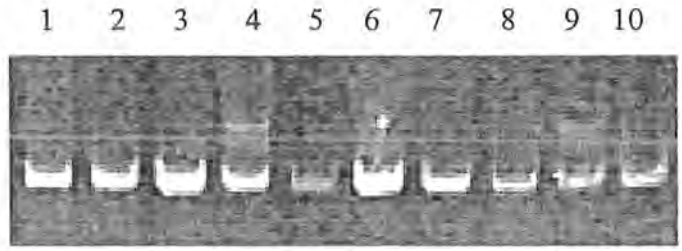

Family E

Lane 1- III-2 Lane 5- IV-3 Lane 9- III-3
Lane 2- IV-1 Lane 6- IV-7 Lane 10- IV-5
Lane 3- IV-2 Lane 7- IV-6
Lane 4- III-1 Lane 8- IV-4

Figure 3.34: Electropherogram of ethidium bromide stained 8% non-denaturing polyacrylamide gel for marker D21S212 at 58.54 cM on chromosome 21 showing homozygosity among the affected individuals (IV-1, IV-2, IV-3, IV-4, IV-5, IV-6, and IV-7) of family E. The Roman numerals indicate the generation number of the individuals within a pedigree while Arabic numerals indicate their positions within a generation.

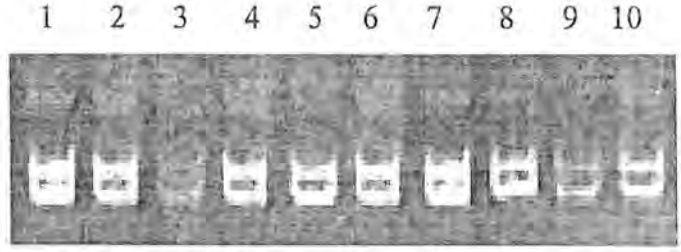

Family E

Lane 1- III-2 Lane 5- IV-3 Lane 9- III-3
Lane 2- IV-1 Lane 6- IV-7 Lane 10- IV-5
Lane 3- IV-2 Lane 7- IV-6
Lane 4- III-1 Lane 8- IV-4

Figure 3.35: Electropherogram of ethidium bromide stained 8% non-denaturing polyacrylamide gel for marker D21S1411 at 61.33 cM on chromosome 21q22.3 showing homozygosity among the affected individuals (IV-1, IV-2, IV-3, IV-4, IV-5, IV-6, and IV-7) of family E. The Roman numerals indicate the generation number of the individuals within a pedigree while Arabic numerals indicate their positions within a generation.

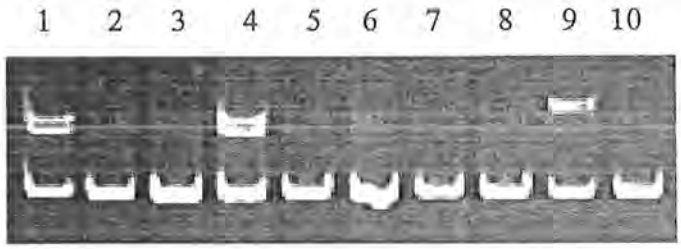

Family E

Lane 1- III-2 Lane 5- IV-3 Lane 9- III-3
Lane 2- IV-1 Lane 6- IV-7 Lane 10- IV-5
Lane 3- IV-2 Lane 7- IV-6
Lane 4- III-1 Lane 8- IV-4

Figure 3.36: Electropherogram of ethidium bromide stained 8% non-denaturing polyacrylamide gel for marker D21S1446 at 69.08 cM on chromosome 21q22.3 showing homozygosity among the affected individuals (IV-1, IV-2, IV-3, IV-4, IV-5, IV-6, and IV-7) of family E. The Roman numerals indicate the generation number of the individuals within a pedigree while Arabic numerals indicate their positions within a generation.

ALOPECIAS

There are many forms of inherited alopecia, which vary in age of onset, severity, and associated ectodermal abnormalities. The identification of hereditary alopecias genes is an essential step in understanding the molecular mechanism of hair loss.

Hair-follicle morphogenesis is a multistep process that requires a series of epithelial-mesenchymal interactions to execute the program of developmental events. Hair follicles vary considerably in size and shape, depending on their location, but they all have the same basic structure. The mature hair follicle is composed of several concentric cylinders of epithelial cells, known as root sheaths, which surround the hair shaft (Sperling, 1991). Hair follicle cycles through periods of growth (anagen), involution (catagen), and rest (telogen) before regenerating at the onset of a new anagen growth phase. Hair-follicle stem cells communicate with the underlying dermal papilla cells and proliferate at anagen onset to generate the progenitor matrix cells required for new hair growth (Moore and Lemischka, 2006). The molecules that control morphogenesis and cycling of hair-follicles and the mechanisms underlying hair loss are poorly understood. A powerful approach to advance our understanding of the pathophysiology of hair loss is to identify the genes underlying isolated and syndromic forms of hair loss. This provides an opportunity to identify factors which are directly involved in hair growth.

Families with Hereditary Alopecias

For the study, presented here, four families (F-I) with autosomal recessive form of hereditary alopecias were ascertained from different parts of Pakistan.

Family F

The family F, demonstrating localized autosomal recessive hypotrichosis, belongs to district Hafizabad of the Punjab province, Pakistan. The family members are engaged in local market business. Family members rarely marry outside the community and consequently consanguineous unions are common. The four generation pedigree (Figure 4.1) consists of fourteen individuals including three affected females (IV-1, IV-2 and IV-5). Pedigree analysis is suggestive of autosomal recessive mode of inheritance and therefore, it is highly likely that all affected individuals are homozygous for the same mutation.

All the three affected individuals of the family F, showed typical features of the hereditary hypotrichosis. At birth, hairs were present on the scalp, but regrew sparsely after ritual shaving, which is usually performed a week after birth. The affected individuals are nearly devoid of normal eyebrows, eyelashes, axillary hair, and body hair (Figure 4.2). Teeth, nails, sweating and hearing are normal in all affected individuals. The affected individuals were in good general health, with no evidence for immune system dysfunction or unusual susceptibility to skin tumors. Heterozygous carrier individuals had normal hairs, and were clinically indistinguishable from genotypically normal individuals.

A skin biopsy from an affected individual (IV-1) revealed the complete absence of normal hair follicle structures. These structures were replaced by comedolike remnants hair follicle. The remnants of the hair follicle infundibulum undergo hyperkeratinization (Figure 4.3). Despite the disintegration of the hair follicle epithelial structures, the sebaceous glands appear morphologically normal but lost their connection with the remnants of the hair follicle infundibulum.

After informed consent was obtained, peripheral blood samples were collected from eight members including three affected (IV-1, IV-2 and IV-5) and five normal (III-1, III-2, IV-3, IV-4 and IV-6) individuals.

Family G

Family G, demonstrating autosomal recessive form of alopecia and mental retardation syndrome (APMR), is located in Sargodha district of the Punjab province, Pakistan. The family members are engaged in local market business. They follow the local tradition of marrying within the family, resulting in a high rate of consanguineous unions. The four generation pedigree (Figure 4.4) comprised of seventeen individuals including an affected male (V-1) and two affected females (V-2 and V-3). Pedigree analysis is suggestive of autosomal recessive mode of inheritance and consanguineous loops could account of all the affected persons being homozygous for an abnormal allele.

In all the three affected individuals of the family, hairs were completely absent by birth from all areas of normal hair growth including scalp, eyebrows, eyelashes, axillary and pubic hair. Affected individuals (Figure 4.5) showed normal hearing, teeth and nails, and no abnormality in sweating was observed. All the affected

individuals were severely mentally retarded (IQ ranges from 25 to 30). No other clinical signs including seizures were detected in any of the affected individuals. The affected individuals were in good general health, with no evidence of immune system dysfunction or unusual susceptibility to skin tumors. Heterozygous carrier individuals had normal hairs, and were clinically indistinguishable from genotypically normal individuals.

A skin biopsy (Figure 4.6) from an affected individual (V-1) revealed the complete absence of normal hair follicle structures. The remnants of the hair follicle infundibulum undergo hyperkeratinization. Despite the disintegration of the hair follicle epithelial structures, the sebaceous glands appear morphologically normal but lost their connection with the remnants of the hair follicle infundibulum.

After informed consent was obtained, blood samples collected from seven family members, including three affected (V-1, V-2 and V-3) and four normal (IV-1, IV-2, V-4, and V-5) individuals, were processed for DNA extraction.

Family H

Family H was ascertained from Pashto speaking population of Quetta district of the Balochistan province, Pakistan. The members of this tribe follow the tradition of marrying within the community. The family history presented in the pedigree (Figure 4.7) suggests that three individuals of the family including a male (IV-4) and two females (IV-5 and IV-6) are affected with localized hereditary hypotrichosis. Affected individuals of the family underwent examination at Department of Dermatology, Civil Hospital Quetta, Pakistan. In all the three affected individuals of the family, hair started disappearing from the scalp at the age of 10 years. Affected individuals showed sparse eyebrows and eyelashes (Figure 4.8). However, teeth, nails, sweating and hearing were normal in all the affected individuals. Heterozygous carrier individuals had normal hair, and were clinically indistinguishable from genotypically normal individuals.

After informed consent was obtained, the DNA was extracted from the blood samples collected from seven individuals of the family, including three affected (IV-4, IV-5 and IV-6) and four normals (III-1, IV-1, IV-2 and IV-3).

Family I

Family I with alopecia resides in Hyderabad district of Sindh province, Pakistan. The

family members are engaged in local market business. They follow the local tradition of marrying within the family, resulting in high rate of consanguineous matings. The four generation pedigree (Figure 4.9) comprised of eleven individuals including an affected female (IV-1) and an affected male (IV-3). Pedigree analysis is suggestive of autosomal recessive mode of inheritance and consanguineous loops could account of all the affected persons being homozygous for an abnormal allele.

In both the affected individuals of the family, hairs were completely absent by birth from all areas of normal hair growth including scalp, eyebrows, eyelashes, axillary and pubic hair. Affected individuals showed normal hearing, teeth and nails and no abnormalities in sweating were observed. They were in good general health, with no evidence for immune system dysfunction or unusual susceptibility to skin tumors. Heterozygous carrier individuals had normal hairs, and were clinically indistinguishable from genotypically normal individuals.

After informed consent was obtained, blood samples collected from five family members, including two affected (IV-1 and IV-3) and three normal (III-1, III-2 and IV-2) individuals, were processed for DNA extraction.

Linkage Studies and Mutation Search in Families F-I

A candidate gene approach was first used to localize the alopecia locus segregating in the four families (F, G, H and I). The families were tested for linkage by using microsatellite markers tightly linked to candidate genes involved in different forms of alopecias (Table 2.2). These included: desmoglein 4 (*DSG4*) gene at 18q12.1; hairless (*HR*) gene at 8p21.2; Lipase H (*LIPH*) gene at 3q27; envoplakin (*EVPL*) gene at 17q25.1; loricrin (*LOR*) gene at 1q21.3; plakophilin (*PKP1*) gene at 1q32.1; ED2 gene gap junction protein ß-6 (*GJB6*) gene at 13q12.11; ED3 gene ectodysplasin1 anhidrotic receptor (*EDAR*) at 2q12.3; ED4 gene poliovirus receptor-like 1 (*PVRL1*) gene at 11q23.3; transglutaminase I (*TGM1*) gene at 14q11.2; corneodesmosin (*CDSN*) gene at 6q21.33.

In family F (Figure 4.1), all the three affected members (IV-1, IV-2 and IV-5) were homozygous for the markers D3S2314, D3S3609, D3S3578 and D3S3583 (Figures 4.10-4.13) linked to AH/LAH2 locus, thus suggesting linkage to this region on chromosome 3q27. Twenty additional markers (D3S3546, D3S3022, D3S1746, D3S3668, D3S3555, D3S1763, D3S1243, D3S2433, D3S1574, D3S3725, D3S2427,

D3S3676, D3S2412, D3S3037, D3S1232, D3S1602, D3S3651, D3S3628, D3S2398, D3S1661) (Figures 4.14-4.33) were selected from the Rutgers combined linkage-physical map of the human genome (Kong *et al.*, 2004) and typed in all the family members. Five of the markers (D3S3723, D3S1617, D3S1262, D3S2311 and D3S2436) were un-informative and, therefore, not included in the analysis. Analysis of the marker genotypes within this region with PEDCHECK (O'Connell and Weeks, 1998) did not elucidate any genotyping errors. Haplotypes (Figure 4.34) were generated using SIMWALK2 (Weeks *et al.*, 1995; Sobel and Lange, 1996). The maximum two-point LOD score of 1.88 (Table 4.1) was obtained with several microsatellite markers. Multipoint linkage analysis generated a maximum LOD score of 2.76 at markers D3S3555, D3S1763, D3S1243, D3S2433, D3S1574, D3S3725, D3S2427, D3S3676, D3S2412, D3S3037, D3S1232, D3S2314, D3S3609, D3S3578 and D3S3583, which is same to the 2.7 theoretical maximum for this family.

The human *LIPH* gene (NM_139248), located at 3q27 and identified earlier by Sonoda *et al.* (2002), was sequenced in the affected and normal individuals of the family F. Primer3 software (Rozen and Skaletsky, 2000) was used to design primers for the ten exons and splice junctions of the *LIPH* gene. Sequencing was performed with the Big Dye Terminator v3.1 Cycle Sequencing Kit, together with an ABI Prism 310 Genetic Analyzer (Applera, Foster City, CA, USA). Sequence variants were identified via Bioedit sequence alignment editor version 6.0.7.

The coding portion and intron-exon borders of the *LIPH* gene were sequenced in three affected and four normal individuals of the family. Sequence analysis of exon 2 revealed a deletion of five consecutive nucleotides (ATATA) in three affected individuals (Figure 4.35). The deletion spans from nucleotide position 346 to 350 (c.346–350delATATA). This mutation, which leads to frameshift and premature termination codon 12 bp downstream in the same exon, is predicted to add four amino acids downstream of the mutation. This deletion mutation was present in heterozygous state in the obligate heterozygous carriers of the family F.

To ensure that the mutation does not represent a neutral polymorphism in this population, a panel of 50 unrelated unaffected ethnically matched control individuals (100 chromosomes) of Pakistani origin was screened for the mutation and it was not identified outside the family.

To identify the underlying gene in the family G, linkage analysis was performed by using microsatellite markers closely linked to previously reported three alopecia and mental retardation loci, including APMR1 (D3S3699, D3S3609; Figures 4.36-4.37), APMR2 (D3S3723, D3S2427; Figures 4.38-4.39) and APMR3 (D18S1100, D18S1102; Figures not shown). In the course of initial screening, evidence for linkage was found with APMR1 (John *et al.*, 2006) and APMR2 (Wali *et al.*, 2006b) loci on chromosome 3. For fine mapping 25 additional markers (D3S3626, D3S3022, D3S1299, D3S1746, D3S1763, D3S3622, D3S1282, D3S2433, D3S3676, D3S3037, D3S3730, D3S1617, D3S3686, D3S3628, D3S3596) (Figures 4.40-4.54) were selected from the Rutgers combined linkage-physical map of the human genome (Kong *et al.*, 2004). Ten of the markers (D3S1548, D3S2421, D3S2412, D3S3715, D3S3511, D3S1618, D3S1571, D3S1602, D3S1262, D3S2436) were non-informative in this family and, therefore, not included in the analysis. All affected members of the family were homozygous for 15 markers spanning from D3S1746 (175 cM) to D3S3628 (215.71 cM).

The data was analyzed using two-point and multipoint linkage analysis. The two-point analysis generated a maximum LOD score of 1.74 (θ=0) for several markers (Table 4.2). Multipoint analysis supported linkage to this region with maximum LOD score exceeding 3.17 at markers D3S2433, D3S2427 and D3S3676.

Haplotype analysis (Figure 4.55) located the APMR locus between markers D3S3622 (183.76 cM) and D3S3596 (216.29 cM), spanning 32.53 cM region on chromosome 3q26.2–q28. This region corresponds to 20.14 Mb according to combined linkage-physical map of the human genome (Kong *et al.*, 2004). The APMR locus identified in family G overlaps with both APMR1 [D3S1232 (202.3 cM) – D3S2436 (213.79 cM)] and APMR2 [D3S1564 (185.79 cM) – D3S2427 (195.85 cM)] linkage intervals (Figure 4.56).

Sequence analysis of five candidate genes, *LIPH* (MIM 607365), *ETS* variant gene 5 (MIM 601600), *TNFSF10* (MIM 603598), *AP2M1* (MIM 601024) and *CAM-K2N2* (MIM 608721) from DNA samples of two affected individuals of the family revealed no pathogenic sequence variants.

The family H was first tested for linkage by using microsatellite markers linked to candidate genes involved in the related phenotypes of alopecias (Table 2.2). After

linkage to the known genes was excluded, a genome wide scan was carried out using 396 highly polymorphic microsatellite markers from linkage mapping set 13 (Invitrogen Co. San Diego, California USA). Five chromosomal regions including D1S1151 at 1p36.22, D3S1544 at 3q12.2, D8S1832 at 8q24.13, D10S1700 at 10q26.3 and D12S291 at 12q12 were found to be homozygous in all the three affected family members (IV-4, IV-5 and IV-6). Each of the five regions was saturated with additional markers selected from Rutgers combined linkage-physical map of the human genome (Kong *et al.,* 2004). All the family members were genotyped with these markers. However, linkage was not detected with any of these regions.

The family I was tested for linkage by using polymorphic microsatellite markers linked to the hairless (*HR*) gene on chromosome 8p21.2. Genotyping of five members of the family I including two affected (IV-1 and IV-3) and three unaffected (III-1, III-2 and IV-2) individuals with polymorphic microsatellite markers D8S322, D8S282, D8S560, D8S298 (Figures 4.57-4.60), established linkage to the *HR* locus. Subsequently, the entire coding region as well as the intron-exon boundaries of *HR* gene was sequenced in two affected individuals (IV-1 and IV-3), but failed to identify functional sequence variant suggesting that the mutation is probably present in the regulatory sequence of the gene.

DISCUSSION

For the work, presented here, four families (F, G, H, I) with hereditary alopecias have been located and studied from different regions of Pakistan. Affected individuals in all the four families showed clinical features of hereditary hypotrichosis, including sparse to absent scalp hairs, sparse eyebrows and eyelashes, and sparse axillary and pubic hairs. In family G in addition to having features of hypotrichosis, affected individuals were severely mentally retarded.

To elucidate the gene defect in the families, co-segregation and homozygosity analysis were performed with microsatellite markers corresponding to candidate genes involved in hair loss and other related phenotypes (Table 2.2). A minimum of two or three microsatellite markers from each of the candidate regions of these loci were genotyped in all the available individuals of the four families (F-I). In family F, linkage was established to lipase-H (*LIPH*) gene on chromosome 3q27-q28. In family G, linkage was established to APMR1 locus on chromosome 3q27. In family H, linkage to all the known loci was conclusively excluded, indicating the involvement of a novel locus responsible for alopecia in this family. In family I, linkage was established to hairless (*HR*) gene on chromosome 8p21.2.

In family F, sequence analysis of exon 2 of *LIPH* gene, located at AH/LAH2 locus on chromosome 3q27, revealed a novel five base pair deletion mutation (c.346–350delATATA) (Figure 4.35). This deletion mutation results in a frameshift and downstream premature termination codon, thereby predicting to cause nonsense-mediated decay of the mRNA or instability of the truncated protein (Maquat, 1996). To date only three mutations (all deletions) in *LIPH* gene have been reported. The first mutation was reported by Kazantseva *et al.* (2006) in large number of affected individuals of two populations from the Volga-Ural region of Russia. The mutation involved a deletion of 985 bp of exon 4 and the flanking intronic sequences of *LIPH* gene eliminating the evolutionary conserved domain of the protein. The mutation identified in family F is the second mutation reported in *LIPH* gene. The third deletion mutation of two base-pairs (c.659-660delTA), located in exon 5 of the *LIPH* gene, was identified recently in two families originated from Pashto speaking population in North Western Frontier Province of Pakistan (Jelani *et al.*, 2008).

The 45 kb *LIPH* gene was cloned and characterized by Sonoda *et al.* (2002). It has ten

exons and expresses in several tissues including prostate, testis, ovary, colon, pancreas, kidney and lung. Kazantseva *et al.* (2006) has detected the expression of *LIPH* in the hair follicle bulge in anagen phase of hair growth. The LIPH protein has a striking sequence similarity to phospholipases and members of the large triglyceride lipase family. The 55 kDa LIPH protein has an N-terminal signal sequence followed by a catalytic domain containing the putative catalytic triad ser154, asp178, and his249. In addition, *LIPH* has 12 residue lid region and four potential N-linked glycosylation sites.

LIPH is a phosphatidic acid-selective phospholipase A1 that produces 2-acyl lysophosphatidic acid (LPA), which is a lipid mediator with wide variety of biological properties including stimulation of cell proliferation, migration, survival, wound healing in skin, cell clustering (Balazs *et al.*, 2001; Weiner *et al.*, 2001; Moolenaar *et al.*, 2004). LIPH has been shown to exert stimulatory effect on proliferation and migration of cells via a G-protein couple receptor P2Y5 encoded by a gene *P2RY5* (Pasternack *et al.*, 2008; Shimomura *et al.*, 2008). Recently, Shimomura *et al.* (2008), Pasternack *et al.* (2008) and Azeem *et al.* (2008) have shown that mutations in *P2RY5* gene result in autosomal recessive hypotrichosis simplex and autosomal recessive woolly hair. Shimomura *et al.* (2008) have provided evidence that *P2RY5* expresses in hair follicle, which has been shown earlier to have an important role in shaping the growing hair (Schlake, 2007). Pasternack *et al.* (2008) have further shown that in contrast to wild-type P2Y5, which co-localized at the plasma membrane with cadherins, truncated P2Y5 accumulated in the endoplasmic reticulum, suggesting a loss of function mutation. Takahashi *et al.* (2008) have shown that both LPA and phosphatidic acid have roles to promote hair growth *in vivo*. Taken together, the mutational and functional studies of *LIPH* and *P2RY5* genes, suggested an integrated model in which LPA, Lipase H and P2Y5 are involved in regulation of hair growth.

In family G, linkage analysis was performed by using microsatellite markers closely linked to previously reported three alopecia and mental retardation loci including APMR1 at 3q26.33-q27.3, APMR2 at 3q26.2-26.31 and APMR3 at 18q11.2-12.2. Recombinations observed in the affected individuals (V-1, V-2 and V-3) showed that APMR locus in family G overlaps with APMR1 (D3S1232 - D3S2436) and APMR2 (D3S1564 - D3S2427) locus. It should also be noted that there is a difference in the clinical phenotypes of the patients of APMR1 and APMR2 families. Patients in the

APMR1 family are severely mentally retarded (IQ from 25 to 30), while for those in the APMR2 family, the mental retardation varies from mild to moderate (IQ from 53 to 61). Since the clinical features of family G are more similar to APMR1, therefore, it is more likely that a gene responsible for APMR1 is also involved in causing APMR phenotypes in family G.

Through a UCSC Genome Browser database search (Karolchik *et al.,* 2003), the linkage interval of APMR locus in family G contains several known and predicted genes and expressed sequence tags (ESTs). Among others, this linkage interval contains human ETS variant gene 5 (*ETV5* MIM 601600), which is involved in the regulation of transcription, *LIPH* (MIM 607365) that regulates hair growth, *TNFSF10* (MIM 603598), *AP2M1* (MIM 601024) and *CAM-K2N2* (MIM 608721) genes. These genes were sequenced in two affected individuals of family G; however, no disease causing mutation was detected.

In family H a genome scan with 390 microsatellite markers, spaced approximately at 10 cM intervals, failed to identify the diseased locus. Therefore, in order to identify the disease locus in this family, it is proposed that a second genome scan may be carried out with microsatellite markers spaced at interval of 5 cM.

In family I linkage was established to hairless (*HR*) gene on chromosome 8p21.2. The entire coding region, as well as intron-exon boundaries of *HR* gene were sequenced in two affected individuals of family I, but failed to identify any functional sequence variant suggesting that the mutation is probably present in the regulatory sequence of the gene.

In human, the *HR* gene appears to function at the cellular transition from the natal to postnatal hair cycle. *HR* gene encodes a putative zinc-finger transcription factor protein of 1189 amino acids. The *HR* protein interacts with and influences the transcriptional activity of several nuclear factors, including thyroid hormone receptor, retinoic acid receptor-related orphan receptor-α and vitamin D receptor (Potter *et al.,* 2001; Hsieh *et al.,* 2003). In *hr* mutant mice, hair follicle morphogenesis and initial hair growth is normal. Hair follicle is the most complex form of all epithelial organ systems and has been slow to yield its molecular secrets.

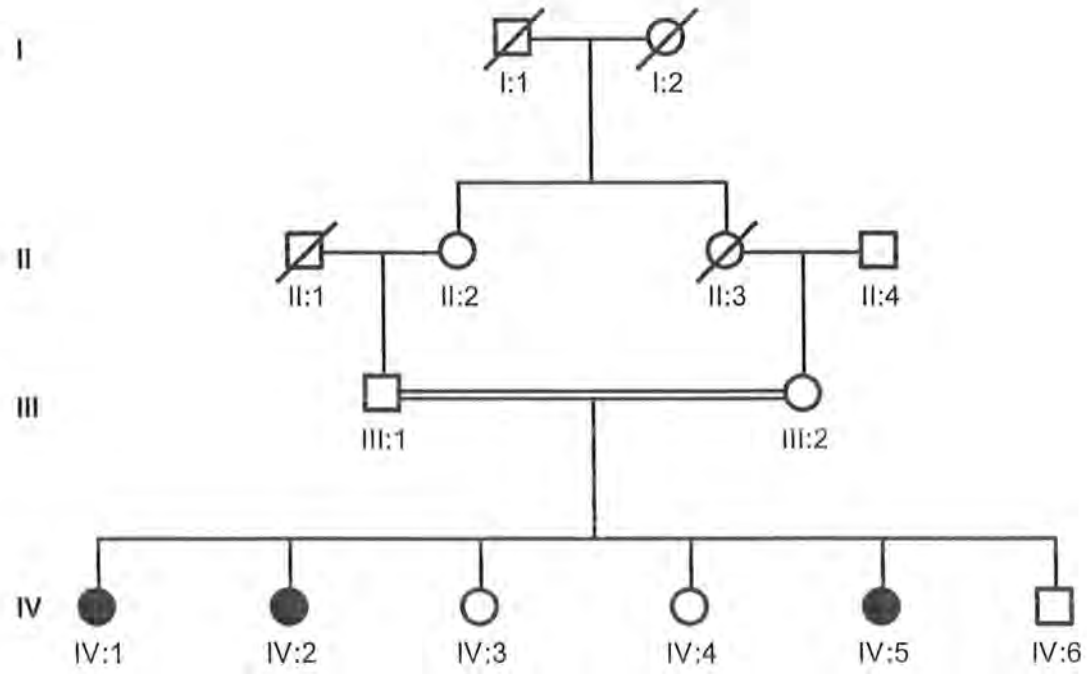

Figure 4.1: Pedigree of family F with autosomal recessive hypotrichosis. Circles represent females, squares represent males. Filled circles and squares represent affected individuals. Double lines indicate consanguineous marriages. Cross lines on the symbols represent deceased individuals.

Figure 4.2: Clinical presentation of autosomal recessive hypotrichosis phenotype in family F. Phenotypic appearance of an affected individual (IV-1) of the family showing sparse hairs on scalp, sparse eyebrows and eyelashes.

Figure 4.3: Scalp skin biopsy of an affected individual (IV-1) of family F reveals keratin-filled cyst within a single hair follicle remnant. *epi* epidermis, *sg* sebaceous glands, *swg* sweat glands, *hf* hair follicle

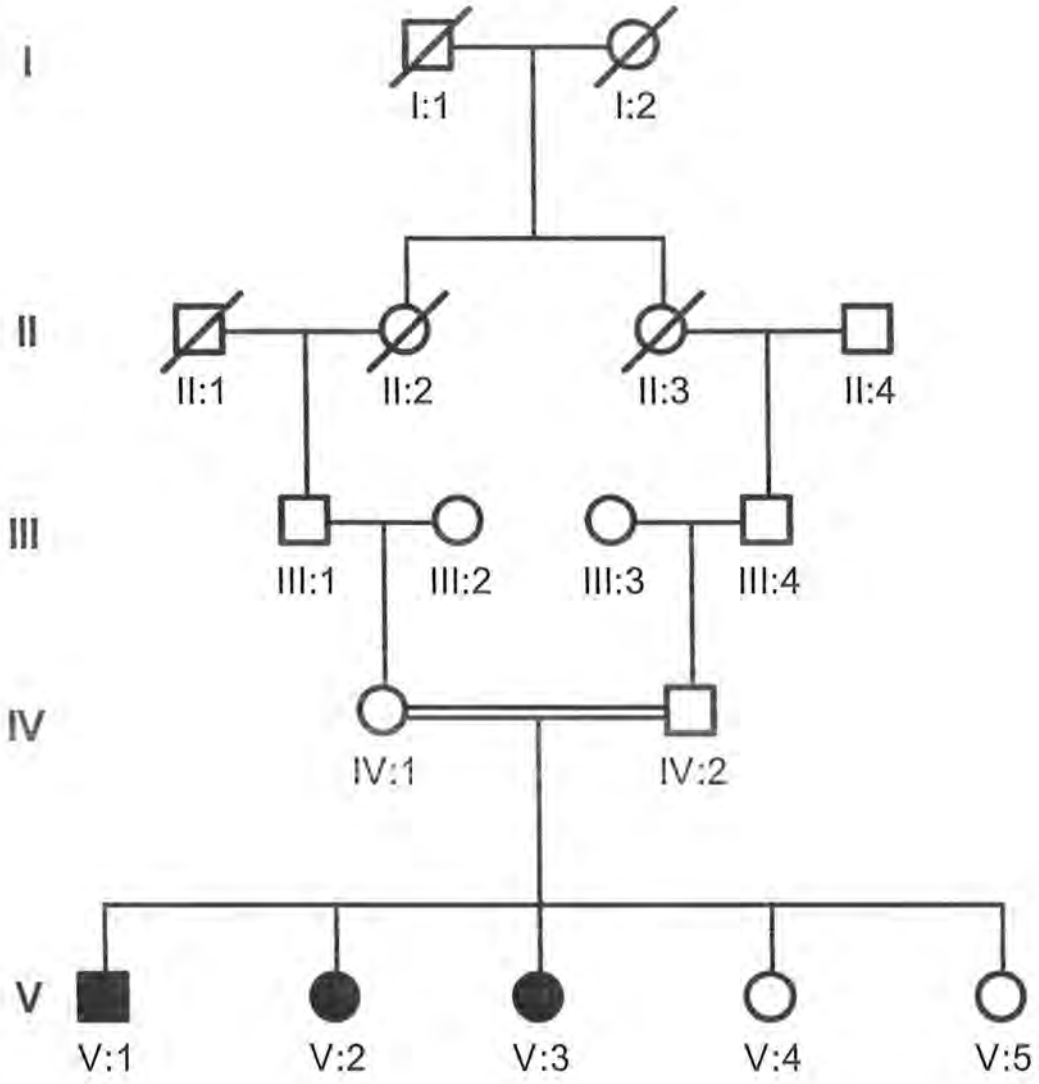

Figure 4.4: Pedigree of family G with alopecia and mental retardation (APMR). Circles represent females, squares represent males. Filled circles and squares represent affected individuals. Double lines indicate consanguineous marriages. Cross lines on the symbols represent deceased individuals.

Figure 4.5: Clinical presentation of APMR family. Phenotypic appearance of an affected individual (V-1) of family G showing complete absence of hair on scalp and missing eyebrows and eyelashes.

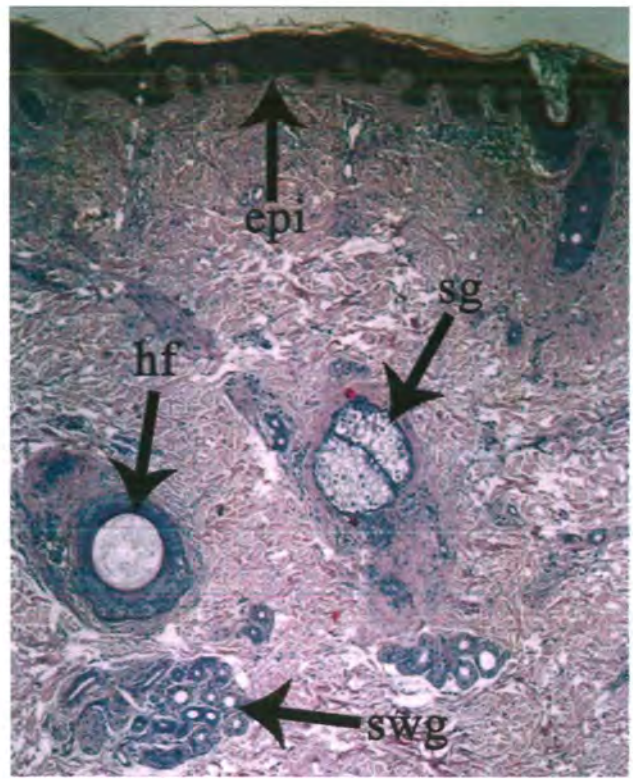

Figure 4.6: Scalp skin biopsy from an affected individual (V-1) of family G revealed complete absence of normal hair follicle structures. The remnants of the hair follicle infundibulum undergo hyperkeratinization. *epi* epidermis, *sg* sebaceous glands, *swg* sweat glands, *hf* hair follicle

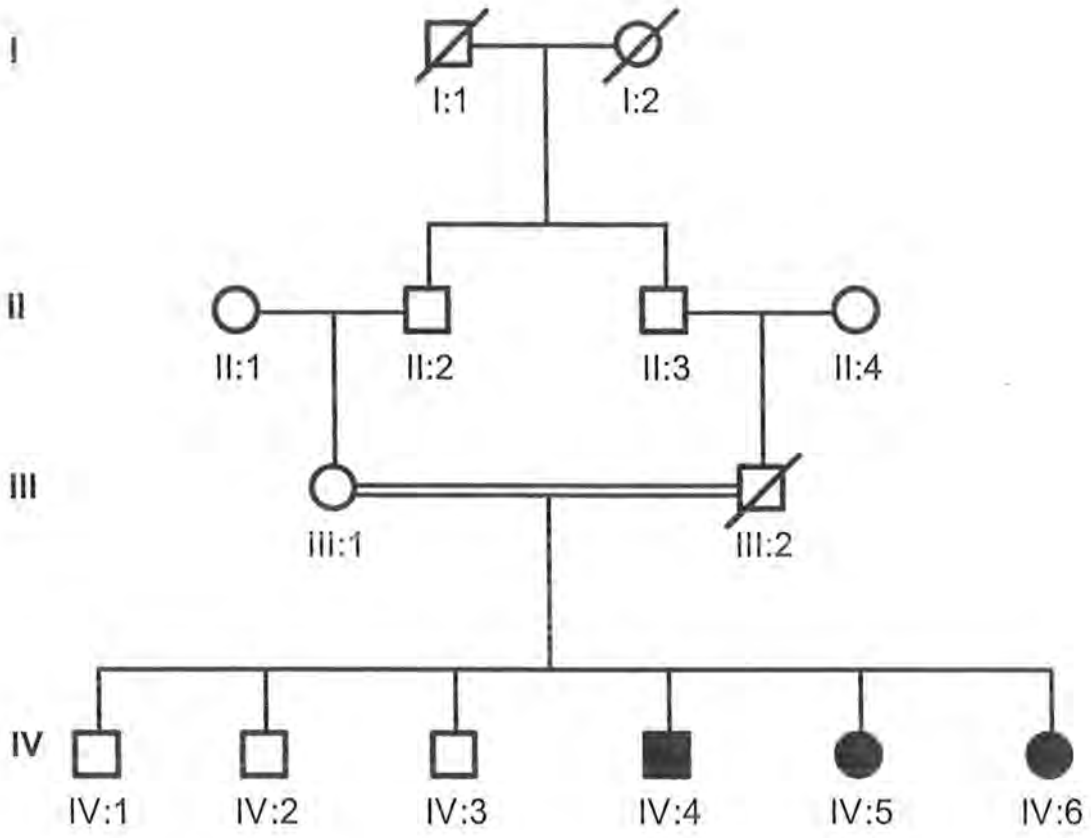

Figure 4.7: Pedigree of family H with autosomal recessive hypotrichosis. Circles represent females, squares represent males. Filled circles and squares represent affected individuals. Double lines indicate consanguineous marriages. Cross lines on the symbols represent deceased individuals.

Figure 4.8: Clinical presentation of family H. Phenotypic appearance of an affected individual (IV-4) of family H showing complete absence of hair on scalp and missing eyebrows and eyelashes.

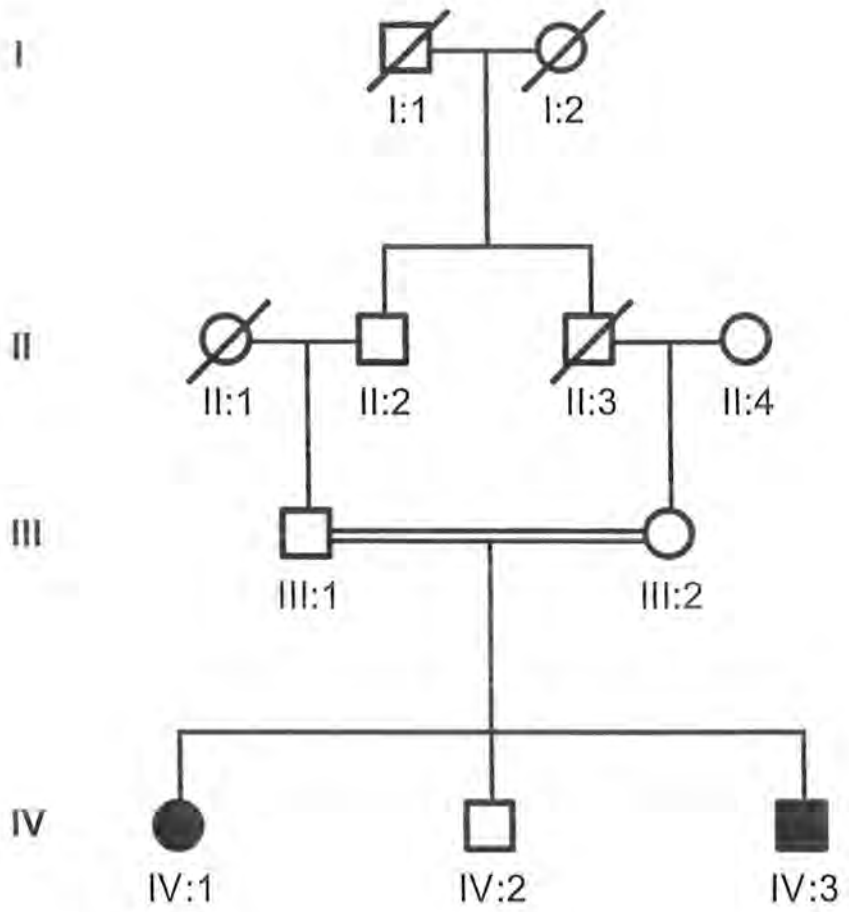

Figure 4.9: Pedigree of family I with autosomal recessive hypotrichosis. Circles represent females, squares represent males. Filled circles and squares represent affected individuals. Double lines indicate consanguineous marriages. Cross lines on the symbols represent deceased individuals.

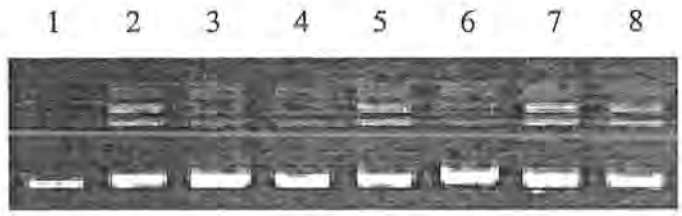

Family F

Lane 1- IV-1	Lane 5- III-2
Lane 2- III-1	Lane 6- IV-3
Lane 3- IV-2	Lane 7- IV-6
Lane 4- IV-5	Lane 8- IV-4

Figure 4.10: Electropherogram of ethidium bromide stained 8% non-denaturing polyacrylamide gel for marker D3S2314 at 201.92 cM on chromosome 3q26.33 showing homozygosity among the affected individuals (IV-1, IV-2 and IV-5) of family F. The Roman numerals indicate the generation numbers of the individuals within a pedigree while Arabic numerals indicate their positions within a generation.

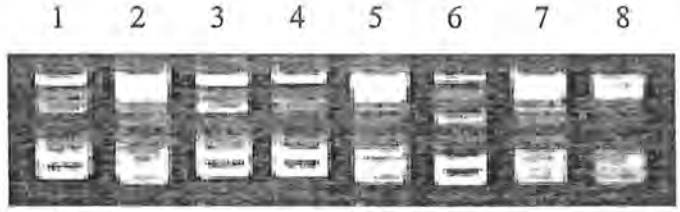

Family F

Lane 1- IV-1	Lane 5- III-2
Lane 2- III-1	Lane 6- IV-3
Lane 3- IV-2	Lane 7- IV-6
Lane 4- IV-5	Lane 8- IV-4

Figure 4.11: Electropherogram of ethidium bromide stained 8% non-denaturing polyacrylamide gel for marker D3S3609 at 205.94 cM on chromosome 3q27.1 showing homozygosity among the affected individuals (IV-1, IV-2 and IV-5) of family F. The Roman numerals indicate the generation numbers of the individuals within a pedigree while Arabic numerals indicate their positions within a generation.

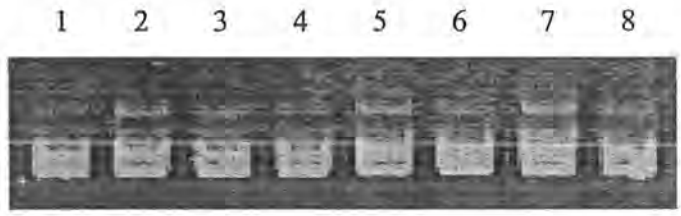

Family F

Lane 1- IV-1	Lane 5- III-2
Lane 2- III-1	Lane 6- IV-3
Lane 3- IV-2	Lane 7- IV-6
Lane 4- IV-5	Lane 8- IV-4

Figure 4.12: Electropherogram of ethidium bromide stained 8% non-denaturing polyacrylamide gel for marker D3S3578 at 205.94 cM on chromosome 3q27.1 showing homozygosity among the affected individuals (IV-1, IV-2 and IV-5) of family F. The Roman numerals indicate the generation numbers of the individuals within a pedigree while Arabic numerals indicate their positions within a generation.

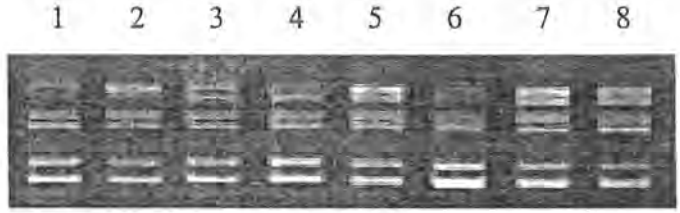

Family F

Lane 1- IV-1	Lane 5- III-2
Lane 2- III-1	Lane 6- IV-3
Lane 3- IV-2	Lane 7- IV-6
Lane 4- IV-5	Lane 8- IV-4

Figure 4.13: Electropherogram of ethidium bromide stained 8% non-denaturing polyacrylamide gel for marker D3S3583 at 205.94 cM on chromosome 3q27.1 showing homozygosity among the affected individuals (IV-1, IV-2 and IV-5) of family F. The Roman numerals indicate the generation numbers of the individuals within a pedigree while Arabic numerals indicate their positions within a generation.

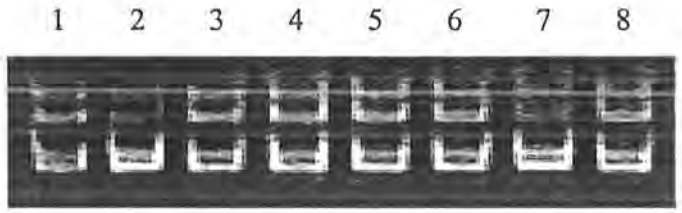

Family F

Lane 1- IV-1	Lane 5- III-2
Lane 2- III-1	Lane 6- IV-3
Lane 3- IV-2	Lane 7- IV-6
Lane 4- IV-5	Lane 8- IV-4

Figure 4.14: Electropherogram of ethidium bromide stained 8% non-denaturing polyacrylamide gel for marker D3S3546 at 163.25 cM on chromosome 3q23. The Roman numerals indicate the generation numbers of the individuals within a pedigree while Arabic numerals indicate their positions within a generation.

Family F

Lane 1- IV-1	Lane 5- III-2
Lane 2- III-1	Lane 6- IV-3
Lane 3- IV-2	Lane 7- IV-6
Lane 4- IV-5	Lane 8- IV-4

Figure 4.15: Electropherogram of ethidium bromide stained 8% non-denaturing polyacrylamide gel for marker D3S3022 at 172.35 cM on chromosome 3q25.1. The Roman numerals indicate the generation numbers of the individuals within a pedigree while Arabic numerals indicate their positions within a generation.

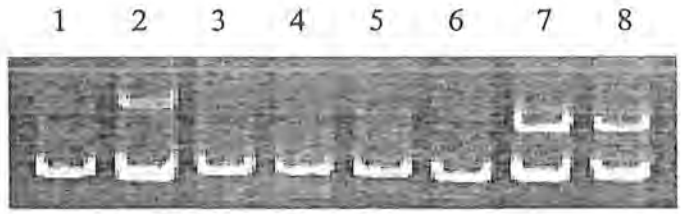

Family F

Lane 1- IV-1	Lane 5- III-2
Lane 2- III-1	Lane 6- IV-3
Lane 3- IV-2	Lane 7- IV-6
Lane 4- IV-5	Lane 8- IV-4

Figure 4.16: Electropherogram of ethidium bromide stained 8% non-denaturing polyacrylamide gel for marker D3S1746 at 175 cM on chromosome 3q25.1. The Roman numerals indicate the generation numbers of the individuals within a pedigree while Arabic numerals indicate their positions within a generation.

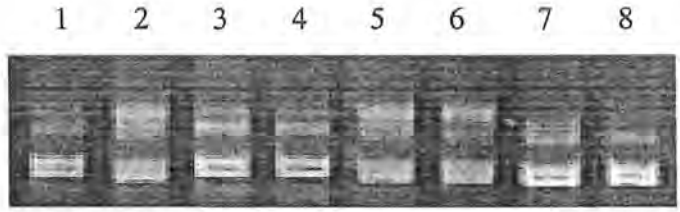

Family F

Lane 1- IV-1	Lane 5- III-2
Lane 2- III-1	Lane 6- IV-3
Lane 3- IV-2	Lane 7- IV-6
Lane 4- IV-5	Lane 8- IV-4

Figure 4.17: Electropherogram of ethidium bromide stained 8% non-denaturing polyacrylamide gel for marker D3S3668 at 181.99 cM on chromosome 3q26.1. The Roman numerals indicate the generation numbers of the individuals within a pedigree while Arabic numerals indicate their positions within a generation.

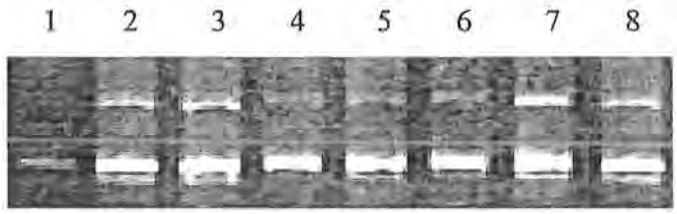

Family F

Lane 1- IV-1	Lane 5- III-2
Lane 2- III-1	Lane 6- IV-3
Lane 3- IV-2	Lane 7- IV-6
Lane 4- IV-5	Lane 8- IV-4

Figure 4.18: Electropherogram of ethidium bromide stained 8% non-denaturing polyacrylamide gel for marker D3S3555 at 182.39 cM on chromosome 3q26.1 showing homozygosity among the affected individuals (IV-1, IV-2 and IV-5) of family F. The Roman numerals indicate the generation numbers of the individuals within a pedigree while Arabic numerals indicate their positions within a generation.

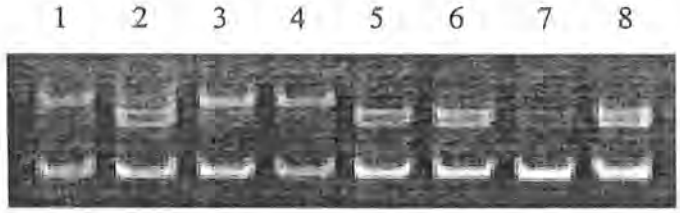

Family F

Lane 1- IV-1	Lane 5- III-2
Lane 2- III-1	Lane 6- IV-3
Lane 3- IV-2	Lane 7- IV-6
Lane 4- IV-5	Lane 8- IV-4

Figure 4.19: Electropherogram of ethidium bromide stained 8% non-denaturing polyacrylamide gel for marker D3S1763 at 182.92 cM on chromosome 3q26.1 showing homozygosity among the affected individuals (IV-1, IV-2 and IV-5) of family F. The Roman numerals indicate the generation numbers of the individuals within a pedigree while Arabic numerals indicate their positions within a generation.

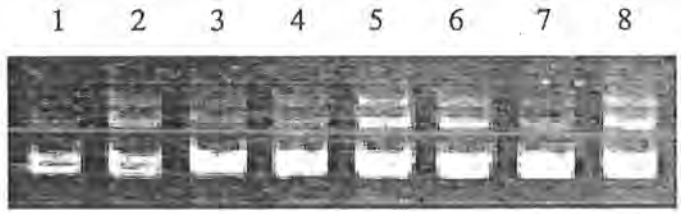

Family F

Lane 1- IV-1	Lane 5- III-2
Lane 2- III-1	Lane 6- IV-3
Lane 3- IV-2	Lane 7- IV-6
Lane 4- IV-5	Lane 8- IV-4

Figure 4.20: Electropherogram of ethidium bromide stained 8% non-denaturing polyacrylamide gel for marker D3S1243 at 184.25 cM on chromosome 3q26.2 showing homozygosity among the affected individuals (IV-1, IV-2 and IV-5) of family F. The Roman numerals indicate the generation numbers of the individuals within a pedigree while Arabic numerals indicate their positions within a generation.

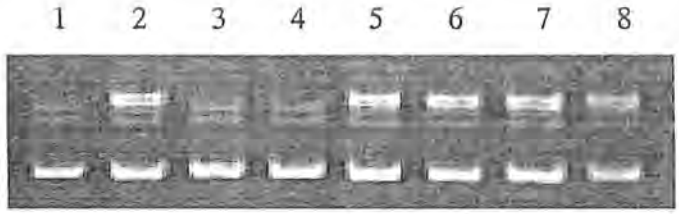

Family F

Lane 1- IV-1	Lane 5- III-2
Lane 2- III-1	Lane 6- IV-3
Lane 3- IV-2	Lane 7- IV-6
Lane 4- IV-5	Lane 8- IV-4

Figure 4.21: Electropherogram of ethidium bromide stained 8% non-denaturing polyacrylamide gel for marker D3S2433 on chromosome 3q26.31 showing homozygosity among the affected individuals (IV-1, IV-2 and IV-5) of family F. The Roman numerals indicate the generation numbers of the individuals within a pedigree while Arabic numerals indicate their positions within a generation.

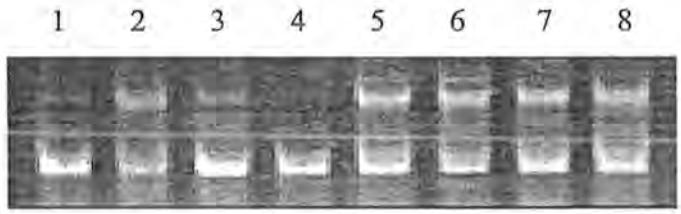

Family F

Lane 1- IV-1	Lane 5- III-2
Lane 2- III-1	Lane 6- IV-3
Lane 3- IV-2	Lane 7- IV-6
Lane 4- IV-5	Lane 8- IV-4

Figure 4.22: Electropherogram of ethidium bromide stained 8% non-denaturing polyacrylamide gel for marker D3S1574 at 187.86 cM on chromosome 3q26.31 showing homozygosity among the affected individuals (IV-1, IV-2 and IV-5) of family F. The Roman numerals indicate the generation numbers of the individuals within a pedigree while Arabic numerals indicate their positions within a generation.

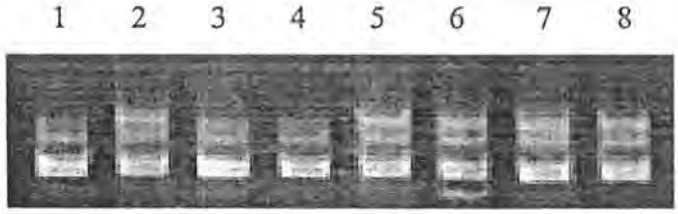

Family F

Lane 1- IV-1	Lane 5- III-2
Lane 2- III-1	Lane 6- IV-3
Lane 3- IV-2	Lane 7- IV-6
Lane 4- IV-5	Lane 8- IV-4

Figure 4.23: Electropherogram of ethidium bromide stained 8% non-denaturing polyacrylamide gel for marker D3S3725 at 188.36 cM on chromosome 3q26.31 showing homozygosity among the affected individuals (IV-1, IV-2 and IV-5) of family F. The Roman numerals indicate the generation numbers of the individuals within a pedigree while Arabic numerals indicate their positions within a generation.

Family F

Lane 1- IV-1	Lane 5- III-2
Lane 2- III-1	Lane 6- IV-3
Lane 3- IV-2	Lane 7- IV-6
Lane 4- IV-5	Lane 8- IV-4

Figure 4.24: Electropherogram of ethidium bromide stained 8% non-denaturing polyacrylamide gel for marker D3S2427 at 195.85 cM on chromosome 3q26.31-q26.32 showing homozygosity among the affected individuals (IV-1, IV-2 and IV-5) of family F. The Roman numerals indicate the generation numbers of the individuals within a pedigree while Arabic numerals indicate their positions within a generation.

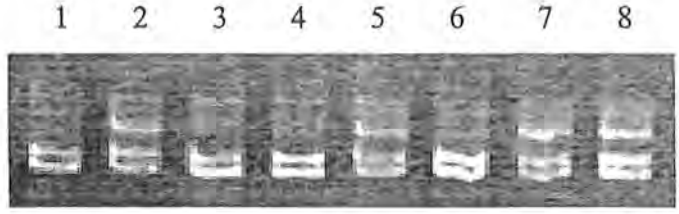

Family F

Lane 1- IV-1	Lane 5- III-2
Lane 2- III-1	Lane 6- IV-3
Lane 3- IV-2	Lane 7- IV-6
Lane 4- IV-5	Lane 8- IV-4

Figure 4.25: Electropherogram of ethidium bromide stained 8% non-denaturing polyacrylamide gel for marker D3S3676 at 196.01 cM on chromosome 3q26.32 showing homozygosity among the affected individuals (IV-1, IV-2 and IV-5) of family F. The Roman numerals indicate the generation numbers of the individuals within a pedigree while Arabic numerals indicate their positions within a generation.

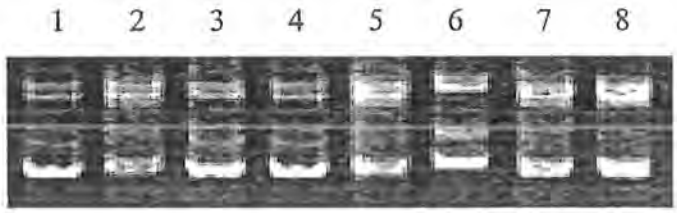

Family F

Lane 1- IV-1	Lane 5- III-2
Lane 2- III-1	Lane 6- IV-3
Lane 3- IV-2	Lane 7- IV-6
Lane 4- IV-5	Lane 8- IV-4

Figure 4.26: Electropherogram of ethidium bromide stained 8% non-denaturing polyacrylamide gel for marker D3S2412 at 197.17 cM on chromosome 3q26.32 showing homozygosity among the affected individuals (IV-1, IV-2 and IV-5) of family F. The Roman numerals indicate the generation numbers of the individuals within a pedigree while Arabic numerals indicate their positions within a generation.

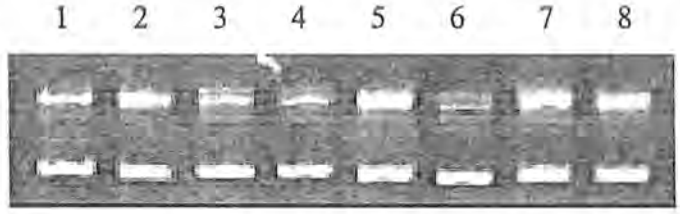

Family F

Lane 1- IV-1	Lane 5- III-2
Lane 2- III-1	Lane 6- IV-3
Lane 3- IV-2	Lane 7- IV-6
Lane 4- IV-5	Lane 8- IV-4

Figure 4.27: Electropherogram of ethidium bromide stained 8% non-denaturing polyacrylamide gel for marker D3S3037 on chromosome 3q26.32. The Roman numerals indicate the generation numbers of the individuals within a pedigree while Arabic numerals indicate their positions within a generation.

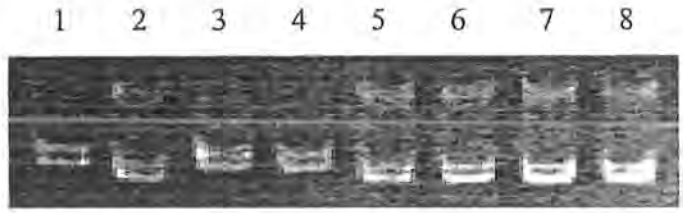

Family F

Lane 1- IV-1	Lane 5- III-2
Lane 2- III-1	Lane 6- IV-3
Lane 3- IV-2	Lane 7- IV-6
Lane 4- IV-5	Lane 8- IV-4

Figure 4.28: Electropherogram of ethidium bromide stained 8% non-denaturing polyacrylamide gel for marker D3S1232 on chromosome 3q26.33 showing homozygosity among the affected individuals (IV-1, IV-2 and IV-5) of family F. The Roman numerals indicate the generation numbers of the individuals within a pedigree while Arabic numerals indicate their positions within a generation.

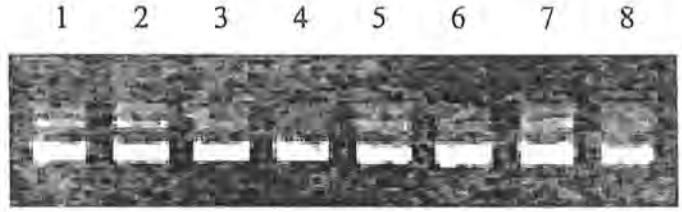

Family F

Lane 1- IV-1	Lane 5- III-2
Lane 2- III-1	Lane 6- IV-3
Lane 3- IV-2	Lane 7- IV-6
Lane 4- IV-5	Lane 8- IV-4

Figure 4.29: Electropherogram of ethidium bromide stained 8% non-denaturing polyacrylamide gel for marker D3S1602 at 209.79 cM on chromosome 3q27.2-q27.3. The Roman numerals indicate the generation number of the individuals within a pedigree while Arabic numerals indicate their positions within a generation.

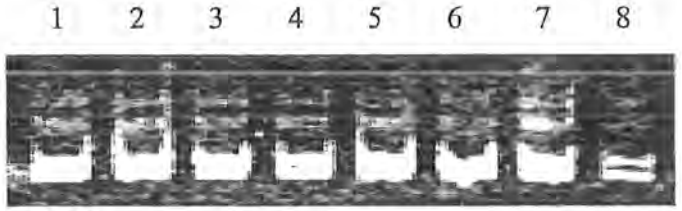

Family F

Lane 1- IV-1	Lane 5- III-2
Lane 2- III-1	Lane 6- IV-3
Lane 3- IV-2	Lane 7- IV-6
Lane 4- IV-5	Lane 8- IV-4

Figure 4.30: Electropherogram of ethidium bromide stained 8% non-denaturing polyacrylamide gel for marker D3S3651 at 214.9 cM on chromosome 3q27.3. The Roman numerals indicate the generation numbers of the individuals within a pedigree while Arabic numerals indicate their positions within a generation.

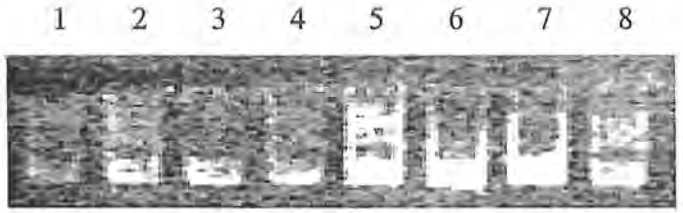

Family F

Lane 1- IV-1	Lane 5- III-2
Lane 2- III-1	Lane 6- IV-3
Lane 3- IV-2	Lane 7- IV-6
Lane 4- IV-5	Lane 8- IV-4

Figure 4.31: Electropherogram of ethidium bromide stained 8% non-denaturing polyacrylamide gel for marker D3S3628 at 215.71 cM on chromosome 3q27.3. The Roman numerals indicate the generation numbers of the individuals within a pedigree while Arabic numerals indicate their positions within a generation.

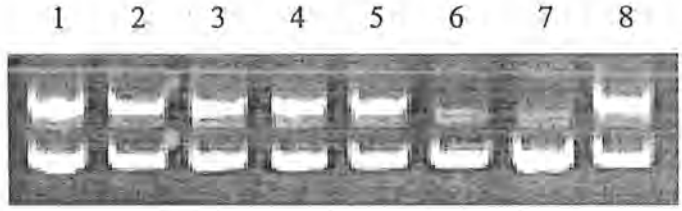

Family F

Lane 1- IV-1	Lane 5- III-2
Lane 2- III-1	Lane 6- IV-3
Lane 3- IV-2	Lane 7- IV-6
Lane 4- IV-5	Lane 8- IV-4

Figure 4.32: Electropherogram of ethidium bromide stained 8% non-denaturing polyacrylamide gel for marker D3S2398 at 219.79 cM on chromosome 3q28. The Roman numerals indicate the generation numbers of the individuals within a pedigree while Arabic numerals indicate their positions within a generation.

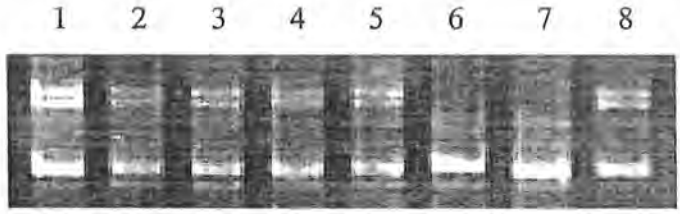

Family F

Lane 1- IV-1	Lane 5- III-2
Lane 2- III-1	Lane 6- IV-3
Lane 3- IV-2	Lane 7- IV-6
Lane 4- IV-5	Lane 8- IV-4

Figure 4.33: Electropherogram of ethidium bromide stained 8% non-denaturing polyacrylamide gel for marker D3S1661 at 220.19 cM on chromosome 3q28. The Roman numerals indicate the generation numbers of the individuals within a pedigree while Arabic numerals indicate their positions within a generation.

Table 4.1: Two point LOD score results between the AH locus and chromosome 3q27 markers

Marker	Rutger map (cM)[a]	Physical position[b]	LOD score at recombination fraction θ =						
			0	0.01	0.05	0.1	0.2	0.3	0.4
D3S3546	152.41	144,198,259	−1.57	−0.93	−0.38	−0.17	−0.04	−0.02	−0.03
D3S3022	161.15	150,771,025	1.88	1.83	1.64	1.4	0.93	0.49	0.14
D3S1746	164.04	153,212,439	0.97	0.95	0.87	0.76	0.54	0.32	0.13
D3S3668	171.06	165,829,800	1.88	1.83	1.64	1.4	0.93	0.49	0.14
D3S3555	171.50	167,352,572	0.97	0.95	0.87	0.76	0.54	0.32	0.13
D3S1763	172.05	168,722,402	1.88	1.83	1.64	1.4	0.93	0.49	0.14
D3S1243	173.38	169,835,456	1.88	1.83	1.64	1.4	0.93	0.49	0.14
D3S2433	NA	173,178,370	1.88	1.83	1.64	1.4	0.93	0.49	0.14
D3S1574	176.98	173,161,822	1.88	1.83	1.64	1.4	0.93	0.49	0.14
D3S3725	177.24	173,292,342	1.88	1.83	1.64	1.4	0.93	0.49	0.14
D3S2427	184.55	177,267,503	1.88	1.83	1.64	1.4	0.93	0.49	0.14
D3S3676	184.55	177,871,163	1.88	1.83	1.64	1.4	0.93	0.49	0.14
D3S2412	185.85	178,547,264	1.88	1.83	1.64	1.4	0.93	0.49	0.14
D3S3037	NA	178,924,191	1.88	1.83	1.64	1.4	0.93	0.49	0.14
D3S1232	189.00	182,902,479	1.88	1.83	1.64	1.4	0.93	0.49	0.14
D3S2314	190.04	183,613,382	1.88	1.83	1.64	1.4	0.93	0.49	0.14
D3S3609	193.97	185,519,714	1.88	1.83	1.64	1.4	0.93	0.49	0.14
D3S3578	193.97	185,567,441	1.88	1.83	1.64	1.4	0.93	0.49	0.14
D3S3583	193.97	185,767,863	1.88	1.83	1.64	1.4	0.93	0.49	0.14
D3S1602	197.63	187,514,449	−inf	−1.86	−0.62	−0.21	0.02	0.05	0.02
D3S3651	202.71	189,123,933	−inf	−1.86	−0.62	−0.21	0.02	0.05	0.02
D3S3628	203.50	189,256,383	−inf	−3.44	−1.5	−0.78	−0.24	−0.06	−0.01
D3S2398	207.05	190,903,729	−1.35	−0.67	−0.17	−0.04	−0.02	−0.02	−0.01
D3S1661	207.72	191,166,400	−1.35	−0.67	−0.17	−0.04	−0.02	−0.02	−0.01

[a] Average-sex distance in cM according to the Rutgers combined linkage-physical human genome map (Kong *et al.*, 2004)

[b] The physical position is based according to build 36 of the human genome (International Human Genome Sequence Consortium, 2001)

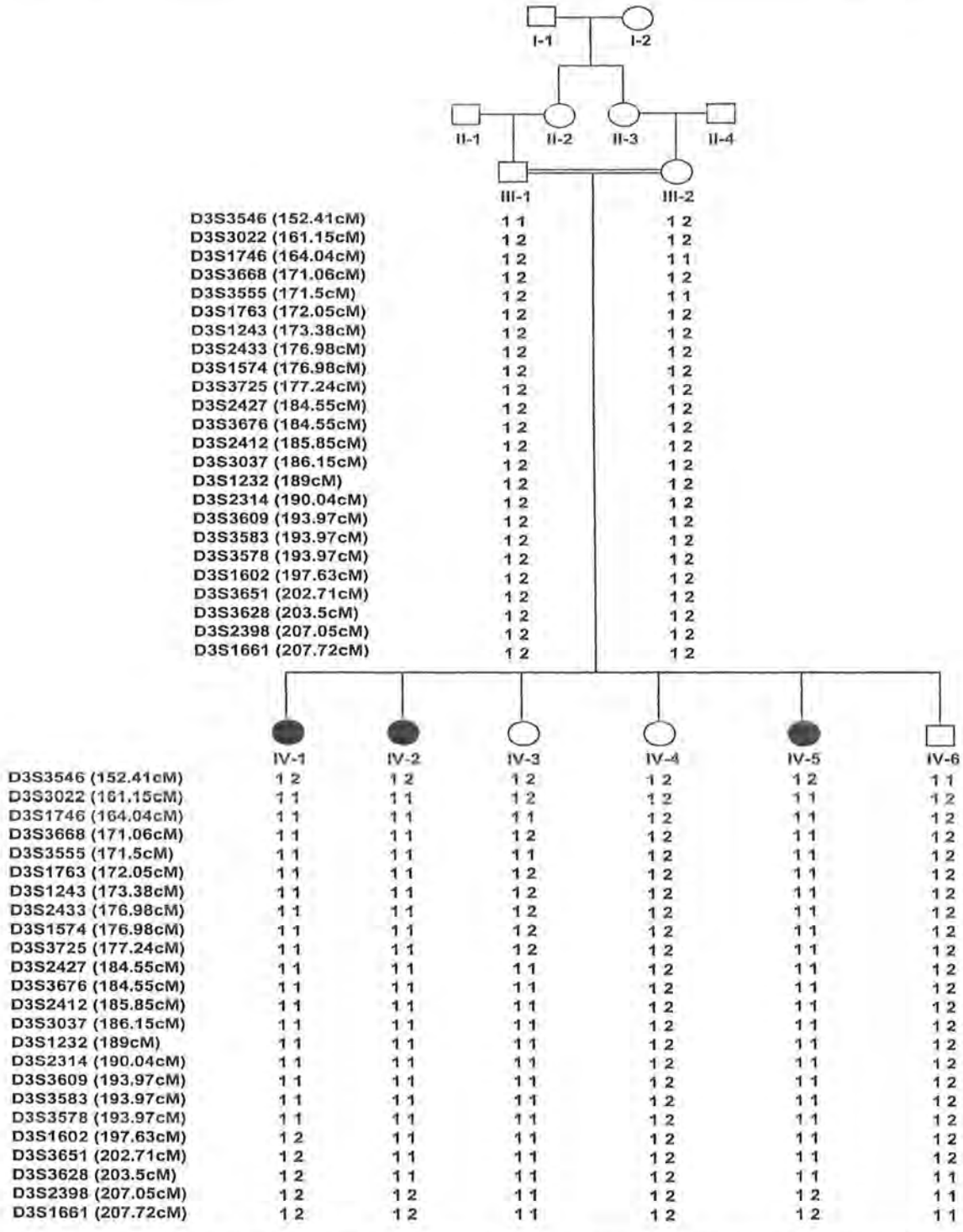

Figure 4.34: Pedigree of family F that segregates autosomal recessive hypotrichosis (AH/LAH2). Haplotypes for most closely linked short tandem repeats polymorphism (STRPs) are shown below each symbol. Map distances are given in centimorgans (cM) according to the Rutgers linkage-physical map of the human genome. The disease-associated haplotypes are shown beneath each symbol. Haplotypes were generated by SIMWALK2

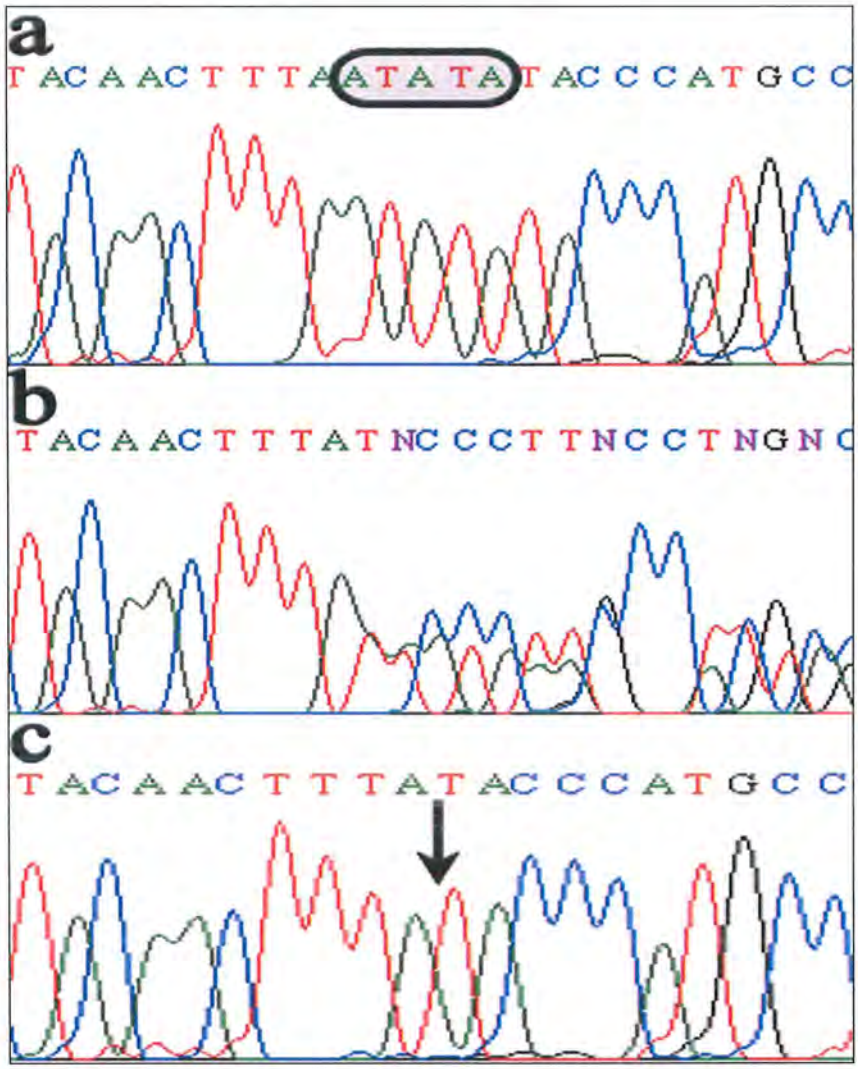

Figure 4.35: Sequence analysis of the *LIPH* gene mutation. DNA sequence of exon 2 from control individual (**a**), heterozygous carrier (**b**) and homozygous affected individual (**c**). The boxed area containing 5 bp sequence ATATA in (**a**) represents the sequence deleted in the homozygous state in affected individual (**c**), resulting in the frameshift and downstream premature termination codon.

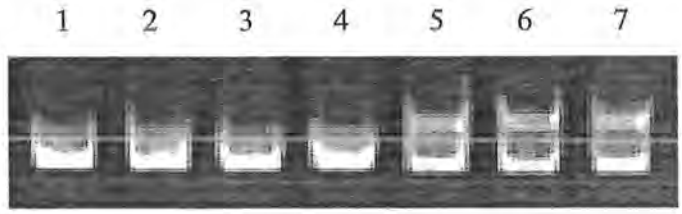

Family G

Lane 1- V-1
Lane 2- IV-1
Lane 3- V-2
Lane 4- V-3
Lane 5- V-4
Lane 6- V-5
Lane 7- IV-2

Figure 4.36: Electropherogram of ethidium bromide stained 8% non-denaturing polyacrylamide gel for marker D3S3699 at 200.19 cM on chromosome 3q26.33 showing homozygosity among the affected individuals (V-1, V-2 and V-3) of family G. The Roman numerals indicate the generation numbers of the individuals within a pedigree while Arabic numerals indicate their positions within a generation.

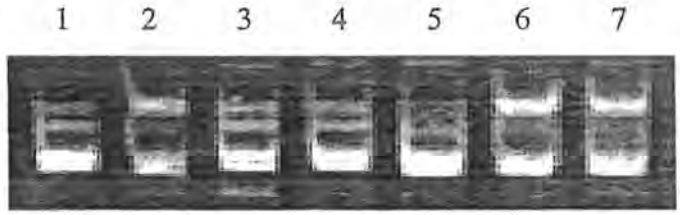

Family G

Lane 1- V-1
Lane 2- IV-1
Lane 3- V-2
Lane 4- V-3
Lane 5- V-4
Lane 6- V-5
Lane 7- IV-2

Figure 4.37: Electropherogram of ethidium bromide stained 8% non-denaturing polyacrylamide gel for marker D3S3609 at 205.94 cM on chromosome 3q27.1 showing homozygosity among the affected individuals (V-1, V-2 and V-3) of family G. The Roman numerals indicate the generation numbers of the individuals within a pedigree while Arabic numerals indicate their positions within a generation.

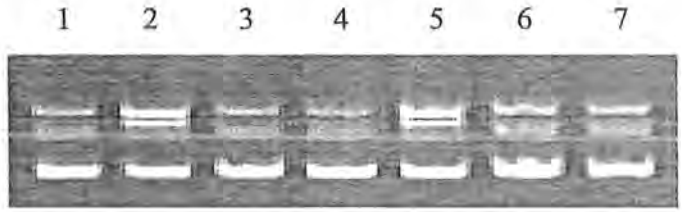

Family G

Lane 1- V-1
Lane 2- IV-1
Lane 3- V-2
Lane 4- V-3
Lane 5- V-4
Lane 6- V-5
Lane 7- IV-2

Figure 4.38: Electropherogram of ethidium bromide stained 8% non-denaturing polyacrylamide gel for marker D3S3723 at 185.79 on chromosome 3q26.31 showing homozygosity among the affected individuals (V-1, V-2 and V-3) of family G. The Roman numerals indicate the generation numbers of the individuals within a pedigree while Arabic numerals indicate their positions within a generation.

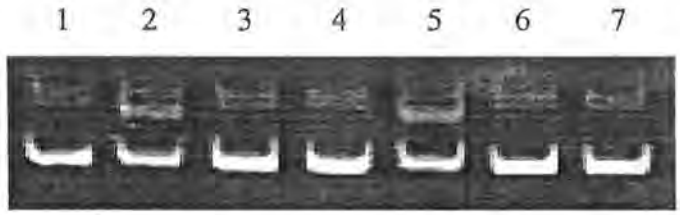

Family G

Lane 1- V-1
Lane 2- IV-1
Lane 3- V-2
Lane 4- V-3
Lane 5- V-4
Lane 6- V-5
Lane 7- IV-2

Figure 4.39: Electropherogram of ethidium bromide stained 8% non-denaturing polyacrylamide gel for marker D3S2427 at 195.85 cM on chromosome 3q26.31-q26.32 showing homozygosity among the affected individuals (V-1, V-2 and V-3) of family G. The Roman numerals indicate the generation numbers of the individuals within a pedigree while Arabic numerals indicate their positions within a generation.

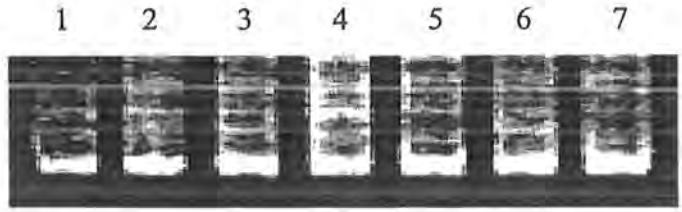

Family G

Lane 1- V-1
Lane 2- IV-1
Lane 3- V-2
Lane 4- V-3
Lane 5- V-4
Lane 6- V-5
Lane 7- IV-2

Figure 4.40: Electropherogram of ethidium bromide stained 8% non-denaturing polyacrylamide gel for marker D3S3626 on chromosome 3q24. The Roman numerals indicate the generation numbers of the individuals within a pedigree while Arabic numerals indicate their positions within a generation.

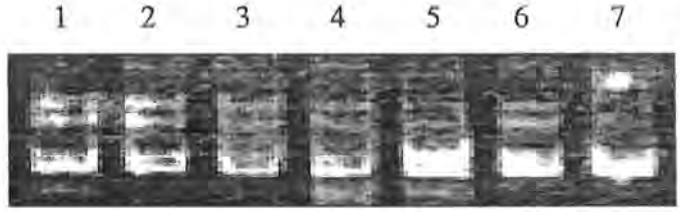

Family G

Lane 1- V-1
Lane 2- IV-1
Lane 3- V-2
Lane 4- V-3
Lane 5- V-4
Lane 6- V-5
Lane 7- IV-2

Figure 4.41: Electropherogram of ethidium bromide stained 8% non-denaturing polyacrylamide gel for marker D3S3022 at 172.35 cM on chromosome 3q25.1. The Roman numerals indicate the generation numbers of the individuals within a pedigree while Arabic numerals indicate their positions within a generation.

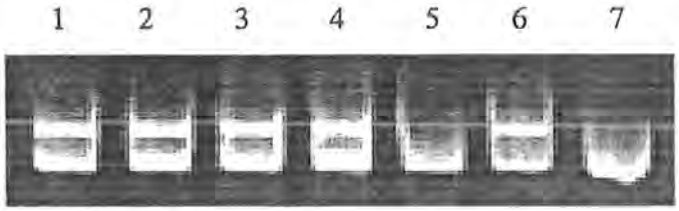

Family G

Lane 1- V-1
Lane 2- IV-1
Lane 3- V-2
Lane 4- V-3
Lane 5- V-4
Lane 6- V-5
Lane 7- IV-2

Figure 4.42: Electropherogram of ethidium bromide stained 8% non-denaturing polyacrylamide gel for marker D3S1299 at 172.95 cM on chromosome 3q25.1 showing homozygosity among the affected individuals (V-1, V-2 and V-3) of family G. The Roman numerals indicate the generation numbers of the individuals within a pedigree while Arabic numerals indicate their positions within a generation.

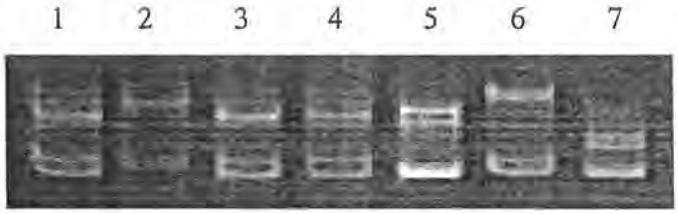

Family G

Lane 1- V-1
Lane 2- IV-1
Lane 3- V-2
Lane 4- V-3
Lane 5- V-4
Lane 6- V-5
Lane 7- IV-2

Figure 4.43: Electropherogram of ethidium bromide stained 8% non-denaturing polyacrylamide gel for marker D3S1746 at 175 cM on chromosome 3q25.1 showing homozygosity among the affected individuals (V-1, V-2 and V-3) of family G. The Roman numerals indicate the generation numbers of the individuals within a pedigree while Arabic numerals indicate their positions within a generation.

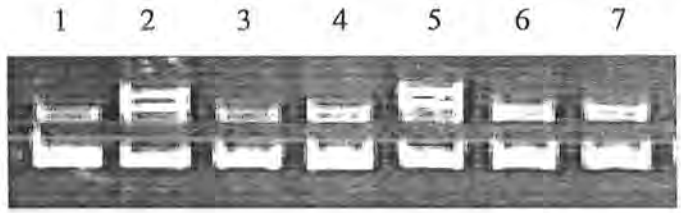

Family G

Lane 1- V-1
Lane 2- IV-1
Lane 3- V-2
Lane 4- V-3
Lane 5- V-4
Lane 6- V-5
Lane 7- IV-2

Figure 4.44: Electropherogram of ethidium bromide stained 8% non-denaturing polyacrylamide gel for marker D3S1763 at 182.92 cM on chromosome 3q26.1 showing homozygosity among the affected individuals (V-1, V-2 and V-3) of family G. The Roman numerals indicate the generation numbers of the individuals within a pedigree while Arabic numerals indicate their positions within a generation.

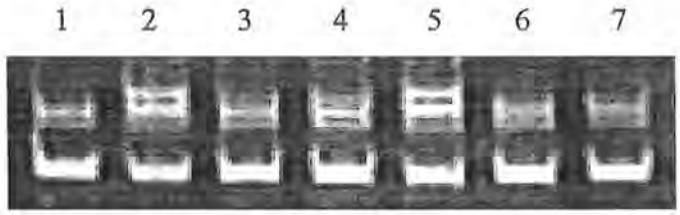

Family G

Lane 1- V-1
Lane 2- IV-1
Lane 3- V-2
Lane 4- V-3
Lane 5- V-4
Lane 6- V-5
Lane 7- IV-2

Figure 4.45: Electropherogram of ethidium bromide stained 8% non-denaturing polyacrylamide gel for marker D3S3622 at 183.76 cM on chromosome 3q26.1 showing homozygosity among the affected individuals (V-1, V-2 and V-3) of family G. The Roman numerals indicate the generation numbers of the individuals within a pedigree while Arabic numerals indicate their positions within a generation.

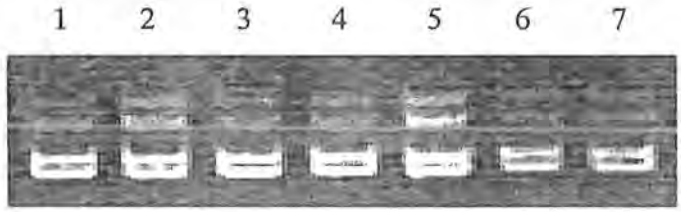

Family G

Lane 1- V-1
Lane 2- IV-1
Lane 3- V-2
Lane 4- V-3
Lane 5- V-4
Lane 6- V-5
Lane 7- IV-2

Figure 4.46: Electropherogram of ethidium bromide stained 8% non-denaturing polyacrylamide gel for marker D3S1282 at 184.79 cM on chromosome 3q26.2 showing homozygosity among the affected individuals (V-1, V-2 and V-3) of family G. The Roman numerals indicate the generation numbers of the individuals within a pedigree while Arabic numerals indicate their positions within a generation.

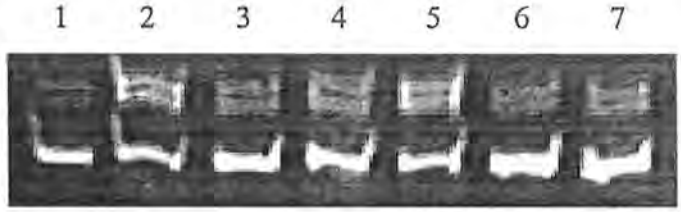

Family G

Lane 1- V-1
Lane 2- IV-1
Lane 3- V-2
Lane 4- V-3
Lane 5- V-4
Lane 6- V-5
Lane 7- IV-2

Figure 4.47: Electropherogram of ethidium bromide stained 8% non-denaturing polyacrylamide gel for marker D3S2433 on chromosome 3q26.31 showing homozygosity among the affected individuals (V-1, V-2 and V-3) of family G. The Roman numerals indicate the generation numbers of the individuals within a pedigree while Arabic numerals indicate their positions within a generation.

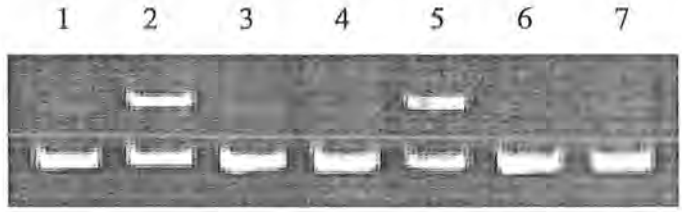

Family G

Lane 1- V-1
Lane 2- IV-1
Lane 3- V-2
Lane 4- V-3
Lane 5- V-4
Lane 6- V-5
Lane 7- IV-2

Figure 4.48: Electropherogram of ethidium bromide stained 8% non-denaturing polyacrylamide gel for marker D3S3676 at 196.01 cM on chromosome 3q26.32 showing homozygosity among the affected individuals (V-1, V-2 and V-3) of family G. The Roman numerals indicate the generation numbers of the individuals within a pedigree while Arabic numerals indicate their positions within a generation.

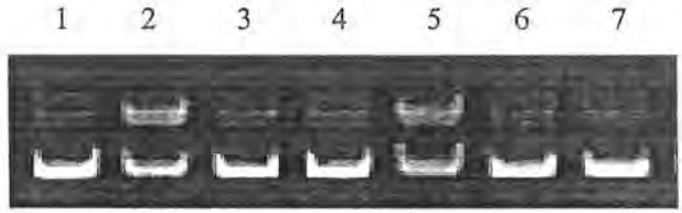

Family G

Lane 1- V-1
Lane 2- IV-1
Lane 3- V-2
Lane 4- V-3
Lane 5- V-4
Lane 6- V-5
Lane 7- IV-2

Figure 4.49: Electropherogram of ethidium bromide stained 8% non-denaturing polyacrylamide gel for marker D3S3037 on chromosome 3q26.32 showing homozygosity among the affected individuals (V-1, V-2 and V-3) of family G. The Roman numerals indicate the generation numbers of the individuals within a pedigree while Arabic numerals indicate their positions within a generation.

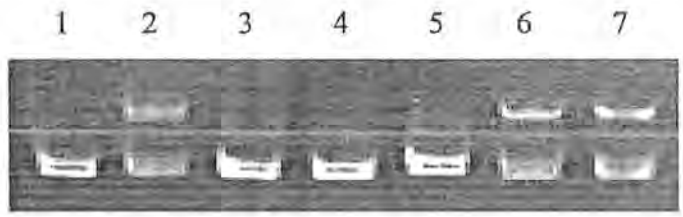

Family G

Lane 1- V-1
Lane 2- IV-1
Lane 3- V-2
Lane 4- V-3
Lane 5- V-4
Lane 6- V-5
Lane 7- IV-2

Figure 4.50: Electropherogram of ethidium bromide stained 8% non-denaturing polyacrylamide gel for marker D3S3730 at 199.44 cM on chromosome 3q26.32 showing homozygosity among the affected individuals (V-1, V-2 and V-3) of family G. The Roman numerals indicate the generation numbers of the individuals within a pedigree while Arabic numerals indicate their positions within a generation.

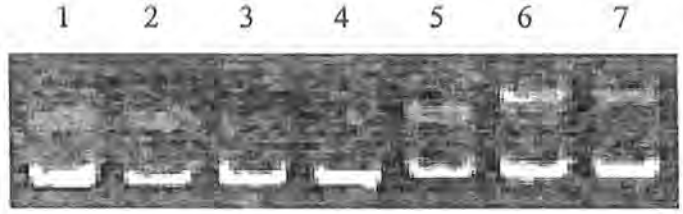

Family G

Lane 1- V-1
Lane 2- IV-1
Lane 3- V-2
Lane 4- V-3
Lane 5- V-4
Lane 6- V-5
Lane 7- IV-2

Figure 4.51: Electropherogram of ethidium bromide stained 8% non-denaturing polyacrylamide gel for marker D3S1617 at 208.48 cM on chromosome 3 showing homozygosity among the affected individuals (V-1, V-2 and V-3) of family G. The Roman numerals indicate the generation numbers of the individuals within a pedigree while Arabic numerals indicate their positions within a generation.

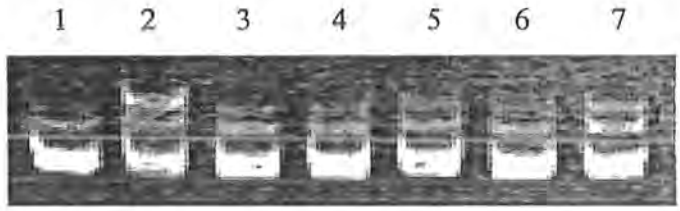

Family G

Lane 1- V-1
Lane 2- IV-1
Lane 3- V-2
Lane 4- V-3
Lane 5- V-4
Lane 6- V-5
Lane 7- IV-2

Figure 4.52: Electropherogram of ethidium bromide stained 8% non-denaturing polyacrylamide gel for marker D3S3686 at 214.27 cM on chromosome 3q27.3 showing homozygosity among the affected individuals (V-1, V-2 and V-3) of family G. The Roman numerals indicate the generation numbers of the individuals within a pedigree while Arabic numerals indicate their positions within a generation.

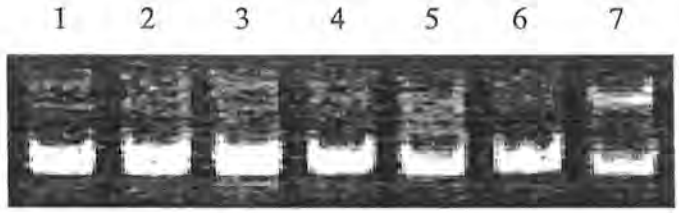

Family G

Lane 1- V-1
Lane 2- IV-1
Lane 3- V-2
Lane 4- V-3
Lane 5- V-4
Lane 6- V-5
Lane 7- IV-2

Figure 4.53: Electropherogram of ethidium bromide stained 8% non-denaturing polyacrylamide gel for marker D3S3628 at 215.71 cM on chromosome 3q27.3 showing homozygosity among the affected individuals (V-1, V-2 and V-3) of family G. The Roman numerals indicate the generation numbers of the individuals within a pedigree while Arabic numerals indicate their positions within a generation.

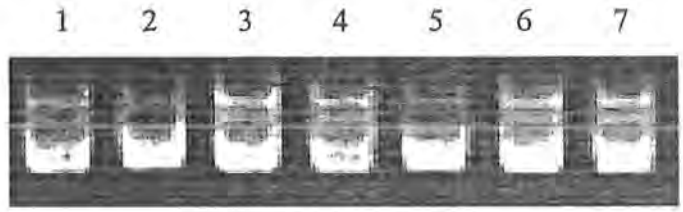

Family G

Lane 1- V-1
Lane 2- IV-1
Lane 3- V-2
Lane 4- V-3
Lane 5- V-4
Lane 6- V-5
Lane 7- IV-2

Figure 4.54: Electropherogram of ethidium bromide stained 8% non-denaturing polyacrylamide gel for marker D3S3596 at 216.29 cM on chromosome 3q27.3-q28 showing homozygosity among the affected individuals (V-1, V-2 and V-3) of family G. The Roman numerals indicate the generation numbers of the individuals within a pedigree while Arabic numerals indicate their positions within a generation.

Table 4.2: Two point LOD score results between the APMR locus and chromosome 33q25.1-q28 markers

Marker	Rutger Map cM[a]	Physical Position [b]	Multipoint LOD Score	Lod Score at Recombination fraction θ =						
				0	0.01	0.05	0.1	0.2	0.3	0.4
D3S3626	NA	149370398	-0.9883	-0.71	-0.42	-0.03	0.12	0.17	0.1	0.03
D3S3022	172.350	150771025	-1.067	-0.71	-0.42	-0.03	0.12	0.17	0.1	0.03
D3S1299	172.950	151666558	-1.1019	-0.71	-0.42	-0.03	0.12	0.17	0.1	0.03
D3S1746	175.000	153212439	1.9833	0.84	0.82	0.72	0.61	0.4	0.22	0.07
D3S1763	182.920	168722402	3.0861	1.14	1.11	0.99	0.85	0.58	0.32	0.11
D3S3622	183.760	169346662	3.1208	1.14	1.11	0.99	0.85	0.58	0.32	0.11
D3S1282	184.790	170372832	3.1379	1.74	1.7	1.51	1.28	0.83	0.42	0.11
D3S3723	185.790	173233404	3.1412	1.74	1.7	1.51	1.28	0.83	0.42	0.11
D3S2433	NA	177267390	3.1701	1.74	1.7	1.51	1.28	0.83	0.42	0.11
D3S2427	195.850	177267503	3.1701	1.74	1.7	1.51	1.28	0.83	0.42	0.11
D3S3676	196.010	177871163	3.1701	1.74	1.7	1.51	1.28	0.83	0.42	0.11
D3S3037	NA	178924199	3.1669	1.74	1.7	1.51	1.28	0.83	0.42	0.11
D3S3730	199.440	180029355	3.1649	1.74	1.7	1.51	1.28	0.83	0.42	0.11
D3S3699	200.190	180779759	3.1613	1.74	1.7	1.51	1.28	0.83	0.42	0.11
D3S3609	205.940	185519714	3.0838	1.74	1.7	1.51	1.28	0.83	0.42	0.11
D3S1617	208.480	187367069	2.9949	1.14	1.11	0.99	0.85	0.58	0.32	0.11
D3S3686	214.240	188900158	2.5704	1.14	1.11	0.99	0.85	0.58	0.32	0.11
D3S3628	215.710	189256383	2.2066	1.14	1.11	0.99	0.85	0.58	0.32	0.11
D3S3596	216.290	189489034	-0.4613	-0.41	-0.13	0.24	0.36	0.34	0.2	0.06

[a]Average-sex distance in cM according to the Rutgers combined linkage-physical human genome map (Kong *et al.*, 2004)

[b]The physical position is based according to build 36 of the human genome (International Human Genome Sequence Consortium, 2001)

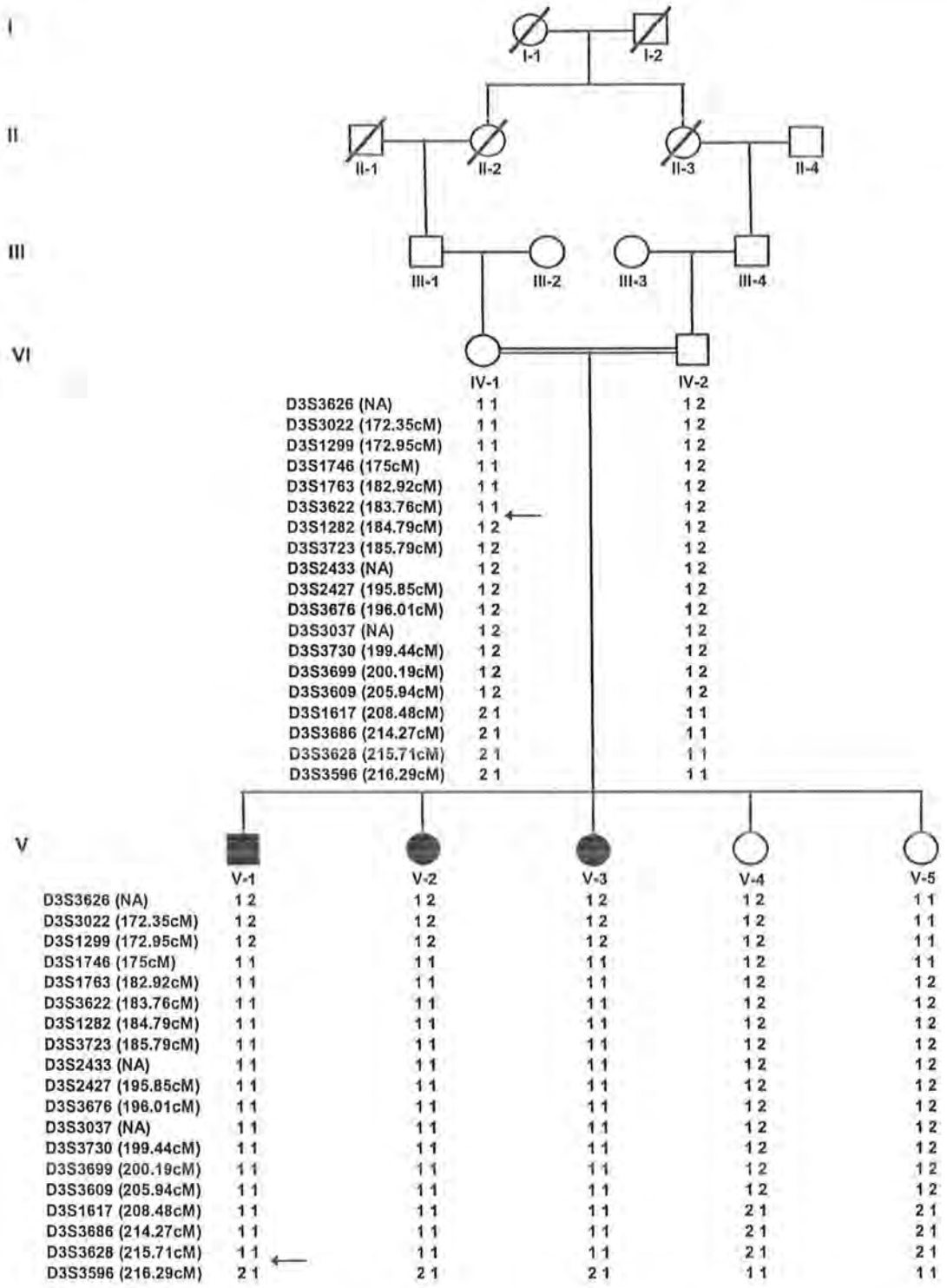

Figure 4.55: Pedigree of family G with alopecia and mental retardation (APMR). Haplotypes for the most closely linked short tandem repeats polymorphism (STRPs) are shown below each symbol. Mapped distances are given in centimorgans (cM) according to the Rutgers linkage-physical map of the human genome. Arrows indicate key recombination events.

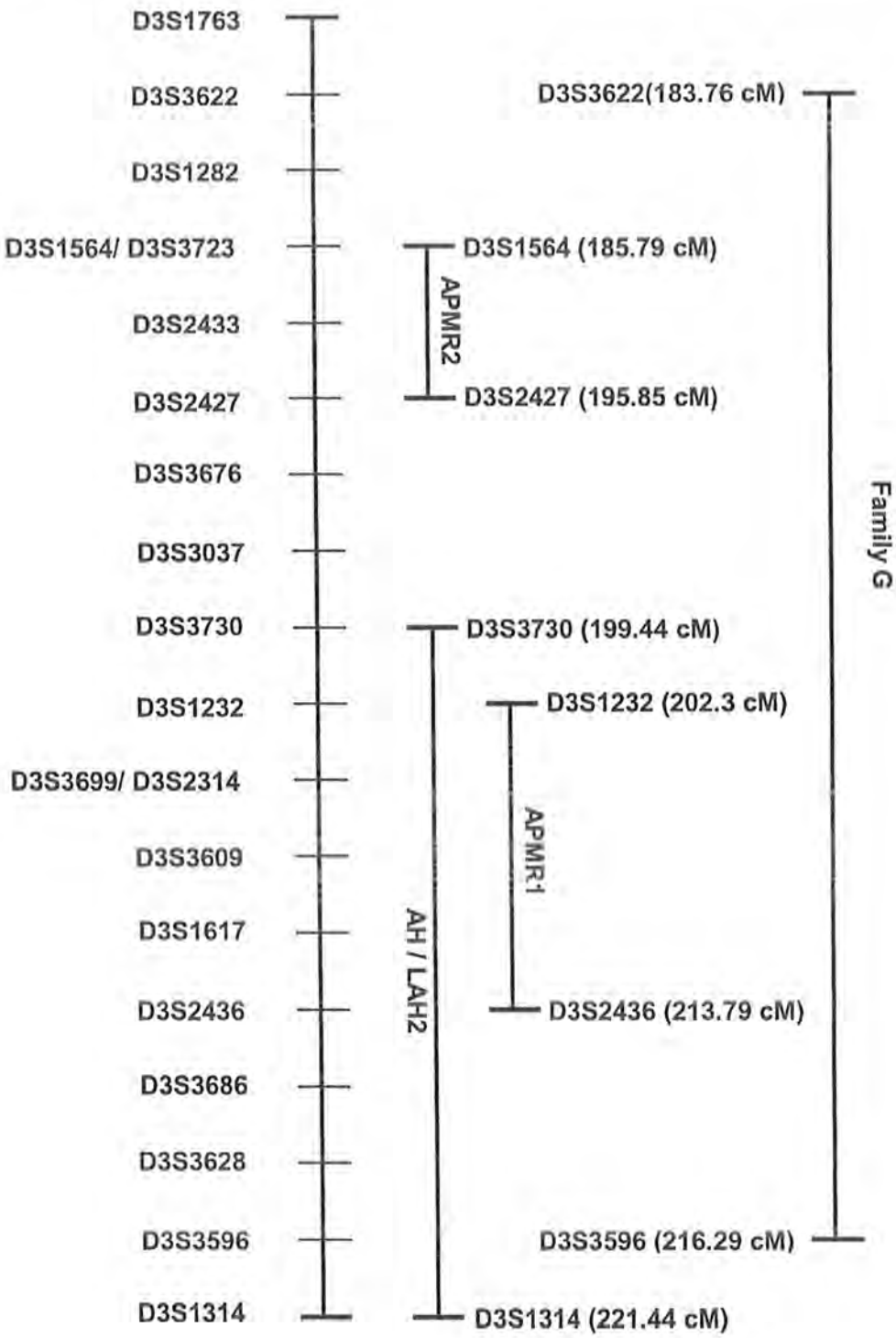

Figure 4.56: Comparison of the linkage interval of AH/LAH2, APMR1 and APMR2 with APMR locus identified in family G on chromosome 3q26.2-q28. Genetic map distances in centimorgans (cM) are according to the Rutgers linkage-physical map of the human genome (Kong *et al.*, 2004).

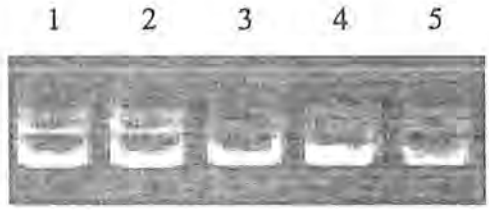

Family I

Lane 1- III-2
Lane 2- III-1
Lane 3- IV-1
Lane 4- IV-3
Lane 5- IV-2

Figure 4.57: Electropherogram of ethidium bromide stained 8% non-denaturing polyacrylamide gel for marker D8S322 on chromosome 8p21.3 showing homozygosity among the affected individuals (IV-1 and IV-3) of family I. The Roman numerals indicate the generation numbers of the individuals within a pedigree while Arabic numerals indicate their positions within a generation.

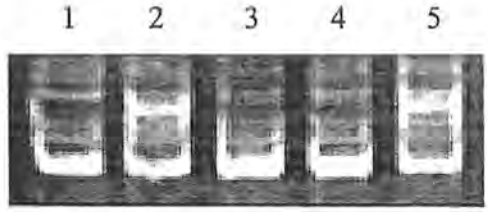

Family I

Lane 1- III-2
Lane 2- III-1
Lane 3- IV-1
Lane 4- IV-3
Lane 5- IV-2

Figure 4.58: Electropherogram of ethidium bromide stained 8% non-denaturing polyacrylamide gel for marker D8S282 at 39.38 cM on chromosome 8p21.3 showing homozygosity among the affected individuals (IV-1 and IV-3) of family I. The Roman numerals indicate the generation numbers of the individuals within a pedigree while Arabic numerals indicate their positions within a generation.

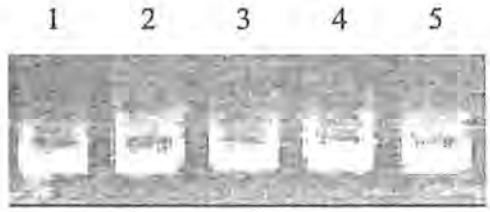

Family I

Lane 1- III-2
Lane 2- III-1
Lane 3- IV-1
Lane 4- IV-3
Lane 5- IV-2

Figure 4.59: Electropherogram of ethidium bromide stained 8% non-denaturing polyacrylamide gel for marker D8S560 at 39.68 cM on chromosome 8p21.3 showing homozygosity among the affected individuals (IV-1 and IV-3) of family I. The Roman numerals indicate the generation numbers of the individuals within a pedigree while Arabic numerals indicate their positions within a generation.

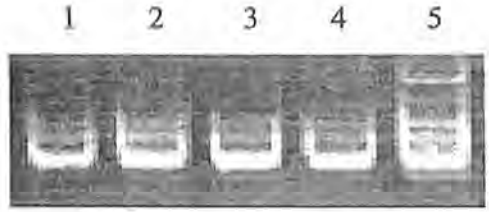

Family I

Lane 1- III-2
Lane 2- III-1
Lane 3- IV-1
Lane 4- IV-3
Lane 5- IV-2

Figure 4.60: Electropherogram of ethidium bromide stained 8% non-denaturing polyacrylamide gel for marker D8S298 at 40.11 cM on chromosome 8p21.3 showing homozygosity among the affected individuals (IV-1 and IV-3) of family I. The Roman numerals indicate the generation numbers of the individuals within a pedigree while Arabic numerals indicate their positions within a generation.

REFERENCES

Abdel-Meguid N, Zaki MS, Hammad SA (2000). Premarital genetic investigations: effect of genetic counselling. East Mediterr Health J 6:652-660.

Abecasis GR, Cherny SS, Cookson WO, Cardon LR (2002). Merlin-rapid analysis of dense genetic maps using sparse gene flow trees. Nat Genet 30:97-101.

Abrams CK, Freidin MM, Verselis VK, Bargiello TA, Kelsell DP, Richard G, Bennett MV, Bukauskas FF (2006). Properties of human connexin 31, which is implicated in hereditary dermatological disease and deafness. Proc Natl Acad Sci USA. 103:5213-5218.

Adato A, Michel V, Kikkawa Y, Reiners J, Alagramam KN, Weil D, Yonekawa H, Wolfrum U, El-Amraoui A, Petit C (2005). Interactions in the network of Usher syndrome type 1 proteins. Hum Mol Genet 14:347-356.

Adato A, Raskin L, Petit C, Bonne-Tamir B (2000). Deafness heterogeneity in a Druze isolate from the Middle East: novel OTOF and PDS mutations, low prevalence of GJB2 35delG mutation and indication for a new DFNB locus. Eur J Hum Genet 8:437-442.

Ahmad W, Irvine AD, Lam H, Buckley C, Bingham EA, Panteleyev AA, Ahmad M, McGrath JA, Christiano AM (1998). A missense mutation in the zinc-finger domain of the human hairless gene underlies congenital atrichia in a family of Irish travellers. Am J Hum Genet 63:984-991.

Ahmad W, Panteleyev AA, Christiano AM (1999). The molecular basis of congenital atrichia in humans and mice: mutations in the hairless gene. J Investig Dermatol Symp Proc 4:240-243.

Ahmad W, Zlotogorski A, Panteleyev AA, Lam H, Ahmad M, ul Haque MF, Abdallah HM, Dragan L, Christiano AM (1999). Genomic organization of the human hairless gene (HR) and identification of a mutation underlying congenital atrichia in an Arab Palestinian family. Genomics 56:141-148.

Ahmed ZM, Morell RJ, Riazuddin S, Gropman A, Shaukat S, Ahmad MM, Mohiddin SA, Fananapazir L, Caruso RC, Husnain T, Khan SN, Riazuddin S, Griffith

AJ, Friedman TB, Wilcox ER (2003). Mutations of MYO6 are associated with recessive deafness, DFNB37. Am J Hum Genet 72:1315-1322.

Ahmed ZM, Riazuddin S, Bernstein SL, Ahmed Z, Khan S, Griffith AJ, Morell RJ, Friedman TB, Riazuddin S, Wilcox ER (2001). Mutations of the protocadherin gene PCDH15 cause Usher syndrome type 1F. Am J Hum Genet 69:25-34.

Alagramam KN, Yuan H, Kuehn MH, Murcia CL, Wayne S, Srisailpathy CR, Lowry RB, Knaus R, Van Laer L, Bernier FP, Schwartz S, Lee C, Morton CC, Mullins RF, Ramesh A, Van Camp G, Hageman GS, Woychik RP, Smith RJ (2001). Mutations in the novel protocadherin PCDH15 cause Usher syndrome type 1F. Hum Mol Genet 10:1709-1718.

Albert S, Blons H, Jonard L, Feldmann D, Chauvin P, Loundon N, Sergent-Allaoui A, Houang M, Joannard A, Schmerber S, Delobel B, Leman J, Journel H, Catros H, Dollfus H, Eliot MM, David A, Calais C, Drouin-Garraud V, Obstoy MF, Tran Ba Huy P, Lacombe D, Duriez F, Francannet C, Bitoun P, Petit C, Garabédian EN, Couderc R, Marlin S, Denoyelle F (2006). SLC26A4 gene is frequently involved in nonsyndromic hearing impairment with enlarged vestibular aqueduct in Caucasian populations. Eur J Hum Genet 14:773-779.

Al-Gazali LI (2005). Attitudes toward genetic counseling in the United Arab Emirates. Community Genet 8:48-51.

Anderson DW, Probst FJ, Belyantseva IA, Fridell RA, Beyer L, Martin DM, Wu D, Kachar B, Friedman TB, Raphael Y, Camper SA (2000). The motor and tail regions of myosin XV are critical for normal structure and function of auditory and vestibular hair cells. Hum Mol Genet 9:1729-1738.

Azeem Z, Jelani M, Naz G, Tariq M, Wasif N, Kamran-Ul-Hassan Naqvi S, Ayub M, Yasinzai M, Amin-Ud-Din M, Wali A, Ali G, Chishti MS, Ahmad W (2008). Novel mutations in G protein-coupled receptor gene (P2RY5) in families with autosomal recessive hypotrichosis (LAH3). Hum Genet 123:515-519.

Balazs L, Okolicany J, Ferrebee M, Tolley B, Tigyi G (2001). Topical application of the phospholipid growth factor lysophosphatidic acid promotes wound healing in vivo. Am J Physiol Regul Integr Comp Physiol 280:466-472.

Bennett RL, Steinhaus KA, Uhrich SB, O'Sullivan CK, Resta RG, Lochner-Doyle D, Markel DS, Vincent V, Hamanishi J (1995). Recommendations for standardized human pedigree nomenclature. Pedigree standardization task force of the national society of genetic counselors. Am J Hum Genet 56:745-752.

Ben-Yosef T, Wattenhofer M, Riazuddin S, Ahmed ZM, Scott HS, Kudoh J, Shibuya K, Antonarakis SE, Bonne-Tamir B, Radhakrishna U, Naz S, Ahmed Z, Riazuddin S, Pandya A, Nance WE, Wilcox ER, Friedman TB, Morell RJ (2001). Novel mutations of TMPRSS3 in four DFNB8/B10 families segregating congenital autosomal recessive deafness. J Med Genet 38:396-400.

Betz RC, Indelman M, Pforr J, Schreiner F, Bauer R, Bergman R, Lentze MJ, Nöthen MM, Cichon S, Sprecher E (2007). Identification of mutations in the human hairless gene in two new families with congenital atrichia. Arch Dermatol Res 299:157-161.

Betz RC, Lee YA, Bygum A, Brandrup F, Bernal AI, Toribio J, Alvarez JI, Kukuk GM, Ibsen HH, Rasmussen HB, Wienker TF, Reis A, Propping P, Kruse R, Cichon S, Nothen MM (2000). A gene for hypotrichosis simplex of the scalp maps to chromosome 6p21.3. Am J Hum Genet 66:1979-1983.

Bitner-Glindzicz M, Lindley KJ, Rutland P, Blaydon D, Smith VV, Milla PJ, Hussain K, Furth-Lavi J, Cosgrove KE, Shepherd RM, Barnes PD, O'Brien RE, Farndon PA, Sowden J, Liu XZ, Scanlan MJ, Malcolm S, Dunne MJ, Aynsley-Green A, Glaser B (2000). A recessive contiguous gene deletion causing infantile hyperinsulinism, enteropathy and deafness identifies the Usher type 1C gene. Nat Genet 26:56-60.

Bittles A (2001). Consanguinity and its relevance to clinical genetics. Clin Genet 60:89-98.

Bittles AH (2002). Endogamy, consanguinity and community genetics. J Genet 81:91-98.

Bittles AH (2005). Endogamy, consanguinity and community disease profiles. Community Genet 8:17-20.

Blanton SH, Liang CY, Cai MW, Pandya A, Du LL, Landa B, Mummalanni S, Li KS, Chen ZY, Qin XN, Liu YF, Balkany T, Nance WE, Liu XZ (2002). A novel locus for autosomal dominant non-syndromic deafness (DFNA41) maps to chromosome 12q24-qter. J Med Genet 39:567–570.

Bolz H, Bolz SS, Schade G, Kothe C, Mohrmann G, Hess M, Gal A (2004). Impaired calmodulin binding of myosin-7A causes autosomal dominant hearing loss (DFNA11). Hum Mutat 24:274-275.

Bork JM, Peters LM, Riazuddin S, Bernstein SL, Ahmed ZM, Ness SL, Polomeno R, Ramesh A, Schloss M, Srisailpathy CR, Wayne S, Bellman S, Desmukh D, Ahmed Z, Khan SN, Kaloustian VM, Li XC, Lalwani A, Riazuddin S, Bitner-Glindzicz M, Nance WE, Liu XZ, Wistow G, Smith RJ, Griffith AJ, Wilcox ER, Friedman TB, Morell RJ (2001). Usher syndrome 1D and nonsyndromic autosomal recessive deafness DFNB12 are caused by allelic mutations of the novel cadherin-like gene CDH23. Am J Hum Genet 68:26-37.

Broman KW, Murray JC, Scheffield VC, White RL, Weber JL (1998). Comprehensive human genetic maps: individual and sex specific variation in recombination. Am J Hum Genet 63:861-869.

Broman KW, Weber JL (1999). Long homozygous chromosomal segments in reference families from the centre d'Etude du polymorphisme humain. Am J Hum Genet 65:1493-500.

Brown KA, Janjua AH, Karbani G, Parry G, Noble A, Crockford G, Bishop DT, Newton VE, Markham AF, Mueller RF (1996). Linkage studies of non-syndromic recessive deafness (NSRD) in a family originating from the Mirpur region of Pakistan maps DFNB1 centromeric to D13S175. Hum Mol Genet 5:169-173.

Carreras D (1996). Monilethrix: a review and case report. Pediatr Dent 18:331-333.

Chavanas S, Bodemer C, Rochat A, Hamel-Teillac D, Ali M, Irvine AD, Bonafe JL, Wilkinson J, Taieb A, Barrandon Y, Harper JI, de Prost Y, Hovnanian A (2000a). Mutations in SPINK5, encoding a serine protease inhibitor, cause Netherton syndrome. Nat Genet 25:141-142.

Chavanas S, Garner C, Bodemer C, Ali M, Teillac DH, Wilkinson J, Bonafe JL, Paradisi M, Kelsell DP, Ansai S, Mitsuhashi Y, Larregue M, Leigh IM, Harper JI, Taïeb A, Prost Y, Cardon LR, Hovnanian A (2000b). Localization of the Netherton syndrome gene to chromosome 5q32, by linkage analysis and homozygosity mapping. Am J Hum Genet 66:914-921.

Chen W, Kahrizi K, Meyer NC, Riazalhosseini Y, Van Camp G, Najmabadi H, Smith RJ (2005). Mutation of COL11A2 causes autosomal recessive non-syndromic hearing loss at the DFNB53 locus. J Med Genet 42:61.

Cichon S, Anker M, Vogt IR, Rohleder H, Pützstück M, Hillmer A, Farooq SA, Al-Dhafri KS, Ahmad M, Haque S, Rietschel M, Propping P, Kruse R, Nothen MM (1998). Cloning, genomic organization, alternative transcripts and mutational analysis of the gene responsible for autosomal recessive universal congenital alopecia. Hum Mol Genet 7:1671-1679.

Cichon S, Kruse R, Hillmer AM, Kukuk G, Anker M, Altland K, Knapp M, Propping P, Nöthen MM (2000). A distinct gene close to the hairless locus on chromosome 8p underlies hereditary Marie Unna type hypotrichosis in a German family. Br J Dermatol 143:811-814.

Cottingham Jr RW, Indury RM, Schaffer AA (1993). Faster sequential genetic linkage computation. Am J Hum Genet 53:252-263.

Couloigner V, Fay M, Djelidi S, Farman N, Escoubet B, Runembert I, Sterkers O, Friedlander G, Ferrary E (2001). Location and function of the epithelial Na channel in the cochlea. Am J Physiol Renal Physiol 280:214-222.

D'Adamo P, Pinna M, Capobianco S, Cesarani A, D'Eustacchio A, Fogu P, Carella M, Seri M, Gasparini P (2003). A novel autosomal dominant non-syndromic deafness locus (DFNA48) maps to 12q13-q14 in a large Italian family. Hum Genet 112:319–320.

Dahl HH, Tobin SE, Poulakis Z, Rickards FW, Xu X, Gillam L, Williams J, Saunders K, Cone-Wesson B, Wake M (2006). The contribution of GJB2 mutations to slight or mild hearing loss in Australian elementary school children. J Med Genet 43:850-855.

del Castillo I, Villamar M, Moreno-Pelayo MA, del Castillo FJ, Alvarez A, Telleria D, Menendez I, Moreno F (2002). A deletion involving the connexin 30 gene in nonsyndromic hearing impairment. N Engl J Med 346:243-249.

Di Palma F, Holme RH, Bryda EC, Belyantseva IA, Pellegrino R, Kachar B, Steel KP, Noben-Trauth K (2001). Mutations in Cdh23, encoding a new type of cadherin, cause stereocilia disorganization in waltzer, the mouse model for Usher syndrome type 1D. Nat Genet 27:103-107.

Dose AC, Burnside B (2000). Cloning and chromosomal localization of a human class III myosin. Genomics 67:333–342.

El-Hazmi MA (1999). Spectrum of genetic disorders and the impact on health care delivery: an introduction. East Mediterr Health J 5:1104-1113.

Elias LA, Wang DD, Kriegstein AR (2007). Gap junction adhesion is necessary for radial migration in the neocortex. Nature 448:901-907.

Everett LA, Green ED (1999). A family of mammalian anion transporters and their involvement in human genetic diseases. Hum Mol Genet 8:1883–1891.

Feinstein A, Engelberg S, Goodman RM (1987). Genetic disorders associated with severe alopecia in children: a report of two unusual cases and a review. J Craniofac Genet Dev Biol 7:301-310.

Friedman TB, Griffith AJ (2003) Human nonsyndromic sensorineural deafness. Annu Rev Genomics Hum Genet 4:341-402

Friedman TB, Hinnant JT, Fridell RA, Wilcox ER, Raphael Y, Camper SA (2000). DFNB3 families and Shaker-2 mice: mutations in an unconventional myosin, myo 15. Adv Otorhinolaryngol 56:131-144.

Friedman TB, Hinnant JT, Ghosh M, Boger ET, Riazuddin S, Lupski JR, Potocki L, Wilcox ER (2002). DFNB3, spectrum of MYO15A recessive mutant alleles and an emerging genotype-phenotype correlation. Adv Otorhinolaryngol 61:124-130.

Friedman TB, Sellers JR, Avraham KB (1999). Unconventional myosins and the genetics of hearing loss. Am J Med Genet 89:147-57.

Gadgil M, Joshi NVC, Manoharan S, Patil S, Prasad UVS (1998). Peopling of India; In Balasubramanian D, Rao NA (ed) The Indian Human Heritage. Hyderabad, Universities Press. pp 100–129.

Greene CC, McMillan PM, Barker SE, Kurnool P, Lomax MI, Burmeister M, Lesperance MM (2001). DFNA25, a novel locus for dominant nonsyndromic hereditary hearing impairment, maps to 12q21-24. Am J Hum Genet 68:254-260.

Gudbjartsson DF, Thorvaldsson T, Kong A, Gunnarsson G, Ingolfsdottir A (2005). Allegro version 2. Nat Genet 37:1015-1016.

Guilford P, Ayadi H, Blanchard S, Chaib H, Le Paslier D, Weissenbach J, Drira M, Petit C (1994). A human gene responsible for neurosensory, non-syndromic recessive deafness is a candidate homologue of the mouse sh-1 gene. Hum Mol Genet 3:989-993.

Guipponi M, Vuagniaux G, Wattenhofer M, Shibuya K, Vazquez M, Dougherty L, Scamuffa N, Guida E, Okui M, Rossier C, Hancock M, Buchet K, Reymond A, Hummler E, Marzella PL, Kudoh J, Shimizu N, Scott HS, Antonarakis SE, Rossier BC (2002). The transmembrane serine protease (TMPRSS3) mutated in deafness DFNB8/10 activates the epithelial sodium channel (ENaC) in vitro. Hum Mol Genet 11:2829-2836.

Hatsell SJ, Eady RA, Wennerstrand L, Dopping-Hepenstal P, Leigh IM, Munro C, Kelsell DP (2001). Novel splice site mutation in keratin 1 underlies mild epidermolytic palmoplantar keratoderma in three kindreds. J Invest Dermatol 116:606-609.

He PP, Zhang XJ, Yang Q, Li M, Liang YH, Yang S, Yan KL, Cui Y, Shen YY, Wang HY, Sun LD, Du WH, Shen YJ, Xu SJ, Huang W (2004). Refinement of a locus for Marie Unna hereditary hypotrichosis to a 1.1-cM interval at 8p21.3. Br J Dermatol 150:837-842.

Hiramatsu T, Sonoda H, Takanezawa Y, Morikawa R, Ishida M, Kasahara K, Sanai Y, Taguchi R, Aoki J, Arai H (2003). Biochemical and molecular characterization of two phosphatidic acid-selective phospholipase A1s, mPA-PLA1alpha and mPA-PLA1beta. J Biol Chem 278:49438-49447.

Hiraoka M, Abe A, Shayman JA (2005). Structure and function of lysosomal phospholipase A2: identification of the catalytic triad and the role of cysteine residues. J Lipid Res 46:2441-2447.

Horev L, Djabali K, Green J, Sinclair R, Martinez-Mir A, Ingber A, Christiano AM, Zlotogorski A (2003). De novo mutations in monilethrix. Exp Dermatol 12:882-885.

Horev L, Glaser B, Metzker A, Ben-Amitai D, Vardy D, Zlotogorski A (2000). Monilethrix: mutational hotspot in the helix termination motif of the human hair basic keratin 6. Hum Hered 50:325-330.

Houseman MJ, Jackson AP, Al-Gazali LI, Badin RA, Roberts E, Mueller RF (2001). A novel mutation in a family with non-syndromic sensorineural hearing loss that disrupts the newly characterised OTOF long isoforms. J Med Genet 38:25.

Hsieh JC, Sisk JM, Jurutka PW, Haussler CA, Slater SA, Haussler MR, Thompson CC (2003). Physical and functional interaction between the vitamin D receptor and hairless corepressor, two proteins required for hair cycling. J Biol Chem 278:38665-38674.

Hur DJ, Raymond GV, Kahler SG, Riegert-Johnson DL, Cohen BA, Boyadjiev SA (2005). A novel MGP mutation in a consanguineous family: review of the clinical and molecular characteristics of Keutel syndrome. Am J Med Genet A 135:36–40.

International Human Genome Sequence Consortium (2001). Initial sequence and analysis of the human genome. Nature 409:860–921.

Ishida-Yamamoto A, Richard G, Takahashi H, Iizuka H (2003). In vivo studies of mutant keratin 1 in ichthyosis hystrix Curth-Macklin. J Invest Dermatol 120:498-500.

Jelani M, Wasif N, Ali G, Chishti MS, Ahmad W (2008). A novel deletion mutation in LIPH gene causes autosomal recessive hypotrichosis (LAH2). Clin Genet (In press)

John P, Ali G, Chishti MS, Naqvi SM, Leal SM, Ahmad W (2006a). Localization of a novel locus for alopecia with mental retardation syndrome to chromosome 3q26.33-q27.3. Hum Genet 118:665-667.

John P, Aslam M, Rafiq MA, Amin-ud-din M, Haque S, Ahmad W (2005). Atrichia with papular lesions in two Pakistani consanguineous families resulting from mutations in the human hairless gene. Arch Dermatol Res 297:226-230.

John P, Tariq M, Arshad Rafiq M, Amin-Ud-Din M, Muhammad D, Waheed I, Ansar M, Ahmad W (2006b). Recurrent intragenic deletion mutation in desmoglein 4 gene underlies autosomal recessive hypotrichosis in two Pakistani families of Balochi and Sindhi origins. Arch Dermatol Res 298:135-137.

Jovine L, Park J, Wassarman PM (2002). Sequence similarity between stereocilin and otoancorin points to a unified mechanism for mechanotransduction in the mammalian inner ear. BMC Cell Biol 3:28.

Karolchik D, Baertsch R, Diekhans M, Furey TS, Hinrichs A, Lu YT, Roskin KM, Schwartz M, Sugnet CW, Thomas DJ, Weber RJ, Haussler D, Kent WJ; University of California Santa Cruz (2003). The UCSC Genome Browser Database. Nucleic Acids Res 31:51-54.

Kazantseva A, Goltsov A, Zinchenko R, Grigorenko AP, Abrukova AV, Moliaka YK, Kirillov AG, Guo Z, Lyle S, Ginter EK, Rogaev EI (2006). Human hair growth deficiency is linked to a genetic defect in the phospholipase gene *LIPH*. Science 314:982-985.

Kazmierczak P, Sakaguchi H, Tokita J, Wilson-Kubalek EM, Milligan RA, Müller U, Kachar B (2007). Cadherin 23 and protocadherin 15 interact to form tip-link filaments in sensory hair cells. Nature 449:87-91.

Keats BJB, Berlin CI (1999). Genomics and hearing impairment. Genome Res 9:7-16.

Keresztes G, Mutai H, Heller S (2003). TMC and EVER genes belong to a larger novel family, the TMC gene family encoding transmembrane proteins. BMC Genomics 4:24.

Kim H, Wajid M, Kraemer L, Shimomura Y, Christiano AM (2007). Nonsense mutations in the hairless gene underlie APL in five families of Pakistani origin. J Dermatol Sci 48:207-211.

Kljuic A, Bazzi H, Sundberg JP, Martinez-Mir A, O'Shaughnessy R, Mahoney MG, Levy M, Montagutelli X, Ahmad W, Aita VM, Gordon D, Uitto J, Whiting D, Ott J, Fischer S, Gilliam TC, Jahoda CA, Morris RJ, Panteleyev AA, Nguyen VT, Christiano AM (2003a). Desmoglein 4 in hair follicle differentiation and epidermal adhesion: evidence from inherited hypotrichosis and acquired pemphigus vulgaris. Cell 113:249-260.

Kljuic A, Gilead L, Martinez-Mir A, Frank J, Christiano AM, Zlotogorski A (2003b). A nonsense mutation in the desmoglein 1 gene underlies striate keratoderma. Exp Dermatol 12:523-527.

Kong A, Gudbjartsson DF, Sainz J, Jonsdottir GM, Gudjonsson SA, Richardsson B, Sigurdardottir S, Barnard J, Hallbeck B, Masson G, Shlien A, Palsson ST, Frigge ML, Thorgeirsson TE, Gulcher JR, Stefansson K (2002). A high-resolution recombination map of the human genome. Nat Genet 31:241-247.

Kong X, Murphy K, Raj T, He C, White PS, Matise TC (2004). A combined linkage-physical map of the human genome. Am J Hum Genet 75:1143-1148.

Kong X, Murphy K, Raj T, He C, White PS, Matise TC (2004). A combined linkage-physical map of the human genome. Am J Hum Genet 75:1143-1148.

Kraemer L, Wajid M, Shimomura Y, Christiano AM (2008). Mutations in the hairless gene underlie APL in three families of Pakistani origin. J Dermatol Sci 50:25-30.

Kubiak RJ, Yue X, Hondal RJ, Mihai C, Tsai MD, Bruzik KS (2001) Involvement of the Arg-Asp-His catalytic triad in enzymatic cleavage of the phosphodiester bond. Biochemistry 40:5422–5432.

Kurima K, Peters LM, Yang Y, Riazuddin S, Ahmed ZM, Naz S, Arnaud D, Drury S, Mo J, Makishima T, Ghosh M, Menon PS, Deshmukh D, Oddoux C, Ostrer H, Khan S, Riazuddin S, Deininger PL, Hampton LL, Sullivan SL, Battey JF Jr, Keats BJ, Wilcox ER, Friedman TB, Griffith AJ (2002). Dominant and recessive deafness caused by mutations of a novel gene, TMC1, required for cochlear hair-cell function. Nat Genet 30:277-284.

Lander ES, Botstein D (1987). Homozygosity mapping: a way to map human recessive traits with the DNA of inbred children. Science 236:1567-1570.

Lee DY, Ahn KS, Lee CH, Rho NK, Lee JH, Lee ES, Steinert PM, Yang JM (2002). Two novel mutations in the keratin 1 gene in epidermolytic hyperkeratosis. J Invest Dermatol 119:976-977.

Lee YJ, Park D, Kim SY, Park WJ (2003). Pathogenic mutations but not polymorphisms in congenital and childhood onset autosomal recessive deafness disrupt the proteolytic activity of TMPRSS3. J Med Genet 40:629-631.

Lefevre P, Rochat A, Bodemer C, Vabres P, Barrandon Y, de Prost Y, Garner C, Hovnanian A (2000). Linkage of Marie-Unna hypotrichosis locus to chromosome 8p21 and exclusion of 10 genes including the hairless gene by mutation analysis. Eur J Hum Genet 8:273-279.

Legan PK, Lukashkina VA, Goodyear RJ, Kossi M, Russell IJ, Richardson GP (2000). A targeted deletion in alpha-tectorin reveals that the tectorial membrane is required for the gain and timing of cochlear feedback. Neuron 28:273-285.

Levy-Nissenbaum E, Betz RC, Frydman M, Simon M, Lahat H, Bakhan T, Goldman B, Bygum A, Pierick M, Hillmer AM, Jonca N, Toribio J, Kruse R, Dewald G, Cichon S, Kubisch C, Guerrin M, Serre G, Nöthen MM, Pras E (2003). Hypotrichosis simplex of the scalp is associated with nonsense mutations in CDSN encoding corneodesmosin. Nat Genet 34:151-153.

Liang Y, Wang A, Probst FJ, Arhya IN, Barber TD, Chen KS, Deshmukh D, Dolan DF, Hinnant JT, Carter LE, Jain PK, Lalwani AK, Li XC, Lupski JR, Moeljopawiro S, Morell R, Negrini C, Wilcox ER, Winata S, Camper SA, Friedman TB (1998). Genetic mapping refines DFNB3 to 17p11.2, suggests multiple alleles of DFNB3, and supports homology to the mouse model shaker-2. Am J Hum Genet 62:904-915.

Liu XZ, Ouyang XM, Xia XJ, Zheng J, Pandya A, Li F, Du LL, Welch KO, Petit C, Smith RJ, Webb BT, Yan D, Arnos KS, Corey D, Dallos P, Nance WE, Chen ZY (2003). Prestin, a cochlear motor protein, is defective in non-syndromic hearing loss. Hum Mol Genet 12:1155-1162.

Liu XZ, Walsh J, Mburu P, Kendrick-Jones J, Cope MJ, Steel KP, Brown SD (1997). Mutations in the myosin VIIA gene cause non-syndromic recessive deafness. Nat Genet 16:188-190.

Liu XZ, Walsh J, Tamagawa Y, Kitamura K, Nishizawa M, Steel KP, Brown SD (1997). Autosomal dominant non-syndromic deafness caused by a mutation in the myosin VIIA gene. Nat Genet 17:268-269.

Liu XZ, Xia XJ, Xu LR, Pandya A, Liang CY, Blanton SH, Brown SD, Steel KP, Nance WE (2000). Mutations in connexin31 underlie recessive as well as dominant non-syndromic hearing loss. Hum Mol Genet 9:63-67.

Lohi H, Kujala M, Makela S, Lehtonen E, Kestila M, Saarialho-Kere U, Markovich D, Kere J (2002). Functional characterization of three novel tissue-specific anion exchangers SLC26A7, -A8, and -A9. J Biol Chem 277:14246-14254.

Lopez-Bigas N, Olive M, Rabionet R, Ben-David O, Martinez-Matos JA, Bravo O, Banchs I, Volpini V, Gasparini P, Avraham KB, Ferrer I, Arbones ML, Estivill X (2001). Connexin 31 (GJB3) is expressed in the peripheral and auditory nerves and causes neuropathy and hearing impairment. Hum Mol Genet 10:947-952.

Magert HJ, Standker L, Kreutzmann P, Zucht HD, Reinecke M, Sommerhoff CP, Fritz H, Forssmann WG (1999). LEKTI, a novel 15-domain type of human serine proteinase inhibitor. J Biol Chem 274:21499-214502.

Maquat LE (1996). Defects in RNA splicing and the consequence of shortened translational reading frames. Am J Hum Genet 59:279-286.

Masmoudi S, Antonarakis SE, Schwede T, Ghorbel AM, Gratri M, Pappasavas MP, Drira M, Elgaied-Boulila A, Wattenhofer M, Rossier C, Scott HS, Ayadi H, Guipponi M (2001). Novel missense mutations of TMPRSS3 in two consanguineous Tunisian families with non-syndromic autosomal recessive deafness. Hum Mutat 18:101-108.

Mburu P, Mustapha M, Varela A, Weil D, El-Amraoui A, Holme RH, Rump A, Hardisty RE, Blanchard S, Coimbra RS, Perfettini I, Parkinson N, Mallon AM, Glenister P, Rogers MJ, Paige AJ, Moir L, Clay J, Rosenthal A, Liu XZ, Blanco G, Steel KP, Petit C, Brown SD (2003). Defects in whirlin, a PDZ

domain molecule involved in stereocilia elongation, cause deafness in the whirler mouse and families with DFNB31. Nat Genet 34:421-428.

Mehdi SQ, Qamar R, Ayub Q, Khaliq S. Mansoor A, Ismail M, Mammer MF, Underhill PA, Cavalli- Sforza LL (1999). The origin of Pakistani populations:evidence from Y chromosome markers. In: Genomic Diversity: Applications in human population Genetics, Papiha S.S., Deka, R. and Chakraborty, R. ed., Kluwer Academic/Plenum Publishers, New York. pp 83-90

Messenger AG, Bazzi H, Parslew R, Shapiro L, Christiano AM (2005). A missense mutation in the cadherin interaction site of the desmoglein 4 gene underlies localized autosomal recessive hypotrichosis. J Invest Dermatol 125:1077-1079.

Mhatre AN, Weld E, Lalwani AK (2003). Mutation analysis of Connexin 31 (GJB3) in sporadic non-syndromic hearing impairment. Clin Genet 63:154–159.

Miano MG, Jacobson SG, Carothers A, Hanson I, Teague P, Lovell J, Cideciyan AV, Haider N, Stone EM, Sheffield VC, Wright AF (2000). Pitfalls in homozygosity mapping. Am J Hum Genet 67:1348-1351.

Migliosi V, Modamio-Hoybjor S, Moreno-Pelayo MA, Rodriguez-Ballesteros M, Villamar M, Telleria D, Menendez I, Moreno F, Del Castillo I (2002). Q829X, a novel mutation in the gene encoding otoferlin (OTOF), is frequently found in Spanish patients with prelingual non-syndromic hearing loss. J Med Genet 39:502-506.

Mirghomizadeh F, Pfister M, Apaydin F, Petit C, Kupka S, Pusch CM, Zenner HP, Blin N (2002). Substitutions in the conserved C2C domain of otoferlin cause DFNB9, a form of nonsyndromic autosomal recessive deafness. Neurobiol Dis 10:157-164.

Mitchem KL, Hibbard E, Beyer LA, Bosom K, Dootz GA, Dolan DF, Johnson KR, Raphael Y, Kohrman DC (2002). Mutation of the novel gene Tmie results in sensory cell defects in the inner ear of spinner, a mouse model of human hearing loss DFNB6. Hum Mol Genet 11:1887-1898.

Mizuno Y, Suga Y, Haruna K, Muramatsu S, Hasegawa T, Kohroh K, Shimizu T, Komatsu N, Ogawa H, Ikeda S (2006). A case of a Japanese neonate with congenital ichthyosiform erythroderma diagnosed as Netherton syndrome. Clin Exp Dermatol 31:677-680.

Mohiddin SA, Ahmed ZM, Griffith AJ, Tripodi D, Friedman TB, Fananapazir L, Morell RJ (2004). Novel association of hypertrophic cardiomyopathy, sensorineural deafness, and a mutation in unconventional myosin VI (MYO6). J Med Genet 41:309-314.

Moolenaar WH, van Meeteren LA, Giepmans BN (2004). The ins and outs of lysophosphatidic acid signaling. Bioessays 26:870-881.

Moore KA, Lemischka IR (2006). Stem cells and their niches. Science 311:1880-1885.

Morton CC (2002). Genetics, genomics and gene discovery in the auditory system. Hum Mol Genet 11:1229-1240.

Moss C, Martinez-Mir A, Lam H, Tadin-Strapps M, Kljuic A, Christiano AM (2004). A recurrent intragenic deletion in the desmoglein 4 gene underlies localized autosomal recessive hypotrichosis. J Invest Dermatol 123:607-610.

Muramatsu S, Kimura T, Ueki R, Tsuboi R, Ikeda S, Ogawa H (2003). Recurrent E413K mutation of hHb6 in a Japanese family with monilethrix. Dermatology 206:338-340.

Mustapha M, Chouery E, Chardenoux S, Naboulsi M, Paronnaud J, Lemainque A, Megarbane A, Loiselet J, Weil D, Lathrop M, Petit C (2002). DFNB31, a recessive form of sensorineural hearing loss, maps to chromosome 9q32-34. Eur J Hum Genet 10:210-212.

Mustapha M, Weil D, Chardenoux S, Elias S, El-Zir E, Beckmann JS, Loiselet J, Petit C (1999). An alpha-tectorin gene defect causes a newly identified autosomal recessive form of sensorineural pre-lingual non-syndromic deafness, DFNB21. Hum Mol Genet 8:409-412.

Naccache SN, Hasson T, Horowitz A (2006). Binding of internalized receptors to the PDZ domain of GIPC/ synectin recruits myosin VI to endocytic vesicles. Proc Natl Acad Sci USA 103:12735-12740.

Nal N, Ahmed ZM, Erkal E, Alper OM, Luleci G, Dinç O, Waryah AM, Ain Q, Tasneem S, Husnain T, Chattaraj P, Riazuddin S, Boger E, Ghosh M, Kabra M, Riazuddin S, Morell RJ, Friedman TB (2007). Mutational spectrum of MYO15A: the large N-terminal extension of myosin XVA is required for hearing. Hum Mutat 28:1014-1019.

Naz S, Alasti F, Mowjoodi A, Riazuddin S, Sanati MH, Friedman TB, Griffith AJ, Wilcox ER, Riazuddin S (2003). Distinctive audiometric profile associated with DFNB21 alleles of TECTA. J Med Genet 40:360-363.

Naz S, Giguere CM, Kohrman DC, Mitchem KL, Riazuddin S, Morell RJ, Ramesh A, Srisailpathy S, Deshmukh D, Riazuddin S, Griffith AJ, Friedman TB, Smith RJ, Wilcox ER (2002). Mutations in a novel gene, TMIE, are associated with hearing loss linked to the DFNB6 locus. Am J Hum Genet 71:632-636.

Naz S, Griffith AJ, Riazuddin S, Hampton LL, Battey JF Jr, Khan SN, Riazuddin S, Wilcox ER, Friedman TB (2004). Mutations of ESPN cause autosomal recessive deafness and vestibular dysfunction. J Med Genet 41:591-595.

Netherton EW (1958). A unique case of trichorrhexis nodosa; bamboo hairs. AMA Arch Derm 78:483-487.

O'Connell JR, Weeks DE (1998). PedCheck: a program for identification of genotype incompatibilities in linkage analysis. Am J Hum Genet 63:259-266.

Ouyang XM, Yan D, Du LL, Hejtmancik JF, Jacobson SG, Nance WE, Li AR, Angeli S, Kaiser M, Newton V, Brown SD, Balkany T, Liu XZ (2005). Characterization of Usher syndrome type I gene mutations in an Usher syndrome patient population. Hum Genet 116:292-299.

Parving A (1983). Epidemiology of hearing loss and aetiological diagnosis of hearing impairment in childhood. Int J Pediatr Otorhinolaryngol 5:151-165.

Pasternack SM, von Kugelgen I, Aboud KA, Lee YA, Ruschendorf F, Voss K, Hillmer AM, Molderings GJ, Franz T, Ramirez A, Nurnberg P, Nothen MM, Betz RC (2008). G protein-coupled receptor P2Y5 and its ligand LPA are involved in maintenance of human hair growth. Nat Genet 40:329-334.

Peltonen L, Palotie A, Lange K (2000). Use of population isolates for mapping complex traits. Nat Rev Genet 3:182-190.

Petersen MB, Willems PJ (2006). Non-syndromic, autosomal-recessive deafness. Clin Genet 69:371-392.

Petit C (1996). Genes responsible for human hereditary deafness: symphony of a thousand. Nat Genet 14:385–391.

Pinheiro M, Freire-Maia N, Gollop TR (1985). Odontoonychodysplasia with alopecia: a new pure ectodermal dysplasia with probable autosomal recessive inheritance. Am J Med Genet 20:197-202.

Plantin P, Delaire P, Guillet MH, Labouche F, Guillet G (1991). Netherton's syndrome. Ann Dermatol Venereol 118:525-530.

Potter GB, Beaudoin GM 3rd, DeRenzo CL, Zarach JM, Chen SH, Thompson CC (2001). The hairless gene mutated in congenital hair loss disorders encodes a novel nuclear receptor corepressor. Genes Dev 15:2687-2691.

Probst FJ, Fridell RA, Raphael Y, Saunders TL, Wang A, Liang Y, Morell RJ, Touchman JW, Lyons RH, Noben-Trauth K, Friedman TB, Camper SA (1998). Correction of deafness in shaker-2 mice by an unconventional myosin in a BAC transgene. Science 280:1444-1447.

Rafiq MA, Ansar M, Mahmood S, Haque S, Faiyaz-ul-Haque M, Leal SM, Ahmad W (2004). A recurrent intragenic deletion mutation in DSG4 gene in three Pakistani families with autosomal recessive hypotrichosis. J Invest Dermatol 123:247-248.

Rafique MA, Ansar M, Jamal SM, Malik S, Sohail M, Faiyaz-Ul-Haque M, Haque S, Leal SM, Ahmad W (2003). A locus for hereditary hypotrichosis localized to human chromosome 18q21.1. Eur J Hum Genet 11:623-628.

Resendes BL, Williamson RE, Morton CC (2001). At the speed of sound: gene discovery in the auditory system. Am J Hum Genet 69:923–935.

Roelandt T, Kraemer L, Van Neste D, Lissens W, Roseeuw D, Christiano AM, Hachem JP (2008). Novel mutation in the human hairless gene once more erroneously diagnosed and treated as 'alopecia areata'. Br J Dermatol 158:834-835.

Rogers MA, Nischt R, Korge B, Krieg T, Fink TM, Lichter P, Winter H, Schweizer J (1995). Sequence data and chromosomal localization of human type I and type II hair keratin genes. Exp Cell Res 220:357-362.

Rothnagel JA, Dominey AM, Dempsey LD, Longley MA, Greenhalgh DA, Gagne TA, Huber M, Frenk E, Hohl D, Roop DR (1992). Mutations in the rod domains of keratins 1 and 10 in epidermolytic hyperkeratosis. Science 257:1128-1130.

Roux AF, Faugere V, Le Guedard S, Pallares-Ruiz N, Vielle A, Chambert S, Marlin S, Hamel C, Gilbert B, Malcolm S, Claustres M, French Usher Syndrome Collaboration (2006). Survey of the frequency of USH1 gene mutations in a cohort of Usher patients shows the importance of cadherin 23 and protocadherin 15 genes and establishes a detection rate of above 90%. J Med Genet 43:763-768.

Rozen S, Skaletsky H (2000). Primer3 on the WWW for general users and for biologist programmers. Methods Mol Biol 132:365-386.

Sambrook J, Fritsch EF, Maniatis T (1989). In: Molecular Cloning: A Laboratory Manual (Irwin N, Ford N, Nolan C, Fergusan M, Ockler M). Cold Spring Harber Laboratory Press, CSH, USA.

Santos RL, El-Shanti H, Sikandar S, Lee K, Bhatti A, Yan K, Chahrour MH, McArthur N, Pham TL, Mahasneh AA, Ahmad W, Leal SM (2006). Novel sequence variants in the TMIE gene in families with autosomal recessive nonsyndromic hearing impairment. J Mol Med 84:226-231.

Santos RL, Wajid M, Khan MN, McArthur N, Pham TL, Bhatti A, Lee K, Irshad S, Mir A, Yan K, Chahrour MH, Ansar M, Ahmad W, Leal SM (2005). Novel sequence variants in the TMC1 gene in Pakistani families with autosomal recessive hearing impairment. Hum Mutat 26:396.

Schaffer AA (1996). Faster linkage analysis computations for pedigrees with loops or unused alleles. Hum Hered 46:226-235.

Scott HS, Kudoh J, Wattenhofer M, Shibuya K, Berry A, Chrast R, Guipponi M, Wang J, Kawasaki K, Asakawa S, Minoshima S, Younus F, Mehdi SQ, Radhakrishna U, Papasavvas MP, Gehrig C, Rossier C, Korostishevsky M,

Gal A, Shimizu N, Bonne-Tamir B, Antonarakis SE (2001). Insertion of beta-satellite repeats identifies a transmembrane protease causing both congenital and childhood onset autosomal recessive deafness. Nat Genet 27:59-63.

Seeman P, Malíkova M, Raskova D, Bendova O, Groh D, Kubalkova M, Sakmaryova I, Seemanova E, Kabelka Z (2004). Spectrum and frequencies of mutations in the GJB2 (Cx26) gene among 156 Czech patients with pre-lingual deafness. Clin Genet 66:152-157.

Sheffield VC, Nishimura DY, Stone EM (1995). Novel approaches to linkage mapping. Curr Opin Genet Dev 5:335-341.

Shimomura Y, Wajid M, Ishii Y, Shapiro L, Petukhova L, Gordon D, Christiano AM (2008). Disruption of P2RY5, an orphan G protein-coupled receptor, underlies autosomal recessive woolly hair. Nat Genet 40:335-339.

Siemens J, Kazmierczak P, Reynolds A, Sticker M, Littlewood-Evans A, Muller U (2002). The Usher syndrome proteins cadherin 23 and harmonin form a complex by means of PDZ-domain interactions. Proc Natl Acad Sci USA 99:14946-14951.

Sobel E, Lange K (1996). Descent graphs in pedigree analysis: applications to haplotyping, location scores, and marker sharing statistics. Am J Hum Genet 58:1323-1337.

Sonoda H, Aoki J, Hiramatsu T, Ishida M, Bandoh K, Nagai Y, Taguchi R, Inoue K, Arai H (2002). A novel phosphatidic acid-selective phospholipase A1 that produces lysophosphatidic acid. J Biol Chem 277:34254-34263.

Sperling LC (1991). Hair anatomy for the clinician. J Am Acad Dermatol 25:1-17

Sprecher E, Chavanas S, DiGiovanna JJ, Amin S, Nielsen K, Prendiville JS, Silverman R, Esterly NB, Spraker MK, Guelig E, de Luna ML, Williams ML, Buehler B, Siegfried EC, Van Maldergem L, Pfendner E, Bale SJ, Uitto J, Hovnanian A, Richard G (2001). The spectrum of pathogenic mutations in SPINK5 in 19 families with Netherton syndrome: implications for mutation detection and first case of prenatal diagnosis. J Invest Dermatol 117:179-187.

Sprecher E, Ishida-Yamamoto A, Becker OM, Marekov L, Miller CJ, Steinert PM, Neldner K, Richard G (2001). Evidence for novel functions of the keratin tail

emerging from a mutation causing ichthyosis hystrix. J Invest Dermatol 116:511-519.

Sprecher E, Tesfaye-Kedjela A, Ratajczak P, Bergman R, Richard G (2004). Deleterious mutations in SPINK5 in a patient with congenital ichthyosiform erythroderma: molecular testing as a helpful diagnostic tool for Netherton syndrome. Clin Exp Dermatol 29:513-517.

Sprecher E, Yosipovitch G, Bergman R, Ciubutaro D, Indelman M, Pfendner E, Goh LC, Miller CJ, Uitto J, Richard G (2003). Epidermolytic hyperkeratosis and epidermolysis bullosa simplex caused by frameshift mutations altering the v2 tail domains of keratin 1 and keratin 5. J Invest Dermatol 120:623-626.

Sreekumar GP, Roberts JL, Wong CQ, Stenn KS, Parimoo S (2000). Marie Unna hereditary hypotrichosis gene maps to human chromosome 8p21 near hairless. J Invest Dermatol 114:595-597.

Sybert VP, Francis JS, Corden LD, Smith LT, Weaver M, Stephens K, McLean WH (1999). Cyclic ichthyosis with epidermolytic hyperkeratosis: A phenotype conferred by mutations in the 2B domain of keratin K1. Am J Hum Genet 64:732-738.

Syder AJ, Yu QC, Paller AS, Giudice G, Pearson R, Fuchs E (1994). Genetic mutations in the K1 and K10 genes of patients with epidermolytic hyperkeratosis. Correlation between location and disease severity. J Clin Invest 93:1533-1542.

Takahashi T, Kamimura A, Hamazono-Matsuoka T, Honda S (2003). Phosphatidic acid has a potential to promote hair growth in vitro and in vivo, and activates mitogen-activated protein kinase/extracellular signal-regulated kinase kinase in hair epithelial cells. J Invest Dermatol 121:448-456.

Tamagawa Y, Kitamura K, Ishida T, Ishikawa K, Tanaka H, Tsuji S, Nishizawa M (1996). A gene for a dominant form of non-syndromic sensorineural deafness (DFNA11) maps within the region containing the DFNB2 recessive deafness gene. Hum Mol Genet 5:849-852.

Temtamy SA, Mannikko M, Abdel-Salam GM, Hassan NA, Ala-Kokko L, Afifi HH (2006). Oto-spondylo-megaepiphyseal dysplasia (OSMED): clinical and

radiological findings in sibs homozygous for premature stop codon mutation in the COL11A2 gene. Am J Med Genet A 140:1189-1195.

Terron-Kwiatkowski A, Paller AS, Compton J, Atherton DJ, McLean WH, Irvine AD (2002). Two cases of primarily palmoplantar keratoderma associated with novel mutations in keratin 1. J Invest Dermatol 119:966-971.

Uyguner O, Emiroglu M, Uzumcu A, Hafiz G, Ghanbari A, Baserer N, Yuksel-Apak M, Wollnik B (2003). Frequencies of gap- and tight-junction mutations in Turkish families with autosomal-recessive non-syndromic hearing loss. Clin Genet 64:65-69.

Vallet V, Chraibi A, Gaeggeler HP, Horisberger JD, Rossier BC (1997). An epithelial serine protease activates the amiloride-sensitive sodium channel. Nature 389:607-610.

Van Camp G, Willems PJ, Smith RJH (1997). Nonsyndromic hearing impairment: unparalleled heterogeneity. Am J Hum Genet 60:758–764.

van Steensel M, Smith FJ, Steijlen PM, Kluijt I, Stevens HP, Messenger A, Kremer H, Dunnill MG, Kennedy C, Munro CS, Doherty VR, McGrath JA, Covello SP, Coleman CM, Uitto J, McLean WH (1999). The gene for hypotrichosis of Marie Unna maps between D8S258 and D8S298: exclusion of the hr gene by cDNA and genomic sequencing. Am J Hum Genet 65:413-419.

van Steensel MA, Steijlen PM, Bladergroen RS, Vermeer M, van Geel M (2005). A missense mutation in the type II hair keratin hHb3 is associated with monilethrix. J Med Genet 42:19.

van Wijk E, van der Zwaag B, Peters T, Zimmermann U, Te Brinke H, Kersten FF, Märker T, Aller E, Hoefsloot LH, Cremers CW, Cremers FP, Wolfrum U, Knipper M, Roepman R, Kremer H (2006). The DFNB31 gene product whirlin connects to the Usher protein network in the cochlea and retina by direct association with USH2A and VLGR1. Hum Mol Genet 15:751-765.

Verpy E, Leibovici M, Zwaenepoel I, Liu XZ, Gal A, Salem N, Mansour A, Blanchard S, Kobayashi I, Keats BJ, Slim R, Petit C (2000). A defect in harmonin, a PDZ domain-containing protein expressed in the inner ear sensory hair cells, underlies Usher syndrome type 1C. Nat Genet 26:51-55.

Verpy E, Masmoudi S, Zwaenepoel I, Leibovici M, Hutchin TP, Del Castillo I, Nouaille S, Blanchard S, Laine S, Popot JL, Moreno F, Mueller RF, Petit C (2001). Mutations in a new gene encoding a protein of the hair bundle cause non-syndromic deafness at the DFNB16 locus. Nat Genet 29:345-349.

Veske A, Oehlmann R, Younus F, Mohyuddin A, Müller-Myhsok B, Mehdi SQ, Gal A (1996). Autosomal recessive non-syndromic deafness locus (DFNB8) maps on chromosome 21q22 in a large consanguineous kindred from Pakistan. Hum Mol Genet 5:165-168.

Vreugde S, Ferrai C, Miluzio A, Hauben E, Marchisio PC, Crippa MP, Bussi M, Biffo S (2006). Nuclear myosin VI enhances RNA polymerase II-dependent transcription. Mol Cell 23:749-755.

Wajid M, Bazzi H, Rockey J, Lubetkin J, Zlotogorski A, Christiano AM (2007). Localized autosomal recessive hypotrichosis due to a frameshift mutation in the desmoglein 4 gene exhibits extensive phenotypic variability within a Pakistani family. J Invest Dermatol 127:1779-1782.

Wali A, Ali G, John P, Lee K, Chishti MS, Leal SM, Ahmad W (2007b). Mapping of a gene for alopecia with mental retardation syndrome (APMR3) on chromosome 18q11.2-q12.2. Ann Hum Genet 71:570-577.

Wali A, Ansar M, Khan MN, Ahmad W (2006b). Atrichia with papular lesions resulting from a novel insertion mutation in the human hairless gene. Clin Exp Dermatol 31:695-698.

Wali A, Chishti MS, Ayub M, Yasinzai M, Kafaitullah K, Ali G, John P, Leal SM, Ahmad W (2007a). Localization of a novel autosomal recessive hypotrichosis locus (LAH3) to chromosome 13q14.11-q21.32. Clin Genet 72:23-29.

Wali A, John P, Gul A, Lee K, Chishti MS, Ali G, Hassan MJ, Leal SM, Ahmad W (2006a). A novel locus for alopecia with mental retardation syndrome (APMR2) maps to chromosome 3q26.2-q26.31. Clin Genet 70:233-239.

Wang A, Liang Y, Fridell RA, Probst FJ, Wilcox ER, Touchman JW, Morton CC, Morell RJ, Noben-Trauth K, Camper SA, Friedman TB (1998). Association of unconventional myosin MYO15 mutations with human nonsyndromic deafness DFNB3. Science 280:1447-1451.

Wattenhofer M, Di Iorio MV, Rabionet R, Dougherty L, Pampanos A, Schwede T, Montserrat-Sentis B, Arbones ML, Iliades T, Pasquadibisceglie A, D'Amelio M, Alwan S, Rossier C, Dahl HH, Petersen MB, Estivill X, Gasparini P, Scott HS, Antonarakis SE (2002). Mutations in the TMPRSS3 gene are a rare cause of childhood nonsyndromic deafness in Caucasian patients. J Mol Med 80:124-131.

Wattenhofer M, Sahin-Calapoglu N, Andreasen D, Kalay E, Caylan R, Braillard B, Fowler-Jaeger N, Reymond A, Rossier BC, Karaguzel A, Antonarakis SE (2005). A novel TMPRSS3 missense mutation in a DFNB8/10 family prevents proteolytic activation of the protein. Hum Genet 117:528-535.

Weber T, Zimmermann U, Winter H, Mack A, Kopschall I, Rohbock K, Zenner HP, Knipper M (2002). Thyroid hormone is a critical determinant for the regulation of the cochlear motor protein prestin. Proc Natl Acad Sci USA 99:2901-2906.

Weeks DE, Sobel E, O'Connell JR, Lange K (1995). Computer programs for multilocus haplotyping of general pedigrees. Am J Hum Genet 56:1506-1507.

Weil D, Blanchard S, Kaplan J, Guilford P, Gibson F, Walsh J, Mburu P, Varela A, Levilliers J, Weston MD, Kelley PM, Kimberling WJ, Wagenaar M, Levi-acobas F, Larget-piet D, Munnich A, Steel KP, Brown SDM, Petit C (1995). Defective myosin VIIA gene responsible for Usher syndrome type 1B. Nature 374:60-61.

Weil D, Küssel P, Blanchard S, Lévy G, Levi-Acobas F, Drira M, Ayadi H, Petit C (1997). The autosomal recessive isolated deafness, DFNB2, and the Usher 1B syndrome are allelic defects of the myosin-VIIA gene. Nat Genet 16:191-193.

Weiner JA, Fukushima N, Contos JJ, Scherer SS, Chun J (2001). Regulation of schwann cells morphology and adhesion by receptor-mediated lysophosphatidic acid signaling. J Neurosci 21:7069–7078.

Whittock NV, Ashton GH, Griffiths WA, Eady RA, McGrath JA (2001). New mutations in keratin 1 that cause bullous congenital ichthyosiform erythroderma and keratin 2e that cause ichthyosis bullosa of Siemens. Br J Dermatol 145:330-335.

Whittock NV, Smith FJ, Wan H, Mallipeddi R, Griffiths WA, Dopping-Hepenstal P, Ashton GH, Eady RA, McLean WH, McGrath JA (2002). Frameshift mutation in the V2 domain of human keratin 1 results in striate palmoplantar keratoderma. J Invest Dermatol 118:838-844.

Wilcox ER, Burton QL, Naz S, Riazuddin S, Smith TN, Ploplis B, Belyantseva I, Ben-Yosef T, Liburd NA, Morell RJ, Kachar B, Wu DK, Griffith AJ, Riazuddin S, Friedman TB (2001). Mutations in the gene encoding tight junction claudin-14 cause autosomal recessive deafness DFNB29. Cell 104:165-172.

Winter H, Labreze C, Chapalain V, Surleve-Bazeille JE, Mercier M, Rogers MA, Taieb A, Schweizer J (1998). A variable monilethrix phenotype associated with a novel mutation, Glu402Lys, in the helix termination motif of the type II hair keratin hHb1. J Invest Dermatol 111:169-172.

Winter H, Vabres P, Larregue M, Rogers MA, Schweizer J (2000). A novel missense mutation, A118E, in the helix initiation motif of the type II hair cortex keratin hHb6, causing monilethrix. Hum Hered 50:322-324.

Wulf P, Suter U (1999). Embryonic expression of epithelial membrane protein 1 in early neurons. Brain Res Dev Brain Res 116:169–180.

Xia JH, Liu CY, Tang BS, Pan Q, Huang L, Dai HP, Zhang BR, Xie W, Hu DX, Zheng D, Shi XL, Wang DA, Xia K, Yu KP, Liao XD, Feng Y, Yang YF, Xiao JY, Xie DH, Huang JZ (1998). Mutations in the gene encoding gap junction protein beta-3 associated with autosomal dominant hearing impairment. Nat Genet 20:370-373.

Yang S, Gao M, Cui Y, Yan KL, Ren YQ, Zhang GL, Wang PG, Xiao FL, Du WH, Liang YH, Sun LD, Xu SJ, Huang W, Zhang XJ (2005). Identification of a novel locus for Marie Unna hereditary hypotrichosis to a 17.5 cM interval at 1p21.1-1q21.3. J Invest Dermatol 125:711-714.

Yasunaga S, Grati M, Chardenoux S, Smith TN, Friedman TB, Lalwani AK, Wilcox ER, Petit C (2000). OTOF encodes multiple long and short isoforms: genetic evidence that the long ones underlie recessive deafness DFNB9. Am J Hum Genet 67:591-600.

Yasunaga S, Grati M, Cohen-Salmon M, El-Amraoui A, Mustapha M, Salem N, El-Zir E, Loiselet J, Petit C (1999). A mutation in OTOF, encoding otoferlin, a FER-1-like protein, causes DFNB9, a nonsyndromic form of deafness. Nat Genet 21:363-369.

Yasunaga S, Petit C (2000). Physical map of the region surrounding the OTOFERLIN locus on chromosome 2p22-p23. Genomics 66:110-112.

Zhao Y, Ma ZH, Yang Y, Yang SX, Wu LS, Ding BL, Lin ZM, Wang AP, Bu DF, Tu P (2007). SPINK5 gene mutation and decreased LEKTI activity in three Chinese patients with Netherton's syndrome. Clin Exp Dermatol 32:564-567.

Zheng J, Shen W, He DZ, Long KB, Madison LD, Dallos P (2000). Prestin is the motor protein of cochlear outer hair cells. Nature 405:149-155.

Zheng L, Sekerkova G, Vranich K, Tilney LG, Mugnaini E, Bartles JR (2000). The deaf jerker mouse has a mutation in the gene encoding the espin actin-bundling proteins of hair cell stereocilia and lacks espins. Cell 102:377-385.

Zlotogorski A, Panteleyev AA, Aita VM, Christiano AM (2002). Clinical and molecular diagnostic criteria of congenital atrichia with papular lesions. J Invest Dermatol 118:887-890.

Zwaenepoel I, Mustapha M, Leibovici M, Verpy E, Goodyear R, Liu XZ, Nouaille S, Nance WE, Kanaan M, Avraham KB, Tekaia F, Loiselet J, Lathrop M, Richardson G, Petit C (2002). Otoancorin, an inner ear protein restricted to the interface between the apical surface of sensory epithelia and their overlying acellular gels, is defective in autosomal recessive deafness DFNB22. Proc Natl Acad Sci USA 99:6240-6245.

ELECTRONIC DATABASE INFORMATION

- UCSC Genome Browser: **http://genome.ucsc.edu/cgi-bin/hgGateway**
- Marshfield Medical Research Foundation database website:

  http://research.marshfieldclinic.org/genetics/
- Hereditary Hearing Loss Homepage web site: Van Camp G, Smith RJH Hereditary hearing loss. Homepage: **http://www.webhost.ua.ac.be/hhh/**
- National Center for Biotechnology Information web site: **http://www.ncbi.nlm.nih.gov/**